Hybrid Active Power Filter Technique to Enhance Power Quality of Electric Railway Traction Substation

(Case Study: Minilik Square Traction Substation NS27)

Thesis submitted to Addis Ababa University, Institute of Technology, in partial fulfillment of the requirements for the degree of Masters of Science in Electrical Power Engineering

By

Kibru Zewdie Woldie

GSE/2349/09

Advisor

Dr. Mengesha Mamo

ADDIS ABABA UNVERSITY

ADDIS ABABA INSTITUTE OF TECHNOLOGY

SCHOOL OF ELECTRICAL AND COMPUTER ENGINEERING

ADDIS ABABA

November 2020

Hybrid Active Power Filter Technique to Enhance Power Quality of Electric Railway Traction Substation

(Case Study: Minilik Square Traction Substation NS27)

By

Kibru Zewdie Woldie

Approval by boards of examiners

We certify that we have read this thesis and that in our opinion it is fully accepted in scope and quality as a thesis for the degree of Master of Science in Electrical Power Engineering.

Dr. Yalemzewd Negash Chairman, Department of Graduate Committee	________________ Signature	______________ Date
Dr. Mengesha Mamo Advisor	________________ Signature	______________ Date
Prof. N.P.Singh External Examiner	________________ Signature	______________ Date
Mr. Amare Assefa (PH.D. Candidate) Internal Examiner	________________ Signature	______________ Date

DECLARATION

I certify that

A. The work contained in this thesis is original and has been done by myself under the supervision of my supervisor.
B. The work has not been submitted to any other Institute for Master of Science.
C. I have conformed to the norms and guidelines given in the Ethical Code of Conduct of the Institute.
D. Whenever I have used or quoted materials (data, theoretical analysis, and text) from other sources, I have given due credit to them by citing them in the text of the thesis and giving their details in the references.

Name: Kibru Zewdie Woldie

ID No. : GSE/2349/09

Signature: _______________

Date of submission: November 2020 G.C

Place: Addis Ababa, Ethiopia

This thesis has been submitted with my approval as a university advisor

Advisor's Name: Dr. Mengesha Mamo

Signature: _____________

Place: Addis Ababa, Ethiopia

ABSTRACT

Addis Ababa Light Rail Transit (AALRT) is an electrified railway traction system with large amount of harmonic currents being generated due to the nonlinear characteristics of rectifiers and inverters devices and inject the harmonics back into the grid. This has caused serious impact on the power supply network and resulted in power quality problems within the traction substation that has led to multifunction of some system components. For the overall quality of railway service, there should be reliable, efficient and safe power distribution systems by improving the power quality. The power quality enhancement has been proposed by using hybrid active power filter harmonic current compensation technique. This study presents theoretical and practical aspects in improving the power quality of Minilik Square NS27 railway traction substation network by reducing 11^{th} and 13^{th} harmonic currents using hybrid active power filter (HAPF). Simulation studies of the Minilik Square NS27 railway traction substation network is carried out using MATLAB Simulink in a discrete mode, variable step size with ode45 (Dormand-Prince) solver.

The simulation results show that 11^{th} order current harmonics is reduced from 26.99% to 3.75% while 13^{th} order current harmonics is reduced from 11.05% to 4.38% at the point of common coupling (PCC). Consequently, the total harmonic distortion (THD) of currents at PCC is reduced from 88.19% to 80.55%. It is further noted that at primary side of the transformer 11^{th} order current harmonics is reduced from 17.99% to 1.55% while 13^{th} order current harmonics is reduced from 13.43% to 0.89%. Thus, the overall total harmonic distortion (THD) of currents is reduced from 26.46% to 6.88% on the primary side of the transformer.

Furthermore, it is observed that the distortion power factor is also improved from 0.955 to 0.995 due to the reduction of 11^{th} and 13^{th} order harmonic currents**.** Therefore, the effective value of fundamental current has been improved due to the reduction of 11^{th} and 13^{th} order harmonic currents and consequently the corresponding active power in the traction network is also improved.

Thus, the simulation results demonstrate the effectiveness of the proposed HAPF technique for selective harmonic currents reduction and thereby power quality enhancement of Minilik Square NS27 railway traction substation network of AALRT.

Key words: Hybrid active power filter, harmonic currents, electric traction, twelve pulse rectifier, six pulse rectifier.

ACKNOWLEDGEMENT

I would like to thank Dr. Mengesha Mamo for his kind support and guidance in the preparation of this study.

I am grateful to staff members of Ethiopian Railway Corporation (ERC) and Addis Ababa Light Railway Transit (AALRT) for providing the traction system documents and permitting and scheduling to process the measurement in traction station.

I would also like to thank staff members of Ethiopian Energy Authority (EEA) in providing local harmonic standard documents and harmonic analyzer equipment.

TABLE OF CONTENTS

LIST OF ABBREVIATIONS

<u>Abbreviation</u>	<u>Description</u>
$\alpha\beta$	Alpha Beta
AALRT	Addis Ababa Light Railway Transit
AIS	Air Insulated Station
APF	Active Power Filter
GIS	Gas Insulated Station
FFT	Fast Fourier Transform
HAPF	Hybrid Active Power Filter
HCC	Hysteresis Current Control
kW	Kilo Watt
MVA	Mega Volt Ampere
NS27	North South 27
OCS	Overhead Catenary System
PCC	Point of Common Coupling
PI	Proportional Integral
PWM	Pulse Width Modulation
RMS	Root Mean Square
STD	Standard
THD	Total Harmonic Distortion
VAC	Voltage of alternating current
VDC	Voltage of direct current
VSI	Voltage Source Inverter
VVVF	Variable Voltage Variable Frequency

LIST OF SYMBOLS

Symbols	Nomenclature	Description (SI Unit)
A	Current	Ampere
i_a, i_b, i_c	Source Current	Instantaneous line currents
L1, L2, L3, L4, L5, L6	Phase R, S, T	Line 1, Line 2, Line 3
V_a, V_b, V_c	Source Voltage	Instantaneous phase voltages
γ	Attenuation factor	

LIST OF FIGURES

Page

LIST OF TABLES

Page

Chapter One

Introduction

1.1 Background

Electrified railway traction networks are one of the modern transportation systems with the advantage of environment friendly nature and cheap running cost. At present, in Ethiopia there are electrified traction networks which are in use for passenger and goods transportation. Addis Ababa Light Railway Transit (AALRT) is one of the electrified traction networks and it is dedicated for passenger transportation. AALRT network consists of four GIS substation each with 2x25MVA capacities which are located at the four ends of North to South and East to West railway routes to deliver electric power to all AIS traction substation. All traction substations are built of identical electrical systems which have the same design ratings and system installation. The main traction network electrical components are dry type rectifier tertiary winding transformer of D10/Dy11, 2MVA, 15kV/590V/590V, 3 phase, 50Hz, twelve pulse diode rectifier circuit rectifying 3 Phase 590VAC to 750VDC, DC power transmission system which is rated for 750VDC with ranges of voltage variation from 500VDC to 900VDC, the locomotive system consisting of traction converter box dedicated to convert dc voltage into three phase ac voltage with variable voltage and variable frequency and the traction motor with rated power of 130kW three phase 500VAC to 510VAC squirrel cage asynchronous (induction) motor. The traction substation under the case study is located around Minilik Square which is identified by the code name NS27 [1].

Even though electrified traction networks are in practical use for their advantages mentioned above, these networks are the main cause to power quality issues due to harmonics within the system. Harmonics are generated from the changing load nature and nonlinear characteristics of the power electronic components of the traction system. These generated harmonics creates serious problems within the network and are injected back to the grid causing huge impact on the power distribution network. To reduce the negative effect of harmonics, power quality engineers have proposed numerous techniques and methods to mitigate the harmonics. Hybrid active power filter is one of the harmonic mitigation methods which is selected for its combined feature of passive filter and active power filter.

It is mainly selected for its combined feature which makes the individual components capable to compensate the limitation of each of them. Passive filters are one of the conventional mitigation techniques which are effective under constant load conditions and are used commonly for its low cost, higher efficiency and easy to implement. But they have various limitations with drawbacks which reduce the performance of harmonic mitigation. The drawbacks are: they are not suitable for changing load conditions, they provide resonance affecting the stability of the power distribution systems, its performance is limited to low order harmonics but are inefficient in the application of higher order harmonics, and their filtering characteristics is affected by frequency variation of the power distribution system and tolerances in components values.

Due to the weak performance of passive filters, active power filters are developed to compensate some of the drawbacks of the passive filters. Active power filters are good solution over the passive filters but they are more expensive than the passive filters and their cost will be higher for high rating of active filters. The development of signal processing and power converters permits the use of active power filters (APFs) to enhance the electrical power quality. Hybrid filter topology is developed to improve the performance of the passive filters. Hybrid topologies composed of passive filters connected in series to an active power filter to improve the compensation characteristics of passive filters, and allow the use of active power filters in high power applications at a relatively low cost. The series interconnection of active power filters with passive filters improves most of the technical drawbacks of passive filters.

In this paper, twelve pulse (two six pulses) traction network is discussed based on the actual field measurement against the standard limits and the hybrid active power filter solution is designed using MATLAB/Simulink software. Based on the simulation results discussion and analysis is provided.

1.2 Problem statement

The nonlinear components of the traction network in AALRT system are generating large amount of current harmonics much more beyond the standard harmonic limit requirement. The predominant current harmonic orders in any electrical power supply systems with twelve pulse rectifiers are 11^{th} and 13^{th} current harmonic orders. Because of continuous traction network failure and malfunction of some of the traction network components, Addis Ababa Light Rail Transit technical teams were unable to identify whether the failures are from the network component equipment quality or due to the harmonic currents developed in Minilik Square NS27 railway traction substation network.

This thesis investigates the effects of 11^{th} and 13^{th} current harmonic orders on the performance of Minilik Square NS27 railway traction substation network. The design and MATLAB/Simulink model based implementation of HAPF for Minilik Square NS27 railway traction substation network is investigated to mitigate the problems caused by 11^{th} and 13^{th} order current harmonics.

1.3 Objectives

General Objective: The general objective of the thesis is to enhance the power quality of railway traction substations supply system by mitigating the current harmonics using hybrid active power filter.

Specific Objectives: The specific objectives of this thesis are as follows:

(a) To collect the values of parameters of Minilik Square NS27 railway traction substation network

(b) To measure and analyze the current and voltage harmonics of Minilik Square NS27 railway traction substation network

(c) To identify the existing problems in the railway traction substation network

(d) To design hybrid active power filter for mitigation of 11^{th} and 13^{th} order current harmonics in order to enhance the power quality of the railway traction substation supply system

(e) To develop model of Minilik Square NS27 railway traction substation network with and without hybrid active power filter using MATLAB/Simulink software

(f) To carry out simulation studies using MATLAB/Simulink models of the railway traction substation network with and without hybrid active power filter
(g) To analyze the simulation results and draw conclusions
(h) To make recommendations to AALRT for mitigation of problems caused by 11^{th} and 13^{th} order current harmonics and enhancement of power quality of Minilik Square NS27 railway traction substation supply system

1.4 Literature review

The authors demonstrated and concluded that the hybrid topology of passive filters & active power filters is capable to improve the compensation characteristics of both of passive filters and active filters. This has created the possibility to use the active power filters in high power applications at a relatively low cost [2].

Hybrid combination of passive filters and active power filters improved the filtering characteristics by improving the passive filter limitations. The hybrid combination performs the compensation strategy without depending on the system impedance and resonance problem [3].

Based on the conclusion drawn from the authors, active power filter improves the compensation characteristics of the passive filter in parallel connection [4].

In reference [5], it is stated that the objective of hybrid active power filter is to improve the filtering performance of high order harmonics which is the limitation of passive filters while providing low order harmonic mitigation with cost effective technique.

Hybrid filters are the combination of passive filters and active power filters in which the presence of passive filters in the hybrid topology significantly reduce the rating of active power filter [6].

The authors in reference [7] together concluded that hybrid active power filter provides the efficacious combination of active filter and passive filter by combining the advantages of both filters and by eliminating the limitations of each of the filters.

1.5 Methodology

Hybrid active power filter is implemented with a three phase pulse width modulation voltage source inverter and connected in series with passive filter. The active power filter acts as a controlled voltage source and enables the line currents to become sinusoidal and in phase with respective phase voltage by injecting all or some selected current harmonics to circulate through the hybrid scheme. In other words, the active power filter is connected in series to passive filter, improving most of the technical drawbacks of passive filter compensation characteristic independently of the variation in the selected resonant frequency of filter parameters.

Voltage and current measurements are taken from source and load side of ac network. These measurements are processed to generate reference current signal through harmonic current detection. This reference current signal is fed to voltage source inverter signal triggering gate making capable to generate the corresponding compensating signal to the power system through hybrid active power filter. The traction system with hybrid scheme is simulated for different load conditions for one traction motor, three traction motors and six traction motors load. One and three traction motors load scenarios are selected arbitrary for evaluation of MATLAB/Simulink model which is designed for six traction motors.

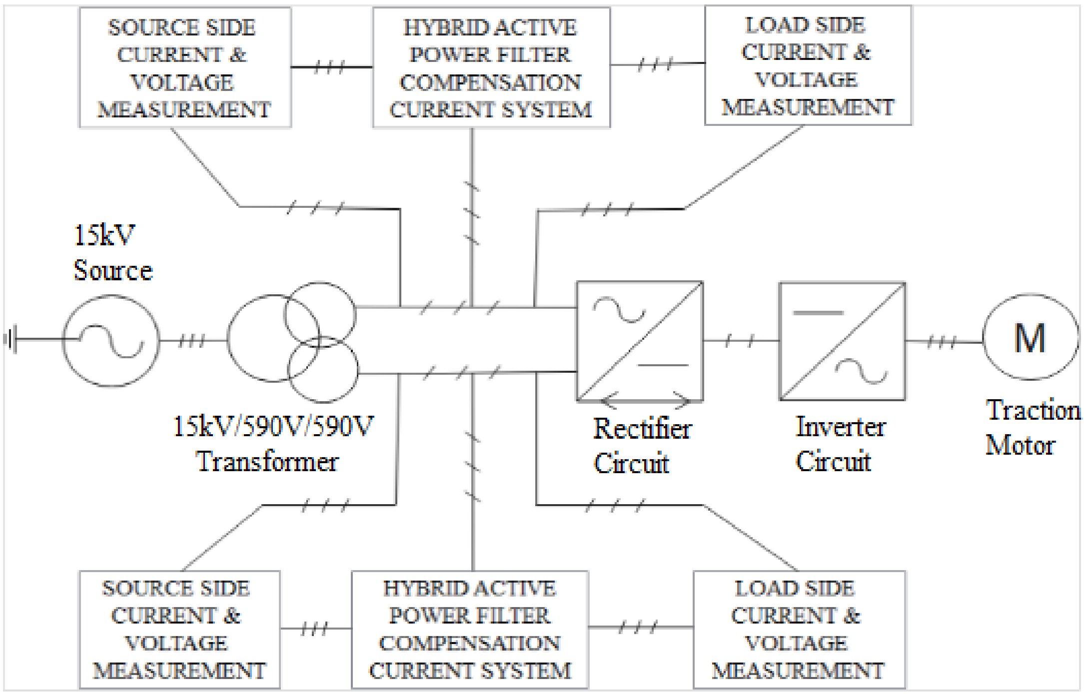

Figure 1.1: Block diagram representation of proposed methodology

1.6 Thesis organization

Chapter 1 provides brief background description about Addis Ababa Light Rail Transit electrified traction network. This chapter also includes problem statement, objectives, literature reviews and methodology.

Chapter 2 presents power quality description and analysis based on traction network data measurement. This chapter also discusses power quality analyses with respect to IEEE standard.

Chapter 3 presents modeling of traction network with and without hybrid active power filter including its detail parameters obtained from measurement and collected information. Designing and modeling of three phase three wire hybrid active power filter and harmonic current compensation procedures based on p-q theory are also included.

Chapter 4 mainly provides simulation results, discussions and analyses of modeled traction network for six traction motors at motor terminal, at PCC and at primary side of the rectifier transformer.

Chapter 5 presents conclusions, recommendations and suggestions for future work.

Chapter Two

Traction network data measurement and analysis

2.1 Introduction

The dry type three winding transformer is the main coupling device between 15kV power provider and AALRT network. The field data measurement is taken at secondary delta and wye outputs of the transformer as indicated on the picture.

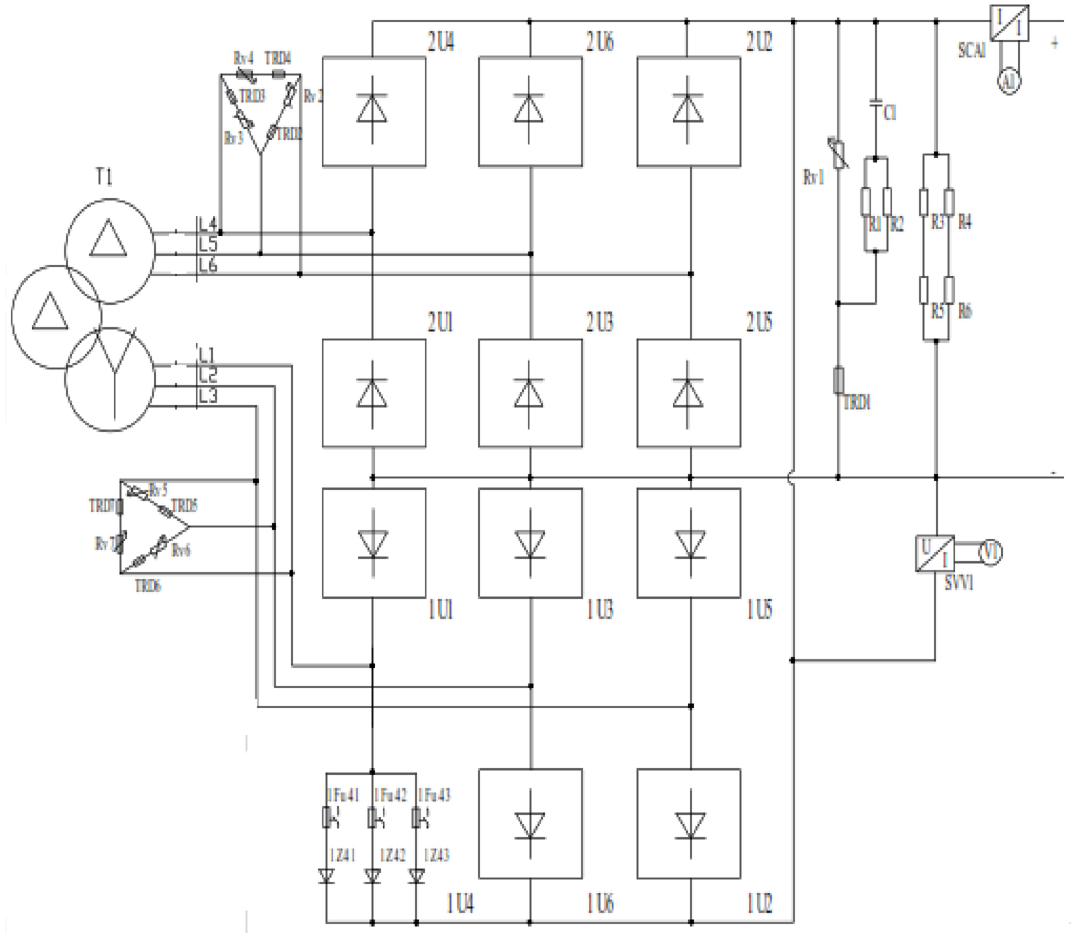

Figure 2.1: Circuit diagram of three winding transformer & twelve pulse rectifier

The lines L1, L2 and L3 are wye connected secondary which are found on the top part of the transformer and the lines L4, L5 and L6 are delta connected secondary on the bottom part of the transformer. The transformer has no neutral line (Appendix B).

The railway traction network diagram is shown below with its components included.

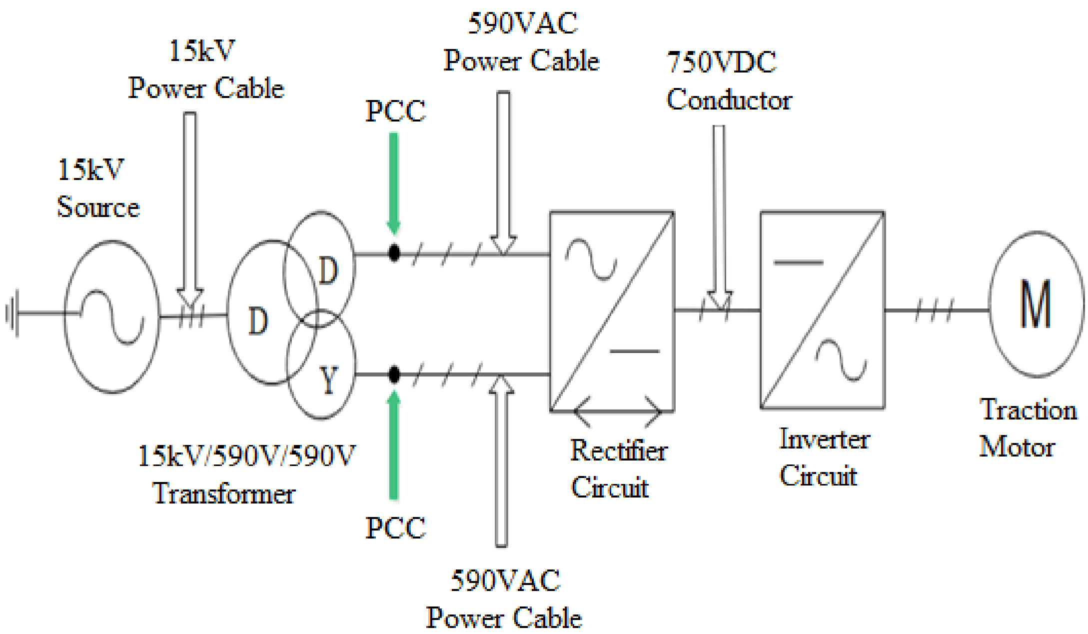

Figure 2.2: Block diagram representation of railway traction network

2.2 Data measuring device and data collection

Field data measuring device is Fluke 435 series II power quality and energy analyzer. This device is designed to work for low voltage system rated up to 1000VAC and a maximum current capacity of 6500A per phase.

The device is made to take measurements for four consecutive days from 10/17/2019 12:53:52 AM or midnight 6:53:52 local time to 10/20/2019 5:33:52PM or evening 11:33:52 local time from delta secondary output and from wye connected secondary output for four consecutive days from 10/20/2019 6:38:24PM or evening 12:38:24 local time to 10/24/2019 2:08:24PM afternoon 8:08:24 local time. The Fluke provides minimum, average and maximum values for each electrical quantity within 10 minute duration of measurement.

Electrical quantities measured at the point of common coupling are: frequency of the system, RMS values of current, RMS values of voltage, voltage THD up to 50th harmonic order, current THD up to 50th harmonic order, peak values of voltage, peak values of current, fundamental voltage, fundamental current, voltage crest factor, current crest factor, power factor, active power, apparent power, reactive power and harmonic power.

The Power Log 430-II software is used to extract measurement from Fluke 435 series II power quality and energy analyzer in spreadsheet of table and spectrums. The maximum measured values of system parameters at PCC is given in the Table 2.1 which is selected for its higher current measurement at PCC at the indicated time from all other values in the data spreadsheet.

Table 2.1: Maximum & average measured values of delta line

10/17/2019 8:03:52AM, (07/02/2012 EC 2:03:52 LT morning)

Function	Phase A		Phase B		Phase C		Phase	
	Aver	Max	Aver	Max	Aver	Max	Aver	Max
Vrms Ph-Ph	569.68	574.92	545.34	567.12	539.08	567.48	551.37	569.84
Current Arms	75.6	478.6	74.4	482.3	72.8	472.6	74.27	477.83
THD V (%)	18.17	23	18.26	23.09	23.99	35.69	20.14	27.26
THD A (%)	94.17	166.55	100.7	177.03	95.33	159.04	96.73	167.54
Peak Voltage	809.6	882.9	808.2	873.5	720	807	779.27	854.47
Peak Current	101.2	909.8	99.6	920.4	97	888.6	99.27	906.27
Fundamental Voltage	328.9	333.7	327.6	333	290.1	325.9	315.53	330.87
Fundamental Current	58.2	423.4	57.4	426.8	56.2	417.4	57.27	422.53
Active Power (kW)	11.24	142.08	10.82	130.74	8.62	88.04	30.68	360.86
Reactive Power (kvar)	1.76	27.7	2.08	27.98	0.94	17.12	4.78	72.80
Harmonic Power (kVA)	21.1	196.88	20.34	198.2	15.9	131.84	57.34	526.92
Apparent Power (kVA)	24	240.02	23.12	241.66	18.2	159.2	65.32	640.88
Power Factor (PF)	0.42	0.86	0.40	0.83	0.42	0.83	0.41	0.84

2.3 IEEE standard and data analysis

The international standard which is IEEE STD 519-2018 is used for measured data analysis and for selection of point of common coupling.

Based on IEEE STD 519-2018 voltage distortion limits

Table 2.2: IEEE STD 519-2018 voltage distortion limits

Bus voltage V at PCC	Individual Harmonic (%)	Total Harmonic Distortion (%)
V≤1.0kV	5	8
1kV<V≤69kV	3	5

Based on IEEE STD 519-2018 current distortion limits for systems rated from 120V through 69kV

Table 2.3: IEEE STD 519-2018 current distortion limits

	Maximum Harmonic Order Distortion in percent Individual Harmonic Order (odd harmonic) = H_n = h					
I_{SC}/I_L	$3 \leq h < 11$	$11 \leq h < 17$	$17 \leq h < 23$	$23 \leq h < 35$	$35 \leq h \leq 50$	THD
<20	4.0	2.0	1.5	0.6	0.3	5.0
20<50	7.0	3.5	2.5	1.0	0.5	8.0
50<100	10.0	4.5	4.0	1.5	0.7	12.0
100<1000	12.0	5.5	5.0	2.0	1.0	15.0
>1000	15.0	7.0	6.0	2.5	1.4	20.0

where $I_{SC}/I_L$is the ratio of short-circuit current available at the Point of Common Coupling (PCC) to the maximum fundamental load current. Even harmonics are limited to 25% of the odd harmonic limits above.

The IEE 519 for maximum current harmonic distortion is given based on the ratio of short circuit current (I_{SC}) to the maximum fundamental load current (I_L) under normal load operating condition.

The measurements are taken on both secondary output of the transformer. The maximum fundamental current at PCC given in Table 2.1 for delta connected I_L = 422.53A. The capacity of the transformer is 2MVA. Assuming that the two secondary outputs of the transformer shares equally the system load at the PCC, each line has a maximum loading capacity of 1MVA. At PCC the voltage level is 590VAC. Therefore, the short circuit currents can be calculated as following.

$$I_{FL\,Delta} = \frac{1{,}000{,}000}{590\sqrt{3}} = 978.56\text{A and}$$

$$I_{FL\,Wye} = \frac{1{,}000{,}000}{590\sqrt{3}} = 978.56\text{A ,}$$

where I_{FL} is a full load current at PCC

Considering the base impedance of the system is the impedance of rectifier transformer at secondary side. The value of base impedance is 7.75% = 0.0775pu which is taken from the name plate of the transformer. Therefore, the short circuit current at PCC of the secondary terminal of the transformer is given as (Appendix C):

$$I_{SC} = \frac{978.56}{0.0775} = 12{,}626.58\text{A}$$

The value of $I_{SC}/I_L = \frac{12,626.58}{422.53} = 29.88$,

The current harmonic limits in Table 2.3 are taken from IEEE 519 standard and the harmonic distortion reference values are selected based on the calculated result of I_{SC}/I_L. Calculated value of I_{SC}/I_L is 29.88 which is between 20 and 50 located on the second row of Table 2.3.

Point of Common Coupling (PCC) is defined as following based on the internationally accepted standards.

IEEE STD 519-1992 – Page 75

The recommendation described in this document attempts to reduce the harmonic effects at any point in the entire system by establishing limits on certain harmonic indices (currents and voltages) at the point of common coupling (PCC), a point of metering, or any point as long as both the utility and the consumer can either access the point for direct measurement of the harmonic indices meaning to both or can estimate the harmonic indices at point of interference through mutually agreeable methods. Within an industrial plant, the pinot of common coupling is the point between the nonlinear load and other loads.

IEEE STD 519-2014 – Page 2

The limits in this recommended practice are intended for application at a point of common coupling between the system owner or operator and a user, where the PCC is usually taken as the point of in the power system closest to the user where the system owner or operator could offer service to another user.

IEEE STD 519-2014 – Page 3

Point of a public power supply system, electrically nearest to a particular load, at which other loads are, or could be connected. The PCC is a point located upstream of the considered installation.

IEEE STD 3002.8 - 2018

Point of a public power supply system, electrically nearest to a particular load, at which other loads are, or could be connected. The PCC is a point located upstream of the considered installation. This definition is in agreement with the earlier definition for PCC.

Based on the above definitions for PCC and considering the actual existing conditions in our specific project of study, the PCC is selected at the secondary side of transformer which is low voltage side of the three winding transformer as shown above in Figure 2.2 for the following reasons.

(a) The available Fluke device maximum limit voltage is 1000VAC.

(b) Installing harmonic compensating devices on the low voltage side is preferred over installing on the medium voltage side as compared to the physical size and the cost of medium voltage harmonic compensating devices.

(c) Installing harmonic compensating devices on the low voltage side reduces the amount of some harmonics that would flow through the rectifier transformer which would cause heating effect on the transformer windings.

(d) In addition, DC link capacitor voltage (15kV) should also be higher than the system PCC voltage for the active filter to inject compensation current to the network.

(e) The concern of utility provider is to control the power quality towards its upstream on the 15kV primary side of the transformer, thus if power quality of the low voltage side is in the acceptable harmonic range, the power quality will also be improved on the primary side of the transformer.

2.4 Power quality analysis in traction system

The Power Log 430-II software histogram representation for each phase individual current harmonic spectrums up to 50th harmonic orders are shown and the corresponding harmonic spectrum values are also tabulated.

2.4.1 Measured current harmonic spectrums of traction substation

Measured individual current harmonic spectrums of the traction substation NS27 is given below in Figure 2.3 & Figure 2.4.

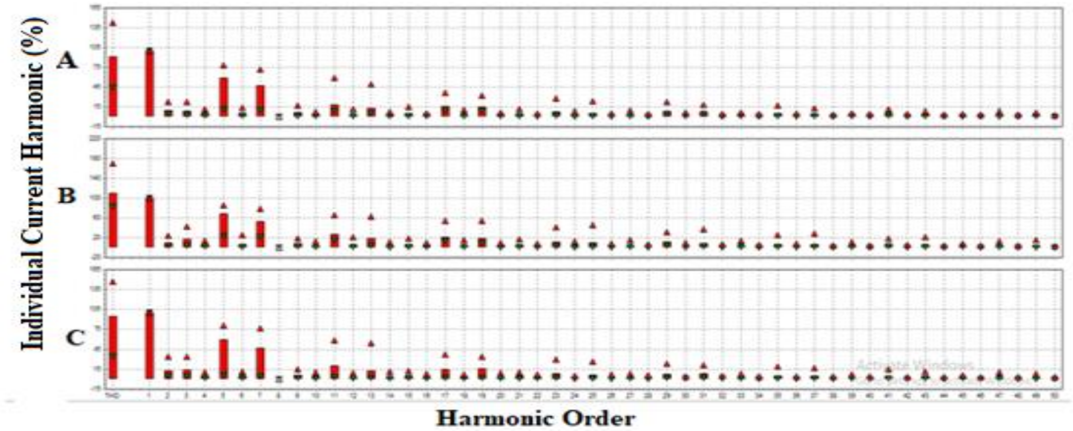

Figure 2.3: Individual current harmonic spectrums of wye line

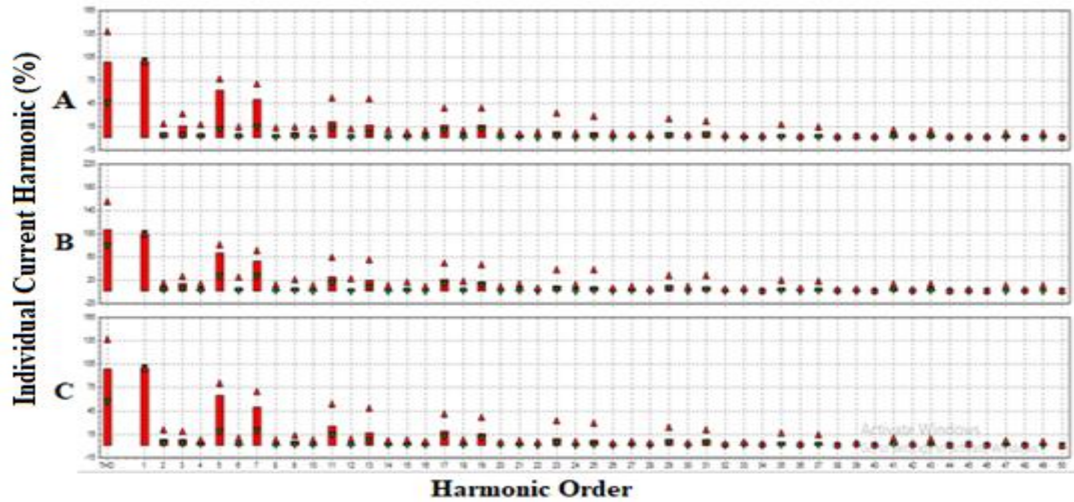

Figure 2.4: Individual current harmonic spectrums of delta line

2.4.2 Measured individual current harmonic values of traction substation

The measured percentage values of individual current harmonics of delta and wye lines of traction substation NS27 are given below in Table 2.4 & Table 2.5.

Table 2.4: Values of individual current harmonics for delta line

H_n	Phase A			Phase B			Phase C		
	Min	Aver	Max	Min	Aver	Max	Min	Aver	Max
2	4.12	10.08	22.99	3.91	9.17	23.87	3.87	12.17	34.09
3	3.03	8.93	22.65	4.66	17.69	42.43	3.99	13.84	33.79
4	2.12	4.59	11.68	2.39	5.38	14.66	2.23	4.4	10.15
5	10.49	58.41	78.26	22.34	67.92	85.79	6.06	59.55	80.41
6	2.02	4.22	13.79	2.03	5.76	25.16	1.93	3.76	11.86
7	9.28	47.06	71.54	21.34	52.27	79.22	4.03	47.05	76.2
8	0	0	0.00	0	0	0.00	0	0	0
9	1.46	6.07	17.28	2.25	8.47	18.98	1.94	8.23	15.1
10	0.76	2.12	7.01	0.99	2.92	12.27	0.88	2.73	11.07
11	8.78	18.6	59.18	13.86	27.38	65.39	3.14	20.65	58.47
12	0.75	2.59	12.06	0.89	4.12	21.80	0.68	1.87	9.49
13	4.89	13.25	49.39	4.38	18.86	62.47	2.44	12.99	54.11
14	0.57	1.72	7.02	0.69	2.77	11.43	0.58	2.48	11.29
15	1.06	4.17	14.79	1.6	5.74	18.58	1.55	3.92	12.6
16	0.75	1.87	5.88	0.8	2.44	10.01	0.72	2.18	8.38
17	8.21	16.14	36.35	12.77	22.05	54.75	1.97	14.87	37.9
18	0.96	2.51	10.74	0.82	3.37	16.37	0.83	1.9	7.58
19	8.06	14.6	32.47	9.22	18.1	54.43	2.13	16.18	33.7
20	0.63	1.61	6.45	0.67	2.35	9.83	0.74	2.17	9.14
21	0.79	3.4	11.82	1.21	4.57	17.35	1.22	3.75	10.4
22	0.41	1.27	5.55	0.54	1.9	8.05	0.46	1.64	7.06
23	2.27	7.36	27.96	3.09	11.67	41.79	1.96	8.26	29.66
24	0.5	1.72	8.10	0.54	2.51	12.69	0.4	1.24	5.07
25	1.57	5.87	23.77	1.3	9.59	46.06	1.16	6.41	26.08
26	0.36	1.13	5.07	0.43	1.73	8.48	0.34	1.48	7.4
27	0.77	2.52	9.25	0.86	3.49	15.68	0.85	2.23	8.42
28	0.48	1.16	4.81	0.54	1.68	6.52	0.42	1.31	5.84
29	4.2	7.78	21.99	4.78	10.82	31.86	1.59	7.03	23.3
30	0.66	1.55	6.76	0.52	1.96	10.33	0.53	1.29	4.55
31	3.9	6.88	17.77	3.43	9.06	36.86	1.69	8.05	21.48
32	0.44	1.08	4.09	0.46	1.41	6.62	0.5	1.34	5.53
33	0.54	1.79	6.56	0.95	3.01	13.64	0.84	2.44	7.9
34	0.27	0.85	4.01	0.38	1.34	5.20	0.33	1.05	4.67
35	0.77	3.87	16.67	1.27	6.02	25.28	1.15	4.30	18.68
36	0.38	1.08	5.32	0.41	1.52	7.91	0.26	0.93	4.07
37	1.00	3.23	12.34	0.78	5.21	28.64	0.66	3.77	16.64
38	0.28	0.84	3.17	0.34	1.09	4.74	0.25	0.92	4.39
39	0.58	1.65	5.36	0.74	2.31	11.47	0.59	1.47	7.15
40	0.36	0.89	3.83	0.42	1.24	4.59	0.29	0.88	3.74
41	2.11	4.09	11.86	2.66	5.56	18.82	1.27	3.49	14.54
42	0.52	1.06	3.81	0.39	1.29	5.84	0.39	0.94	3.39
43	1.02	3.44	8.61	1.45	4.30	21.64	1.43	4.42	12.11
44	0.37	0.86	2.82	0.37	1.01	4.06	0.40	0.91	3.18
45	0.44	1.27	4.69	0.79	2.01	8.80	0.79	1.79	6.02
46	0.21	0.65	3.29	0.32	1.01	4.13	0.28	0.75	2.94
47	0.47	1.95	8.40	0.74	2.83	13.49	0.66	2.14	10.54
48	0.33	0.79	2.72	0.36	1.13	4.74	0.2	0.67	2.62
49	0.69	1.64	5.92	0.48	2.46	15.60	0.41	2.02	8.72
50	0.19	0.61	2.37	0.25	0.74	3.39	0.16	0.54	2.98

where H_n is harmonic orders for n = 2,3,4,5, …, 50

Table 2.5: Values of individual current harmonics for wye line

H_n	Phase A			Phase B			Phase C		
	Min	Aver	Max	Min	Aver	Max	Min	Aver	Max
2	3.15	7.81	19.01	2.93	6.89	15.75	2.76	8.19	20.83
3	3.46	15.62	32.61	3.82	14.03	27.54	2.49	8.7	18.82
4	1.91	5.43	18.43	1.78	4.55	14.14	1.7	3.64	8.43
5	11.16	61.62	77.06	26.16	67.31	81.14	17.86	64.67	80.91
6	1.9	3.79	14.63	1.55	5.06	25.94	1.67	3.56	10.66
7	13.44	50.68	70.66	25.85	53.42	71.73	18.98	49.44	70.46
8	1.2	3.52	14.13	1.13	3.28	13.5	1.14	2.47	8.11
9	1.65	7.04	15.51	1.72	5.87	21.16	1.08	5.99	13.7
10	0.74	2.7	12.92	0.71	2.52	12.12	0.73	1.95	8.22
11	11.44	21.52	52.34	13.61	26.35	60.21	13.94	25.36	53.9
12	0.7	2.14	12.39	0.67	3.41	22.7	0.69	2.1	9.43
13	6.63	17.11	51.26	7.06	19.69	56.07	6.56	17.32	48.65
14	0.58	2.29	11.75	0.58	2.34	11.67	0.55	1.62	7.58
15	1.16	4.19	8.84	1.38	4.05	17.67	0.87	3.56	8.73
16	0.7	2.29	11.02	0.7	2.09	9.9	0.66	1.61	6.68
17	9.55	17.34	40.03	13.53	21.84	50.06	11.93	19.13	41.78
18	0.88	2.06	10.26	0.72	2.81	18.11	0.7	1.86	7.99
19	11.15	17.64	39.59	9.69	17.49	47.57	9.25	16.26	37.6
20	0.62	1.99	9.76	0.52	1.91	9.81	0.52	1.39	5.64
21	0.7	2.87	6.39	0.96	2.72	14.09	0.94	2.56	6.87
22	0.4	1.5	8.48	0.41	1.37	7.34	0.44	1.13	5.17
23	2.26	8.26	33.08	2.58	10.33	38.58	3.15	9.69	32.77
24	0.41	1.24	7.33	0.38	1.89	13.55	0.39	1.22	6.03
25	1.19	7.37	29.41	1.59	8.4	38.19	1.15	7.06	29.22
26	0.36	1.351	7.01	0.36	1.462	7.55	0.33	0.971	4.15
27	0.69	2.176	5.07	0.72	2.205	10.71	0.61	1.773	6.25
28	0.44	1.331	6.24	0.5	1.23	5.03	0.4	0.965	3.94
29	3.7	7.97	25.62	5.39	10.41	28.6	3.94	8.56	24.69
30	0.6	1.285	5	0.5	1.64	9.46	0.43	1.091	4.57
31	4.69	8.59	22.12	3.45	8.05	28.44	3.68	7.62	21.21
32	0.44	1.217	4.94	0.36	1.265	5.73	0.33	0.81	2.81
33	0.52	1.822	4.58	0.7	1.587	7.61	0.72	1.532	5.41
34	0.25	0.961	4.62	0.26	0.843	3.55	0.27	0.745	3.02
35	0.6	4.189	18.42	0.95	5.235	20.19	1.4	4.688	16.91
36	0.28	0.802	3.4	0.24	1.178	6.43	0.25	0.764	3.6
37	0.6	3.938	15.46	0.73	4.296	19.12	0.6	3.559	14.98
38	0.28	0.878	3.49	0.29	1.012	4.19	0.23	0.566	2.27
39	0.66	1.564	3.96	0.65	1.613	5.19	0.51	1.212	4.18
40	0.32	0.953	3.52	0.41	0.895	2.94	0.29	0.572	2.23
41	1.73	3.969	11.82	2.94	5.238	14.44	2.07	4.035	10.67
42	0.47	0.952	3.6	0.41	1.194	4.79	0.32	0.717	2.82
43	2.53	4.306	10.55	1.46	3.614	13.59	1.78	3.61	9.8
44	0.35	0.887	2.88	0.3	0.9	3.35	0.25	0.534	1.7
45	0.46	1.31	3.19	0.41	1.149	4.31	0.58	1.142	3.39
46	0.21	0.729	2.71	0.21	0.674	2.71	0.21	0.532	1.74
47	0.4	1.862	7.5	0.49	2.048	11.01	0.83	2.012	6.9
48	0.23	0.61	2.17	0.18	0.84	3.82	0.2	0.51	2.13
49	0.31	1.45	7.04	0.39	1.65	10.92	0.31	1.41	6.24
50	0.17	0.57	2.08	0.22	0.66	2.66	0.15	0.32	1.02

where H_n is harmonic orders for n = 2,3,4,5, …, 50

The average and maximum values of individual current harmonics for phase A, phase B & phase C are presented below in Table 2.6 & Table 2.7.

Table 2.6: Values of maximum individual current harmonics for delta line

H_n	Phase A Max	Phase B Max	Phase C Max	Phase Average	H_n	Phase A Max	Phase B Max	Phase C Max	Phase Average
2	22.99	23.87	34.09	26.98	27	9.25	15.68	8.42	11.12
3	22.65	42.43	33.79	32.96	28	4.81	6.52	5.84	5.72
4	11.68	14.66	10.15	12.16	29	21.99	31.86	23.30	25.72
5	78.26	85.79	80.41	81.49	30	6.76	10.33	4.55	7.21
6	13.79	25.16	11.86	16.94	31	17.77	36.86	21.48	25.37
7	71.54	79.22	76.2	75.65	32	4.09	6.62	5.53	5.41
8	0.00	0.00	0.00	0.00	33	6.56	13.64	7.90	9.37
9	17.28	18.98	15.10	17.12	34	4.01	5.20	4.67	4.63
10	7.01	12.27	11.07	10.12	35	16.67	25.28	18.68	20.21
11	59.18	65.39	58.47	61.01	36	5.32	7.91	4.07	5.77
12	12.06	21.80	9.49	14.45	37	12.34	28.64	16.64	19.21
13	49.39	62.47	54.11	55.32	38	3.17	4.74	4.39	4.10
14	7.02	11.43	11.29	9.91	39	5.36	11.47	7.15	7.99
15	14.79	18.58	12.60	15.32	40	3.83	4.59	3.74	4.05
16	5.88	10.01	8.38	8.09	41	11.86	18.82	14.54	15.07
17	36.35	54.75	37.90	43.00	42	3.81	5.84	3.39	4.35
18	10.74	16.37	7.58	11.56	43	8.61	21.64	12.11	14.12
19	32.47	54.43	33.70	40.20	44	2.82	4.06	3.18	3.35
20	6.45	9.83	9.14	8.47	45	4.69	8.80	6.02	6.50
21	11.82	17.35	10.40	13.19	46	3.29	4.13	2.94	3.45
22	5.55	8.05	7.06	6.89	47	8.40	13.49	10.54	10.81
23	27.96	41.79	29.66	33.14	48	2.72	4.74	2.62	3.36
24	8.10	12.69	5.07	8.62	49	5.92	15.60	8.72	10.08
25	23.77	46.06	26.08	31.97	50	2.37	3.39	2.98	2.91
26	5.07	8.48	7.40	6.98	THD	142.15	169.92	147.03	153.03

Individual current harmonic values exceeds IEEE 519 standard as given in Table 2.4. For the delta connected secondary output current total harmonic distortion $THD_{minimum}$ = 53.33%, $THD_{average}$ = 98.73%, and $THD_{maximum}$ = 153.03% which is by far beyound the standard minimum THD limit.

Table 2.7: Values of maximum individual current harmonics for wye line

H_n	Phase A Max	Phase B Max	Phase C Max	Phase Average	H_n	Phase A Max	Phase B Max	Phase C Max	Phase Average
2	19.01	15.75	20.83	18.53	27	5.07	10.71	6.28	7.35
3	32.61	27.54	18.82	26.32	28	6.24	5.03	3.94	5.07
4	18.43	14.14	8.43	13.67	29	25.62	28.60	24.69	26.30
5	77.06	81.14	80.91	79.70	30	5.00	9.46	4.57	6.34
6	14.63	25.94	10.66	17.08	31	22.12	28.44	21.21	23.92
7	70.66	71.73	70.46	70.95	32	4.94	5.73	2.81	4.49
8	14.13	13.5	8.11	11.91	33	4.58	7.61	5.41	5.87
9	15.51	21.16	13.7	16.79	34	4.62	3.55	3.02	3.73
10	12.92	12.12	8.22	11.09	35	18.42	20.19	16.91	18.51
11	52.34	60.21	53.9	55.48	36	3.40	6.43	3.60	4.48
12	12.39	22.7	9.43	14.84	37	15.46	19.12	14.98	16.52
13	51.26	56.07	48.65	51.99	38	3.49	4.19	2.27	3.32
14	11.75	11.67	7.58	10.33	39	3.96	5.19	4.18	4.44
15	8.84	17.67	8.73	11.75	40	3.52	2.94	2.23	2.90
16	11.02	9.9	6.68	9.20	41	11.82	14.44	10.67	12.31
17	40.03	50.06	41.78	43.96	42	3.60	4.79	2.82	3.74
18	10.26	18.11	7.99	12.12	43	10.55	13.59	9.80	11.31
19	39.59	47.57	37.6	41.59	44	2.88	3.35	1.70	2.64
20	9.76	9.81	5.64	8.40	45	3.19	4.31	3.39	3.63
21	6.39	14.09	6.87	9.12	46	2.71	2.71	1.74	2.39
22	8.48	7.34	5.17	7.00	47	7.50	11.01	6.90	8.47
23	33.08	38.58	32.77	34.81	48	2.71	3.82	2.13	2.89
24	7.33	13.55	6.03	8.97	49	7.04	10.92	6.24	8.07
25	29.41	38.19	29.22	32.27	50	2.08	2.66	1.02	1.92
26	7.01	7.55	4.15	6.24	THD	138.55	155.52	136.88	143.65

Individual current harmonic values exceeds IEEE 519 standard as given in Table 2.5. For wye connected secondary output current total harmonic distortion $THD_{minimum}$ = 60.00%, $THD_{average}$ = 101.65%, and $THD_{maximum}$ = 143.58% which is by far beyound the standard minimum THD limit.

2.4.3 Measured individual voltage harmonic spectrums of traction substation

Measured individual voltage harmonic spectrums of traction substation NS27 is given below in Figure 2.5 & Figure 2.6.

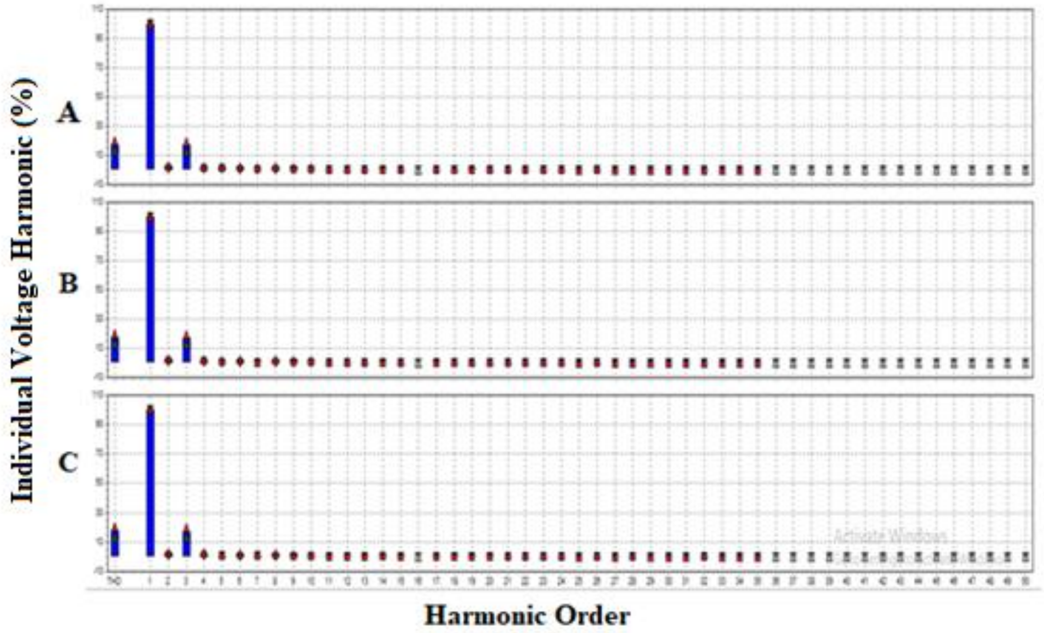

Figure 2.5: Individual voltage harmonic spectrums of wye line

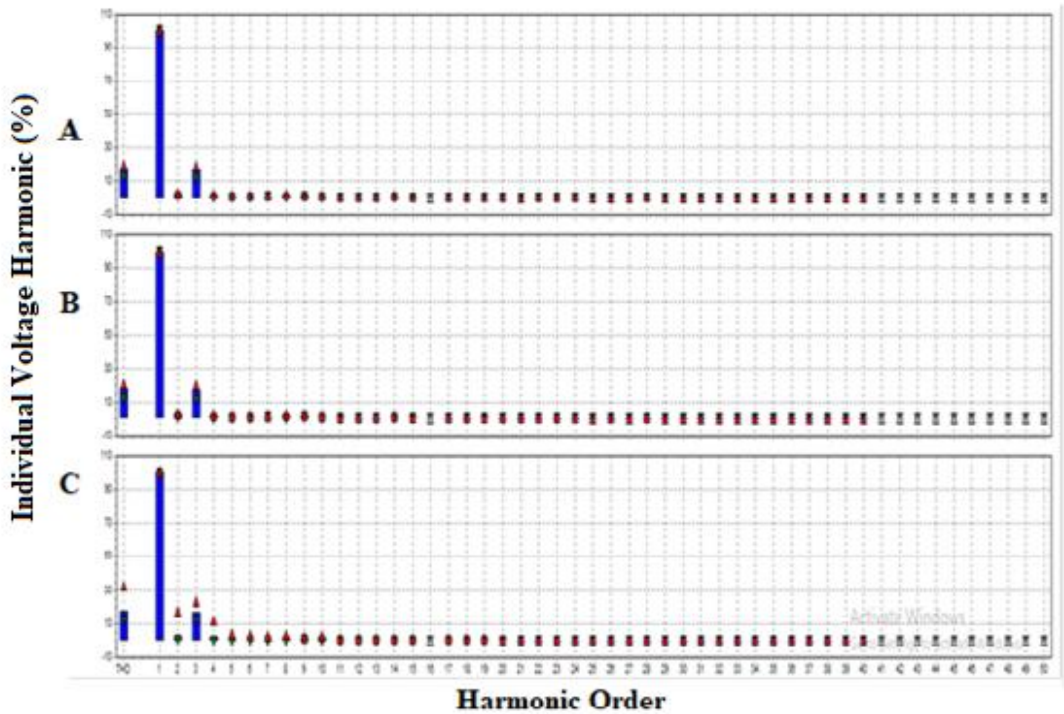

Figure 2.6: Individual voltage harmonic spectrums of delta line

2.4.4 Measured voltage harmonic values of traction substation

The measured percentage values of individual voltage harmonics of delta line of the traction substation given below in Table 2.8 & Table 2.9.

Table 2.8: Values of individual voltage harmonic for delta line

H_n	Phase A			Phase B			Phase C		
	Min	**Aver**	**Max**	**Min**	**Aver**	**Max**	**Min**	**Aver**	**Max**
2	0.39	1.96	3	0.4	1.95	3.02	0.41	2.34	17.68
3	11.52	17.09	19.56	11.69	17.2	19.67	11.69	17.32	23.4
4	0.15	1.64	2.46	0.15	1.65	2.47	0.15	1.88	12.29
5	0.27	0.72	1.25	0.27	0.69	1.42	0.29	0.7	4.52
6	0.09	0.73	1.09	0.09	0.72	1.1	0.09	0.8	3.53
7	0.45	0.736	1.24	0.43	0.733	1.5	0.11	0.635	2.91
8	0.04	1.251	2.04	0.05	1.257	2.05	0.04	1.288	3.37
9	0.52	1.33	1.78	0.52	1.343	1.8	0.53	1.326	2.04
10	0.04	1.004	1.63	0.05	1.013	1.65	0.04	1.054	2.77
11	0.06	0.313	0.97	0.24	0.413	0.64	0.12	0.395	1.37
12	0.12	0.313	0.77	0.12	0.311	0.78	0.12	0.347	1.48
13	0.05	0.275	0.56	0.13	0.326	0.47	0.09	0.331	1.01
14	0.05	0.67	1.12	0.05	0.671	1.13	0.05	0.689	1.62
15	0.11	0.45	0.75	0.09	0.467	0.78	0.12	0.48	1.52
16	0	0	0	0	0	0	0	0	0
17	0.05	0.293	0.5	0.08	0.348	0.57	0.1	0.38	1.39
18	0.05	0.31	0.82	0.04	0.319	0.83	0.05	0.357	1.35
19	0.05	0.341	0.77	0.07	0.363	0.86	0.08	0.469	1.17
20	0.04	0.323	0.6	0.04	0.322	0.6	0.04	0.335	0.97
21	0.05	0.211	0.33	0.08	0.237	0.38	0.06	0.241	0.81
22	0.05	0.272	0.46	0.04	0.274	0.47	0.04	0.292	0.98
23	0.04	0.199	0.2	0.05	0.215	0.37	0.04	0.199	0.82
24	0.08	0.164	0.22	0.09	0.163	0.47	0.08	0.176	0.79
25	0.03	0.127	0.37	0.03	0.13	0.21	0.04	0.131	0.7
26	0.02	0.205	0.35	0.02	0.209	0.36	0.02	0.214	0.75
27	0.03	0.138	0.22	0.03	0.131	0.2	0.03	0.146	0.77
28	0.03	0.192	0.37	0.02	0.2	0.38	0.02	0.207	0.81
29	0.02	0.136	0.22	0.02	0.168	0.29	0.02	0.112	0.75
30	0.02	0.126	0.21	0.03	0.143	0.24	0.03	0.157	0.77
31	0.01	0.131	0.21	0.02	0.899	0.36	0.02	0.16	0.79
32	0.01	0.149	0.27	0.01	0.158	0.18	0.01	0.157	0.75
33	0.04	0.085	0.13	0.03	0.08	0.29	0.03	0.113	0.72
34	0.01	0.127	0.26	0.01	0.133	0.12	0.01	0.142	0.76
35	0.01	0.092	0.15	0.01	0.097	0.28	0.01	0.1	0.73
36	0.02	0.078	0.14	0.02	0.081	0.17	0.02	0.086	0.76
37	0.01	0.076	0.13	0.01	0.079	0.13	0.02	0.078	0.71
38	0.01	0.13	0.22	0.01	0.136	0.12	0.01	0.134	0.74
39	0.03	0.085	0.1	0.03	0.078	0.23	0.03	0.073	0.7
40	0.01	0.086	0.19	0.01	0.089	0.2	0.01	0.099	0.72
41-50	0	0	0	0	0	0	0	0	0

From table 2.8, except the 3rd voltage harmonic, all individual voltage harmonic orders are less than 5% which satisfy the IEEE 519 standard. Because of the 3rd voltage harmonic order, the voltage THD exceeds the IEEE 519 standard for voltage total

2.5 Traction system load parameter and harmonic analysis

In this section, basics of system load parameters such as voltage, current, power and frequency analysis is done based on the result of measurement.

2.5.1 Power analysis at PCC

The total apparent power for a system with harmonic (distortion) power is expressed as following

$$S^2 = P^2 + Q^2 + D^2$$

where S = Apparent power of the system, P = Active Power of the system

Q = Reactive Power of the system, D = Distortion Power (Harmonic Power)

The maximum power measured at PCC which is selected from the data spreadsheet is given below in Table 2.9.

Table 2.9: Maximum power measured at PCC for delta line

	Phase A	Phase B	Phase C	
Function	Max	Max	Max	Total
Active Power (kW)	142.08	130.74	88.04	360.86
Reactive Power (kvar)	27.7	27.98	17.12	72.80
Harmonic Power (kVA)	196.88	198.2	131.84	526.92
Apparent Power (kVA)	240.02	241.66	159.2	640.88
Power Factor (PF)	0.86	0.83	0.83	0.84

The motor load can be determined by transforming the maximum power measured at PCC towards the motor terminal is given below in Table 2.10.

Table 2.10: Traction induction motor load

	Phase A	Phase B	Phase C	Phase
Function	Max	Max	Max	Max
Active Power (kW)	284.16	261.48	176.08	721.72
Reactive Power (kvar)	55.4	55.96	34.24	145.60
Harmonic Power (kVA)	393.76	396.4	263.68	1053.84
Apparent Power (kVA)	480.04	483.32	318.4	1281.76

The rated active power of one locomotive induction motor is 130kW. The maximum active power of the system measured is 721.72kW. The number of locomotives in the network during the field data measuring process for that specific time is six and determined as following.

Number of locomotives = $\frac{721.72}{130} = 5.55 \approx 6$, (six single locomotives were in the network during the time of data collection.

2.5.2 Supply frequency analysis at PCC

The variation of power supply frequency is in the allowable standard range from 49.271Hz to 50.455Hz as the standard is 50±1Hz.

2.5.3 Voltage analysis at PCC

From Table 2.8 individual voltage harmonics, except the value of 3^{rd} harmonic voltage, all voltage harmonic values are below the standard limit requirement of IEEE 519. Thus, voltage harmonics don't contribute significant power quality problems as compared to current harmonics within the traction network.

2.5.4 Current analysis at PCC

From data presented in Table 2.4 and Table 2.5, the values of individual current harmonics at PCC exceeds the IEEE 519 minimum standard limit for each harmonic orders. All current harmonics are present in the system at PCC, except delta connected line where 8^{th} harmonic order is found zero measured value. Therefore, current harmonics contribute significant power quality issues within the traction network.

For comparison purpose measured values of individual current harmonics and IEEE 519 standard harmonic minimum requirements for each harmonic orders are presented below in Table 2.11.

Table 2.11: Individual current harmonic measured values and theoretical IEEE 519 standard

H_n	Wye line per phase (%)			Delta line per phase (%)			Theoretically expected values for six pulse rectifier	Theoretically expected values for 12 pulse rectifier
	Min	Aver	Max	Min	Aver	Max		
2	2.95	7.63	18.53	3.97	10.47	26.98	0.0	0.0
3	3.26	12.78	26.32	3.89	13.49	32.96	0.0	0.0
4	1.80	4.54	13.67	2.25	4.79	12.16	0.0	0.0
5	18.39	64.53	79.70	12.96	61.96	81.49	x	0.0
6	1.71	4.14	17.08	1.99	4.58	16.94	0.0	0.0
7	19.42	51.18	70.95	11.55	48.79	75.65	x	0.0
8	1.16	3.09	11.91	0.00	0.00	0.00	0.0	0.0
9	1.48	6.30	16.79	1.88	7.59	17.12	0.0	0.0
10	0.73	2.39	11.09	0.88	2.59	10.12	0.0	0.0
11	13.00	24.41	55.48	8.59	22.21	61.01	x	x
12	0.69	2.55	14.84	0.77	2.86	14.45	0.0	0.0
13	6.75	18.04	51.99	3.90	15.03	55.32	x	x
14	0.57	2.08	10.33	0.61	2.32	9.91	0.0	0.0
15	1.14	3.93	11.75	1.40	4.61	15.32	0.0	0.0
16	0.69	2.00	9.20	0.76	2.16	8.09	0.0	0.0
17	11.67	19.44	43.96	7.65	17.69	43.00	x	0.0
18	0.77	2.24	12.12	0.87	2.59	11.56	0.0	0.0
19	10.03	17.13	41.59	6.47	16.29	40.20	x	0.0
20	0.55	1.76	8.40	0.68	2.04	8.47	0.0	0.0
21	0.87	2.72	9.12	1.07	3.91	13.19	0.0	0.0
22	0.42	1.33	7.00	0.47	1.60	6.89	0.0	0.0
23	2.66	9.43	34.81	2.44	9.10	33.14	x	x
24	0.39	1.45	8.97	0.48	1.82	8.62	0.0	0.0
25	1.31	7.61	32.27	1.34	7.29	31.97	x	x
29	4.34	8.98	26.30	3.52	8.54	25.72	x	0.0
31	3.94	8.09	23.92	3.01	8.00	25.37	x	0.0
48	0.20	0.65	2.71	0.30	0.86	3.36	0.0	0.0
49	0.34	1.50	8.07	0.53	2.04	10.08	x	x
50	0.18	0.52	1.92	0.20	0.63	2.91	0.0	0.0

where x denotes the existence of indicated harmonic orders in the six and twelve pulse diode rectifiers.

Theoretically, major current harmonic orders which are expected to exist in six pulse rectifier system are 5th, 7th, 11th, 13th , 17th, 19th, 23rd , 25th , 29th, 31st, 35th , 37th , 41st , 43rd , 47th and 49th. And also theoretically expected current harmonic orders to exist in 12 pulse rectifier system are 11th, 13th, 23rd, 25th, 35th, 37th, 47th & 49th and shown below in Table 2.12.

Table 2.12: Major current harmonic values and theoretical IEEE 519 standard

H_n	Wye line per phase			Delta line per phase			Theoretically expected values for six pulse rectifier	Theoretically expected values for 12 pulse rectifier
	Min	Aver	Max	Min	Aver	Max		
5	18.39	64.53	79.70	12.96	61.96	81.49	x	0.0
7	19.42	51.18	70.95	11.55	48.79	75.65	x	0.0
11	13.00	24.41	55.48	8.59	22.21	61.01	x	x
13	6.75	18.04	51.99	3.90	15.03	55.32	x	x
17	11.67	19.44	43.96	7.65	17.69	43.00	x	0.0
19	10.03	17.13	41.59	6.47	16.29	40.20	x	0.0
23	2.66	9.43	34.81	2.44	9.10	33.14	x	x
25	1.31	7.61	32.27	1.34	7.29	31.97	x	x
29	4.34	8.98	26.30	3.52	8.54	25.72	x	0.0
31	3.94	8.09	23.92	3.01	8.00	25.37	x	0.0
35	0.98	4.70	18.51	1.06	4.73	20.21	x	x
37	0.64	3.93	16.52	0.81	4.07	19.21	x	x
41	2.25	4.41	12.31	2.01	4.38	15.07	x	0.0
43	1.92	3.84	11.31	1.30	4.05	14.12	x	0.0
47	0.57	1.97	8.47	0.62	2.31	10.81	x	x
49	0.34	1.50	8.07	0.53	2.04	10.08	x	x
	Total number of harmonic orders exist						16	8

where x denotes the existence of indicated harmonic orders in the rectifiers

As it can be seen from Table 2.12, current harmonic orders 5th, 7th, 17th, 29th, 31st, 41th, and 43th cancel out or their amount would get reduced at the primary side of the rectifier transformer in case of twelve pulse rectifier.

The importance of this study is to show that the possibility to reduce or to remove 11th and 13th current harmonic orders that account the main percentage of current total harmonic distortion. The harmonic amount of 11th orders ranges from minimum value of 8.59% to maximum value of 61.01% and the harmonic amount of 13th order ranges from minimum value of 3.9% to maximum value of 55.32%.

By using the following procedures, the amperage values of 11th and 13th harmonic current value can be determined from individual harmonic distortion (IHD) formulation.

$$IHD_I\ (\%) = \frac{I_h}{I_1} * 100\% \quad \ldots\ldots (1)$$

where IHD_I is current individual harmonic distortion

THD_I is current total harmonic distortion

I_1 is the fundamental current

$I_h = I_2, I_3, I_4, \ldots I_{48}, I_{49}$ and I_{50} are individual current harmonics

The maximum load measured in the network is taken into consideration to design hybrid active power filter parameters. Three load scenarios are selected arbitrary from the spreadsheet table. The three load scenarios are load measurement equivalent to one traction motor, load measurement equivalent to three traction motors and load measurement equivalent to six traction motors. These three load scenarios are given below in Table 2.13.

Table 2.13: Selected three load scenarios

System Parameters	One traction motor	Three traction motors	Six traction motors
Vrms Ph-Ph	567.81	568.42	569.84
Current Arms	94.3	255.57	477.83
THD V (%)	21.65	21.75	27.26
THD A (%)	180.8	197.03	167.54
Peak Voltage	877.9	870.13	854.47
Peak Current	197.6	516.07	906.27
Fundamental Voltage	328.67	330.03	330.87
Fundamental Current	68.93	202.6	422.53
Active Power (kW) = P	66.62	194.32	368.58
Active Power Fundamental (kW) = P_1	66.42	192.10	353.32
Reactive Power (kvar) = Q	10.72	42.18	72.80
Harmonic Power (kVA) = D	127.24	330.86	526.92
Apparent Power (kVA) = S	143.94	384.88	640.88
Apparent Power Fundamental (kVA) = S_1	67.26	196.66	367.40
Power Factor	0.85	0.85	0.84

It is imperative to determine the values of 11th and 13th current harmonic distortion in ampere for each selected three load scenarios. Table 2.14 presents that the total harmonic distortion for that specific load category. Therefore, it is necessary to consider the percentage contribution of 11th and 13th current harmonics to the total harmonic distortion of the system as shown in Table 2.4.

Percentage contribution of 11th harmonic = $\frac{I_{11}}{I_2+I_3+I_4+I_5+\cdots+I_{48}+I_{49}+I_{50}}$ *100%

Percentage contribution of 11th harmonic = $\frac{0.6101}{8.7142}$ *100% = 7%

Percentage contribution of 13th harmonic = $\frac{I_{13}}{I_2+I_3+I_4+I_5+\cdots+I_{48}+I_{49}+I_{50}}$*100%

Percentage contribution of 13th harmonic = $\frac{0.5532}{8.7142}$ *100% = 6.35%

In other words, 11th and 13th orders contribute 7% and 6.35% of harmonics in the systems' current total harmonic distortion respectively. The ampere value of 11th and 13th current harmonic can be calculated using the individual harmonic distortion equation expressed in equation (1). The overall individual harmonic distortion values of 11th and 13th harmonic orders for the railway traction substation are 61.01% and 55.32% respectively.

By using equation (1), the amount 11th and 13th harmonic current value can be determined from individual harmonic distortion (IHD).

$$I_{11}\ (\%) = \frac{I_{11}}{I_1} * 100\% \text{ and } I_{13}\ (\%) = \frac{I_{13}}{I_1} * 100\%$$

a) For six traction motors,

$I_{11} = \frac{I_1 * I_{11}\ (\%)}{100\%}$ = 422.53*0.6101 = 257.79A

$I_{13} = \frac{I_1 * I_{13}\ (\%)}{100\%}$ = 422.53*0.5532 = 233.74A

b) For three traction motors,

$I_{11} = \frac{I_1 * I_{11}\ (\%)}{100\%}$ = 202.6*0.6101 = 123.61A

$I_{13} = \frac{I_1 * I_{13}\ (\%)}{100\%}$ = 202.6*0.5532 = 112.08A

c) For one traction motor,

$I_{11} = \frac{I_1 * I_{11}\ (\%)}{100\%}$ = 68.93*0.6101 = 42.05A

$I_{13} = \frac{I_1 * I_{13}\ (\%)}{100\%}$ = 68.93*0.5532 = 38.13A

Table 2.14: Percentage and ampere values of 11th and 13th current harmonic

System parameters	One traction motor	Three traction motors	Six traction motors
THD A (%)	180.8	197.03	167.54
Fundamental Current (A)	68.93	202.6	422.53
11th Current Harmonic (A) = I_{11}	42.05	123.60	257.79
13th Current Harmonic (A) = I_{13}	38.13	112.08	233.74
(11th +13th) Current Harmonic (A) = I_{11+13}	56.76	166.85	347.98

In similar procedure by using the percentage contribution of 11th and 13th harmonic orders, 11th and 13th harmonic powers are calculated and presented in the following Table 2.15.

Table 2.15: Calculated values of 11th and 13th harmonic powers

System parameters	One traction motor	Three traction motors	Six traction motors
Harmonic Power(kVA) = D	127.24	330.86	526.92
11th Current Harmonic (% contribution)	7.00	7.00	7.00
13th Current Harmonic (% contribution)	6.35	6.35	6.35
11th Harmonic Power (kVA) = D_{11}	8.90	23.16	36.88
13th Harmonic Power (kVA) = D_{13}	8.08	21.00	33.65
(11th +13th) Harmonic Power (kVA) = D_{11+13}	16.98	44.16	70.53

From Table 2.14 and Table 2.15 hybrid active power filter is designed to inject 11th and 13th order harmonic currents to reduce or if possible to eliminate 11th and 13th order harmonic powers specified in the table. The capacity of single tuned pass filter is designed considering the maximum system load for six traction motors in the network.

Chapter Three

Modeling of traction network and hybrid active power filter

3.1 Introduction

For modeling existing traction network, electrical parameters for the traction system components have been identified either from the technical design document or from the nameplate or from manufacturer catalogue or from manufacturer equipment test documents. The modeling is done based on the MATLAB/Simulink electrical block requirements.

The hybrid active power filter (HAPF) topology consists of a three phase three wire power circuit, nonlinear load based on uncontrolled rectifier, reference current estimator system based on the p-q theory, pulse generation system based on hysteresis current controlled technique, voltage source inverter connected in series with single tuned passive filters, and dc bus voltage controller system. This chapter presents the details of MATLAB/Simulink modeling and designing of hybrid active power filter components.

3.2 Modeling of existing traction network

3.2.1 Modeling of 15kV power source

The traction substation (NS27) is fed from 132/15kV, 2x25MVA GIS substation. But for our MATLAB/Simulink modeling purpose, 15kV MATLAB power supply block is used with its standard electrical parameters. The source supply can be represented as three phase voltage source with source resistance Rs and source inductance Ls.

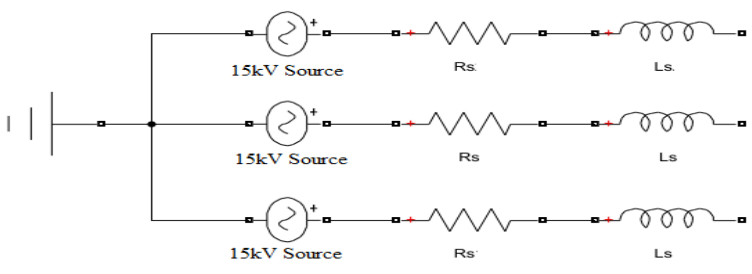

Figure 3.1: Circuit diagram of 15kV power source

The source supply configuration is wye grounded. The rms phase to phase voltage is 15kV at frequency of 50Hz. The value of source impedance Rs is 0.8929Ω and source inducatane Ls is 0.01658H.

3.2.2 Modeling of 15kV AC power cable

The most commonly used representation for AC power cable is π-circuit model. The length of this cable is 120meter. For modeling the power cable the following *RLC* paramenters are also obtained from cable manufacturer. The cable is a single core copper conductor XLPE insulated and PVC sheathed with a nominal cross sectional area of 240mm² and conductor resistance of R_1 = 0.0754Ω/km, capacitance of C_1 = 0.305μF/km and inductance of L_1 = 0.335mH/km. By considering R_1, C_1 and L_1 are positive sequence of 15kV power cable. The zero sequences of the cable can be calculated by multiple of 3.0 and zero sequence resistance R_0 = 0.2262 Ω/km , C_0 = 0.915 μF/km and L_0 = 1.005 mH/km.

a. Positive sequence of resistance (ohm) = 0.009048Ω
b. Zero sequence of resistance (ohm) = 0.027144Ω
c. Positive sequence of inductance (H) = 0.0402mH
d. Zero sequence of inductance (H) = 0.1206mH
e. Positive sequence of capacitance (F) = 0.0366mH
f. Zero sequence of capacitance (F) = 0.1098mH

The π-ciruit models for positive and zero sequences of AC power cable are represented as shown below in Figure 3.2.

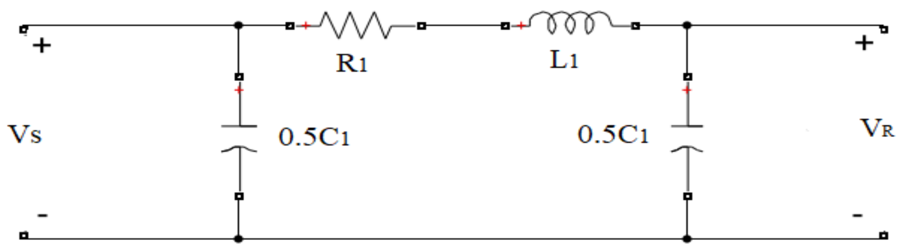

(a)

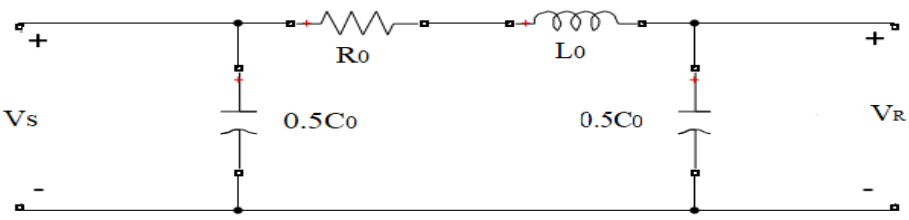

(b)

Figure 3.2: (a) Positive sequence π-ciruit model (b) Zero sequence π-circuit model

3.2.3 Modeling of dry type rectifier transformer

It is a three winding transformer with vector group D10/Dy11 and 2MVA, 15/0.59/0.59kV. The per unit impedance of the transformer taken from its nameplate, is 7.75%. The representation of dry type recifier transformer is given below in Figure 3.3.

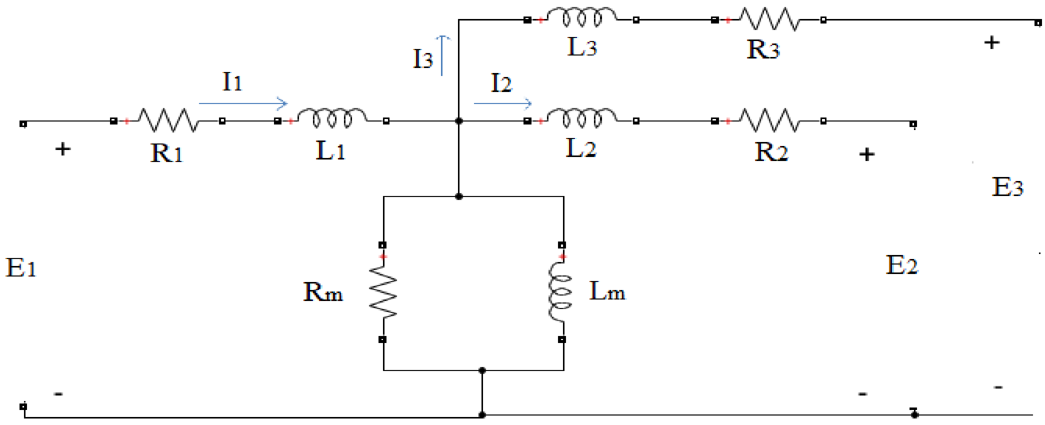

Figure 3.3: Circuit diagram of three winding transformer

The values of three winding transformer resistance, inductance, magnitization resistance and magnitization inductance are given as following:-

a. Winding 1 parameters resistance (R_1 in ohm) and inductance (L_1 in H) = 0.16875 & 0.021486 respectively
b. Winding 2 parameters resistance (R_2 in ohm) and inductance (L_2 in H) = 0.000299 & 0.0000432 respectively
c. Winding 3 parameters resistance (R_3 in ohm) and inductance (L_3 in H) = 0.0000398 & 0.0000099 respectively
d. Magnetization resistance (R_m in ohm) = 42187
e. Magnetization inductance (L_m in H) = 134.29
f. Inductance of Lo zero sequence flux path return (H) = 0.13428

The vector group of the transformer is D10/Dy11. The primary winding leads the secondary winding by phase displacement angle of 60^o and the secondary delta connected winding leads the secondary wye connected winding by phase displacement angle of 30^o.

For twelve pulse rectifier system the following mathematical expression obtained after Fourier series expansion for each of the secodary winding currents with the delta connected winding leading the wye connected winding by 30^o.

$I_2 = k*[\cos\theta + \frac{1}{5}\cos(5\theta) - \frac{1}{7}\cos(7\theta) - \frac{1}{11}\cos(11\theta) + \frac{1}{13}\cos(13\theta) + \frac{1}{17}\cos(17\theta) \ldots]$……..(3.1)

$I_3 = k*[\cos\theta - \frac{1}{5}\cos(5\theta) + \frac{1}{7}\cos(7\theta) - \frac{1}{11}\cos(11\theta) + \frac{1}{13}\cos(13\theta) - \frac{1}{17}\cos(17\theta) \ldots]$……..(3.2)

where k represents the mathematical constant value found in the process of Fourier series expression.

I_2 is the current flowing through wye connected winding 2

I_3 is the current flowing through delta connected winding 3

I_1 is the combined current flowing through primary winding 1 referred to the secondary side of the transformer.

$$I_1 = I_2 + I_3 \quad \ldots\ldots(3.3)$$

$$I_1 = 2k*[\cos\theta - \frac{1}{11}\cos(11\theta) + \frac{1}{13}\cos(13\theta) + \ldots] \quad \ldots\ldots(3.4)$$

The expression in equations (3.1) and (3.2) works for ideal and balanced system components and equipment. From equation (3.4), the dominant current harmonics in twelve pulse rectifier transformer are 11^{th} and 13^{th} order harmonics.

But in practical, as it is found from measurement, all harmonics are found in the traction network due to the non-ideal behavior of the system components.

3.2.4 Modeling of low voltage ac power cable

The cable is a single core copper conductor XLPE insulated and PVC sheathed with a nominal cross sectional area of 3x300mm² per phase and conductor resistance of R_1 = 0.0601Ω/km. The length of this cable is 30meter. The inductive and capacitive parameters of low voltage cables are negligible and are not considered in the modeling of the system. Therefore, the low voltage cable is represented by series resistance element only. The total resistance of this line is 0.001803Ω.

3.2.5 Modeling of diode rectifier

The rectifier circuit consists of two six pulse rectifier diode circuits which are connected in parallel to the system load. The parameter specification of twelve pulse traction substation rectifier is give below in Table 3.1.

Table 3.1: Parameter specification of twelve pulse diode rectifier

Twelve pulse traction substation rectifier		
1	Rated input current	2x1020A
2	Input phase	2x3phase
3	Rated input voltage	590VAC
4	Rated output voltage	750VDC
5	Rated output current	2500A
6	Rated output power	1875kW
7	Rated frequency	50Hz

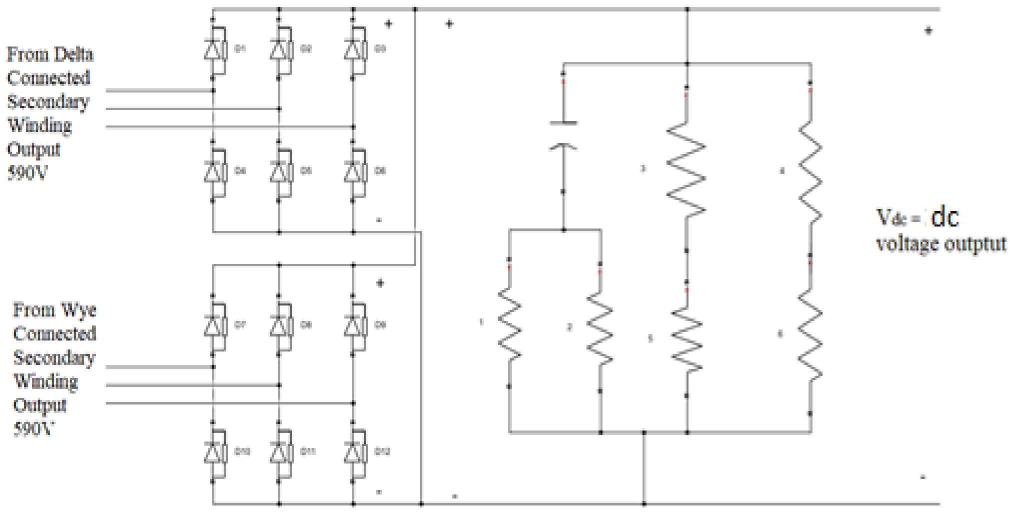

Figure 3.4: Circuit diagram of twelve pulse diode rectifier

The output of the rectifier is filtered using the *RC* filter circuit connected next to the rectifier to smooth the dc output ripple voltage and also to reduce the pulses along with the ripple voltage. The values for the capacitor is 6µF/2000V, resistances R1 & R2 are each 10Ω and resistances R3, R4, R5 & R6 are each 3.9kΩ taken from the technical documents.

3.2.6 Overhead catenary system (OCS)

One of the components of OCS is a copper conductor with a nominal cross sectional of 400mm² to deliver 750VAC power to the locomotive system through pantograph. The total length of the copper conductor connected to the traction substation named NS27 is 1.47km. The resistance of this conductor is 0.047Ω/km which is taken from the manufacture documents and the total resistance of the conductor is 0.06909Ω. The copper conductor is represented by a series resistance element for modeling purpose. Actually, the total effective resistance of this dc cable varies based on the position of the locomotive in the network. The total resistance value given above is the maximum value at the entry point of the locomotive towards NS27 traction substation network.

3.2.7 Traction inverter box

The traction inverter box mainly consists of insulated gate bipolar transistor IGBT inverter, line contactor, chopper power unit, logic control unit and filter unit. IGBT inverter is the main component which is important for interconnecting the DC power network with AC induction motor systems. The role of traction inverter box is to invert DC voltage to variable voltage variable frequency (VVVF) three phase AC voltages. The output of the inverter is filtered out through inductor capacitor circuit to preserve the sinusoidal wave of the output.

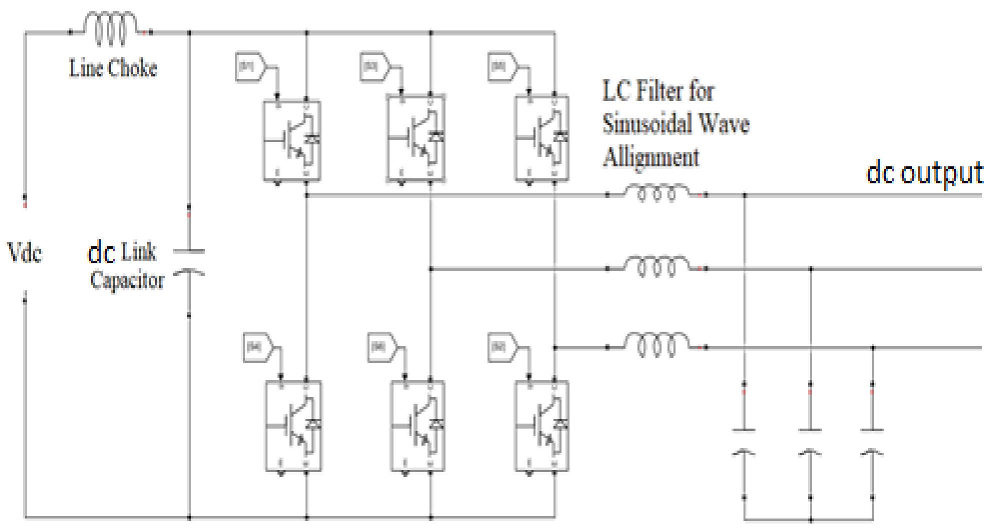

Figure 3.5: Circuit diagram of IGBT/Diode inverter

The parameter specification of inverter is given below in Table 3.2

Table 3.2: Parameter specification of IGBT inverter

Parameter specification of IGBT Inverter		
1	Rated input voltage	750VDC
2	Rated output voltage	3x500VAC
3	Rated output power	130kW
4	Control System	PWM

3.2.8 Pulse width modulation techniques

Pulse width modulation (PWM) technique is used for traction motor IGBT inverter gate signal control. It is most efficient and used to control the ON and OFF time of switching devices in predetermined condition. A designed fixed dc voltage is given to the IGBT inverter input and the power switches are controlled by the PWM control signal to modulate input dc voltage to required ac voltage. Since frequency of operation is inversely dependent upon inverter size, thus reduces the inverter size and increases the switching frequency. MATLAB/Simulink PWM model and input waveform is shown in Figure 3.6.

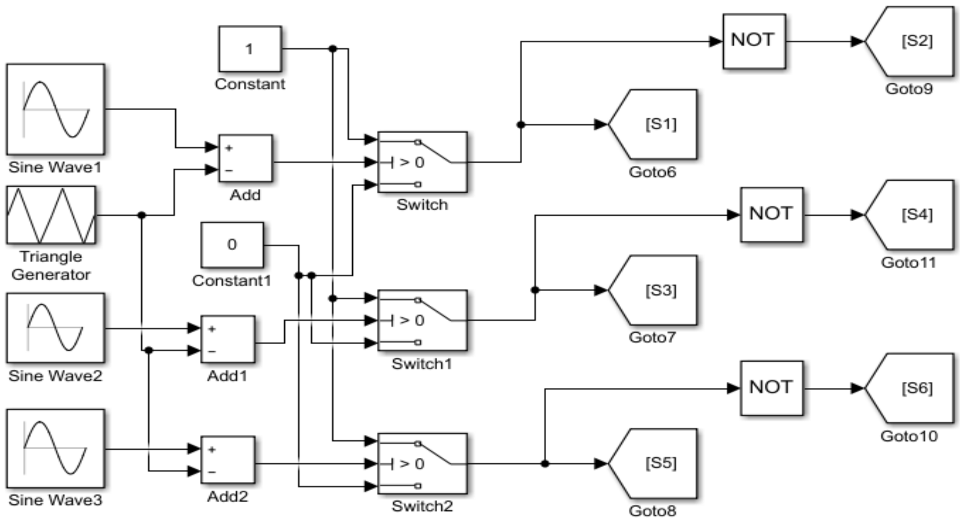

Figure 3.6: MATLAB/Simulink model representation of pulse width modulation

3.2.9 Traction motor

The traction motor is three phase squirrel cage induction motor with the following details.

Table 3.3: Parameter specification of traction motor

Traction motor specification		
1	Rated power	130kW
2	Number of phases	3
3	Number of poles	6 (3 pairs)
4	Rated voltage	3x500VAC
5	Rated current	215A
6	Rated frequency	91Hz
7	Rated rotational speed	1800 r/mim or 188.5 rad per second
8	Maximum rotational speed	4377 r/min or 458.36 rad per second
9	Power Factor	0.74

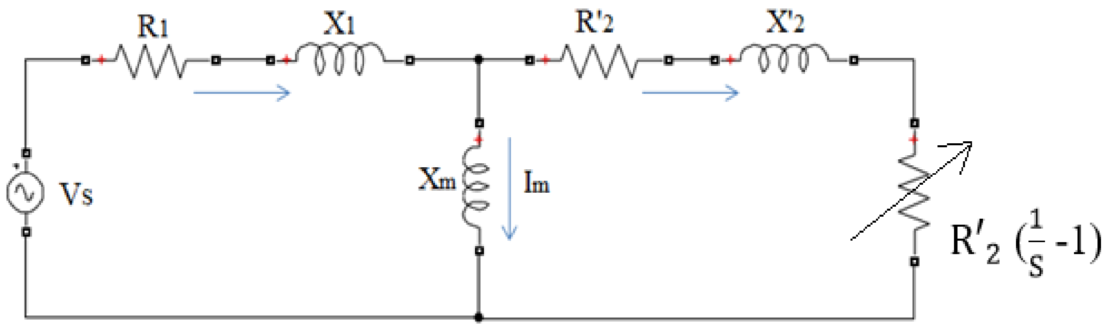

Figure 3.7: Equivalent circuit diagram of induction motor

where R_1 is stator resistance per phase

X_1 is leakage reactance per phase

R'_2 is rotor resistance transferred to the stator side

X'_2 is leakage reactance transferred to the stator side

R'_L is the mechanical power production of the motor

where $R'_L = R'_2\,(\frac{1}{S}-1)$

Induction motor parameters taken from technical documents are given as following.

a) Stator resistance R_1 = 0.5968Ω, Stator Inductance X_1 = 0.0003495H
b) Rotor resistance R'_2 = 0.6258Ω, Rotor Inductance X'_2 = 0.005473H
c) Mutual Inductance X_m = 0.0354H
d) Inertia J = 0.05J(kg.m²)
e) Friction factor = 0.005879
f) Pole pairs = 3 (It is a six pole induction motor)

For any motor load application, it is imperative to know the torque speed characteristic of the induction motor. Consider a three phase squirrel cage induction motor whose stator has three windings displaced in space by 120°. When they are excited with currents that are displaced in time by 120°, a rotating magnetic field rotating at a speed called synchronous speed Ns is set up. The synchronous speed, Ns is given by

$$N_S = \frac{120*f}{P} \quad \text{……………………………………………………………… (3.5)}$$

where f is the frequency of the currents (rated frequency of the motor is 91Hz), P is the number of poles & the synchronous speed is in rpm (revolution per minute)

Thus, $N_S = \frac{120*91}{6} =$ 1820rpm or 190.59 rad per second.

If the rotor of the induction motor rotates at speed, N_r, then the slip, s is defined by

$$s = \frac{N_S - N_r}{N_S} = \frac{190.59 - N_r}{190.59} \text{ rad/sec} \quad \text{……………………………………… (3.6)}$$

The torque (T_m) developed by the induction motor is given by

$$T_m = \frac{3*(I_2)^2*R\prime_2}{s*w_S} = \frac{3{V_S}^2 R\prime_2/s}{w_S[(R_1 + R\prime_2/s)^2 + (X_1 + X\prime_2)^2]} \quad \text{……………..……. (3.7)}$$

where $w_S = 2\pi N_S$, is the synchronous speed in rad/sec, V_S is the voltage applied to the stator

$$T_m = \frac{3*(I_2)^2*0.6258}{2\pi(190.59 - N_r)} = \frac{0.2987975*I_2*I_2}{190.59 - N_r} \quad \text{………………..………….. (3.8)}$$

The torque expression in equation (3.8) is a function of rotor speed and rotor current.

3.2.10 Auxiliary power supply system

Auxiliary power supply system includes auxiliary inverter and batteries. Auxiliary inverter supplies 380VAC and 24VAC to vehicles and charges the batteries. When high input voltage of 750VDC is not available (auxiliary inverter not working) for vehicles, it also supplies vehicles with control power and emergency power supply. The total auxiliary power requirement is 34kW, 380VAC & 50Hz [35]. Auxiliary inverter mainly consists of line contactor group, IGBT inverter power unit, 3-phase 380VAC (with N line for supplying 220VAC) which will be supplied for auxiliary equipment of vehicles. Similarly, it will also convert 750VDC into 24VDC to be supplied as control power supply for vehicle control systems and all equipment.

The complete railway traction network model is presented in three sections for simplicity of demonstration. A railway traction network consists of the following sections which are interconnected to each other.

a. Traction substation**:** This includes 15kV power source, 15kV power cable, dry type three winding transformer (delta-delta-wye), low voltage power cable, twelve pulse diode rectifier and others.

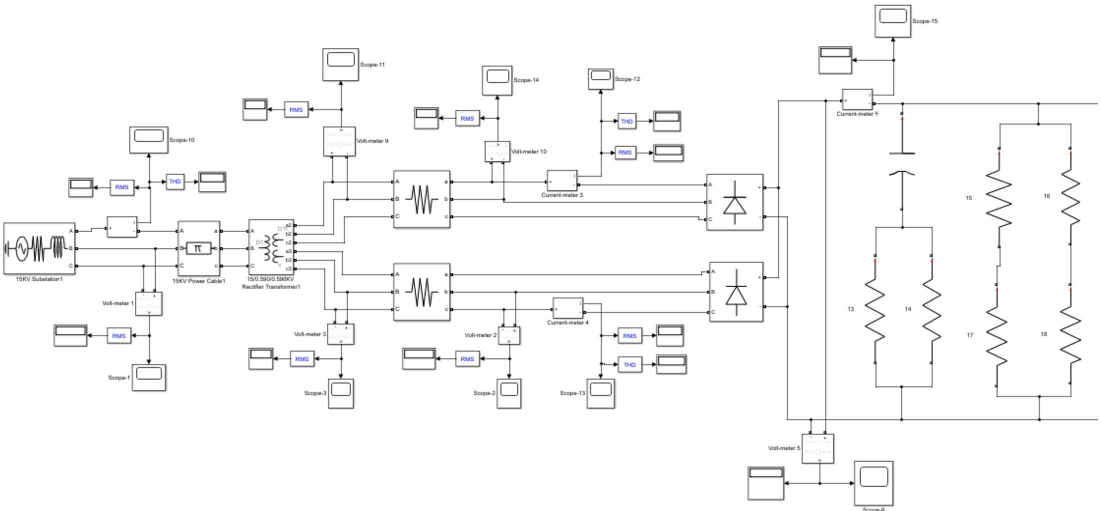

Figure 3.8: MATLAB/Simulink model representation of traction substation

b. Transmission system: The DC overhead conductor or catenary line, the railway (DC power negative line) and the signal control system.

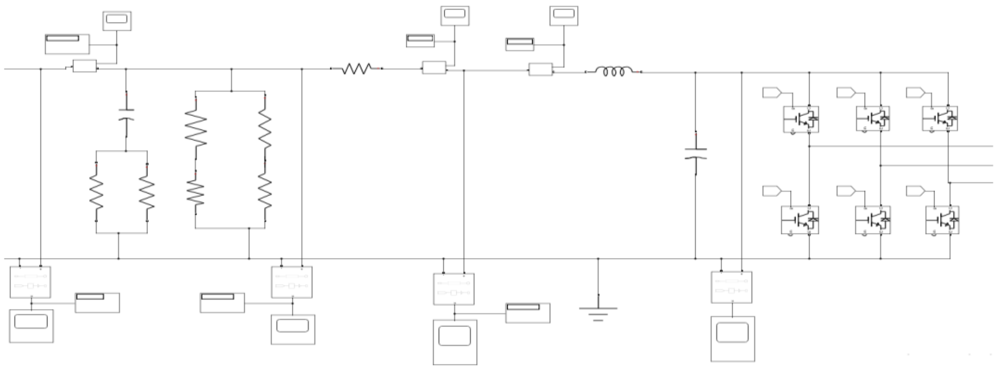

Figure 3.9: MATLAB/Simulink model representation of overhead catenary with rectifier output and inverter input

c. The train or locomotive systems: This is a moving system that mainly consists of the IGBT inverter, the three phase squirrel cage induction motor, auxiliary systems, chopper module, others.

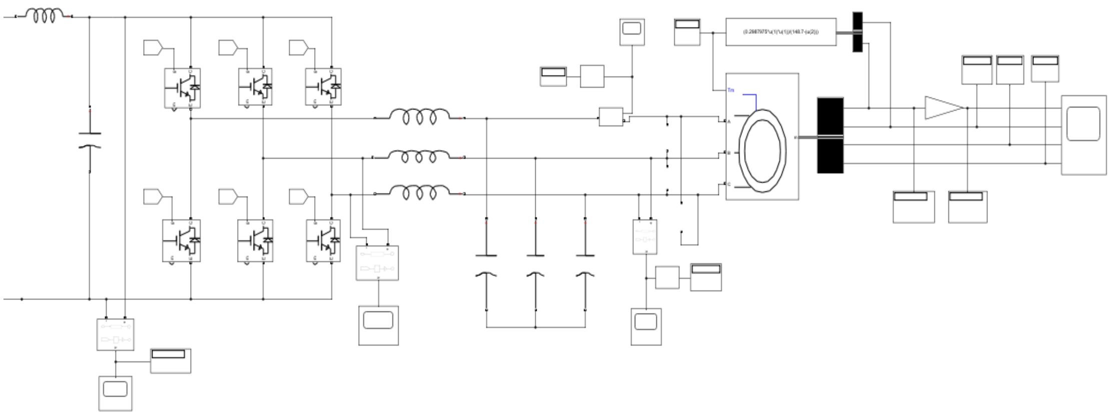

Figure 3.10: MATLAB/Simulink model representation of traction motor and traction inverter

3.3 Designing and modeling of hybrid active power filter

The components of hybrid active power filters are active power and passive filters.

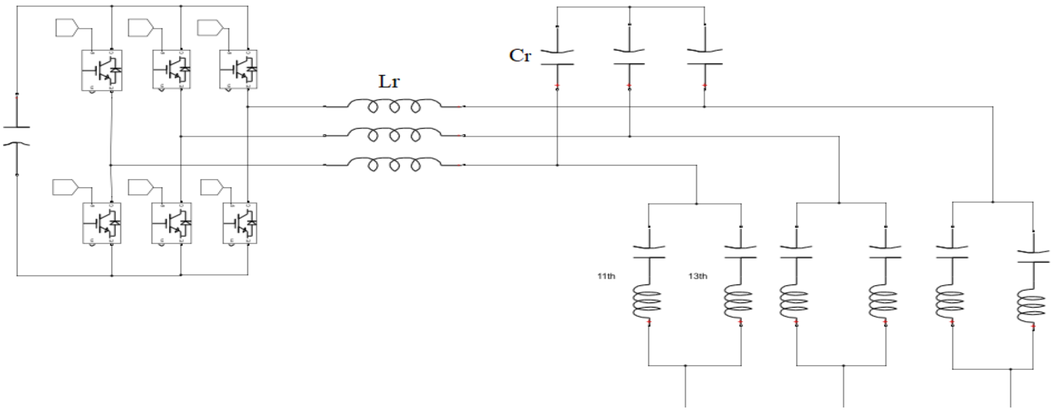

Figure 3.11: Circuit diagram of three phase hybrid active power filter

The active power filter component is IGBT inverter and it is controlled by PWM technique as presented in section 3.2.8.

3.3.1 Principle of operation of hybrid active power filter

The main aim of hybrid combination is to reduce the rating requirements of the active filter component. Lower ratings are achieved by reducing systematically some components of harmonic voltage and or current in the active element [19].

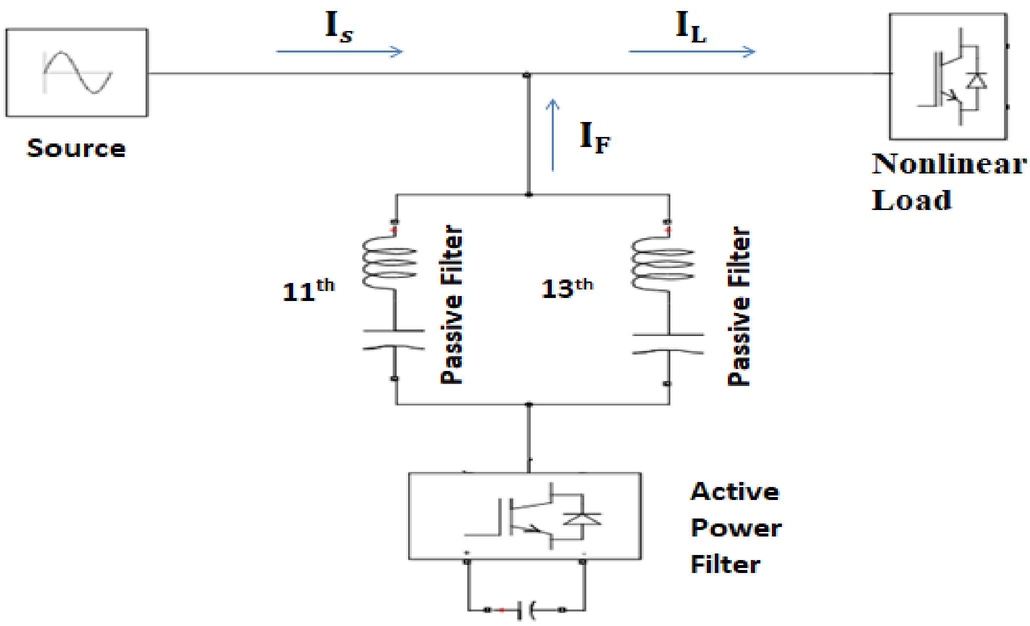

Figure 3.12: Block diagram representation of hybrid series active power filter

The operation principle of the proposed HAPF topology is illustrated in Fig. 3.12. It consists of an active power filter connected in series with passive filters. The two parallel single tuned passive filters are designed to compensate 11th and 13th harmonic currents. The active power filter generates compensation current (I_F) equal to 11th and 13th harmonic currents but in opposite phase and injects into the point of common coupling (PCC) through the passive filters. Therefore, source current (I_S) is desired to be relatively sinusoidal and in phase with the source voltage (V_S) to yield maximum power factor.

The hybrid active power filter topology presented is implemented with a three phase pulse width modulation (PWM) voltage source inverter and connected in series to the passive filter. The active power filter acts as a controlled voltage source for generating the harmonic currents to flow through the hybrid scheme to achieve the intended compensation. In other words, because the active power filter is connected in series to the passive filter, it imposes a voltage signal that forces the circulation of harmonic currents through the passive filters, improving the most of the draw backs of passive filter compensation characteristics, independently of the variation in selected resonant frequency or filter parameters. The compensation of specific current harmonics leads to power factor improvement which is explained below with the help of single phase equivalent circuits shown in Figure 3.13.

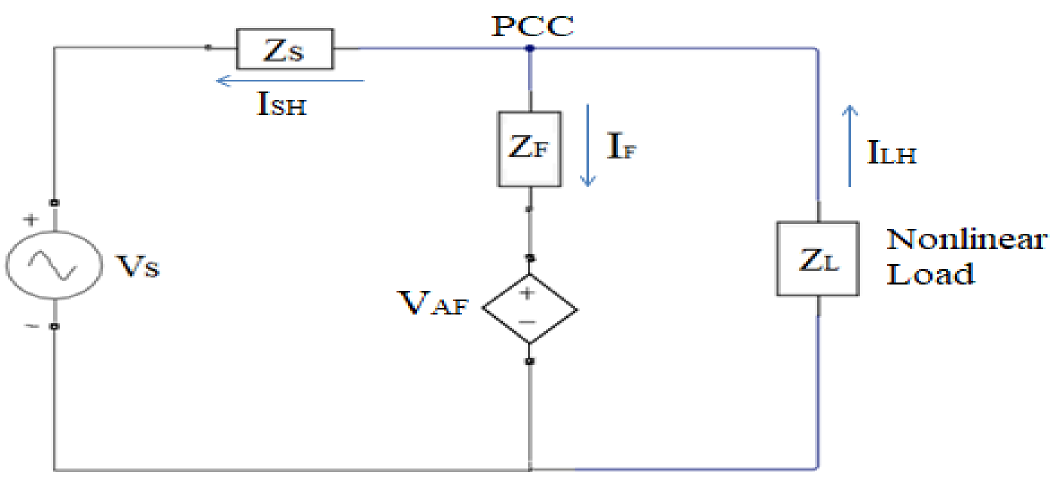

Figure 3.13: Single phase equivalent circuit diagram of hybrid active power filter to reduce harmonic currents

3.3.2 Current harmonic compensation

In Figure 4.2 representing single phase harmonic equivalent circuit of the power system, the source voltage is modeled by V_S which is in series with the source impedance (Z_S) of the power system, the nonlinear load is connected in parallel with the hybrid scheme and is modeled as a source for harmonic I_{LH} [9]. The nonlinear load in this specific study is combination of traction induction motor, diode rectifier and IGBT inverter with capacitors and inductors connected on the output and input of the system.

The series active power filter behaves as a damping resistor which can eliminate resonance between the parallel passive filter and the source impedance. It also prevents flowing of harmonic currents to the power source by presenting zero impedance at the selected frequency of passive filters and a high resistance K (also called the active power filter gain) at the power source or load harmonics. Thus, the series active power filter can be modeled by the active power filter gain K, and its output reference voltage [16].

$$V_{AF} = K*I_{SH} \quad \text{(3.9)}$$

where I_{SH} is the harmonic current flowing towards the power source, K is the active power filter gain and V_{AF} is the harmonic voltage source. At the PCC, the following equations can be obtained by applying Kirchhoff's voltage and current law:

$$V_S - Z_S * I_{SH} + Z_F * I_F - V_{AF} = 0 \quad \text{(3.10)}$$

$$I_{LH} = I_{SH} + I_F \quad \text{(3.11)}$$

By solving for I_F from equation 4.3 and substituting in equation 4.2, the harmonic current of the power source can be expressed as:

$$I_{SH} = \frac{Z_F}{K+Z_F+Z_S} I_{LH} + \frac{V_S}{K+Z_F+Z_S} \quad \text{(3.12)}$$

where Z_S is power source equivalent impedance and Z_F is passive filter equivalent impedance.

Based on equation (3.12), when K is large enough greater than Z_S and Z_F, the power source harmonic currents will be equal to zero (I_{SH}=0). In this case, the source impedance (Z_S) has no impact on the parallel passive filter characteristic, and the power source current harmonics will completely be eliminated.

Thus, $\frac{V_S}{K+Z_F+Z_S} \approx 0$, for $K >> Z_F$ & $K >> Z_S$, And the ratio between the power source harmonic current and the load harmonic current is:

$$\frac{I_{SH}}{I_{LH}} = \frac{Z_F}{K+Z_F+Z_S} \quad \text{……………………..………………….…… (3.13)}$$

When the series active power filter is used along with the passive filter, since the series active power filter behaves as a damping resistor, there is no resonance in the system. If the power source harmonic current (I_{SH}=0), the ac mains voltage will be purely sinusoidal, therefore, the ratio of between the harmonic component of the ac line current (I_{SH}) to the harmonic component of the nonlinear load current (I_{LH}) can be; considered as attenuation factor, γ:

$$\gamma = \frac{I_{SH}}{I_{LH}} = \frac{Z_F}{K+Z_F+Z_S} \quad \text{…….…………………………….……… (3.14)}$$

Above equations shows that the attenuation factor defining the filtering characteristic of the hybrid topology (I_{SH}/I_{LH}), which depends on the value of the passive filter equivalent impedance Z_F, the active power filter gain K, and the source impedance Z_S. To improve the attenuation factor for better compensation performance, K must be increased because Z_F and Z_S are constant. Current harmonic compensation is achieved by reducing the impedance of the hybrid scheme and thus, forcing the current harmonic to follow the low impedance trajectory instead of circulating through the power system. To accomplish this task, the hybrid filter must present a wide bandwidth and very small impedance at the frequency of the harmonics that are being compensated. The hybrid active power filter bandwidth depends on the passive filter parameters and on the active power filter gain [16].

Large values of K improve the hybrid scheme filter compensation performance by reducing the equivalent impedance for different values of frequency, by increasing the hybrid active power filter bandwidth. Thus, large values of K improve hybrid active power filter compensation performance.

The total harmonic distortion (THD) of the line current depends on the value of K,

Solving for I_{SH} using equation (3.14),

$$I_{SH} = \frac{Z_F}{K+Z_F+Z_S} * I_{LH} \quad \text{………………………………………………… (3.15)}$$

$$\mathrm{THD_I}\ (\%) = \frac{\sqrt{\sum_{h=2}^{N} \mathrm{I_{sh}^2}}}{\mathrm{I_{S1}}} * 100\% = \frac{\sqrt{\sum_{h=2}^{N} [\frac{\mathrm{Z_F}}{\mathrm{K+Z_F+Z_S}} * \mathrm{I_{Lh}})]^2}}{\mathrm{I_{S1}}} \quad \ldots\ldots\ldots\ldots\ldots (3.16)$$

From equation (3.15), the total harmonic distortion of the line current decreases if K increases and better hybrid active power filter compensation is obtained for larger values of active power filter gain.

3.3.3 Power factor compensation

Power factor is not only affected by the phase displacement between voltage and current waveforms. The existence of non-fundamental apparent power also affects the power factor. Power factor will decrease in presence of harmonics or non-fundamental apparent power also called distortion power. For power systems with harmonics, power factor is composed of displacement power factor and distortion power factor.

$$\text{Power Factor} = \frac{\text{Active Power}}{\text{Apparent Power}} = \frac{\mathrm{P}}{\mathrm{S}} = \frac{\mathrm{P}}{\mathrm{S_1}} * \frac{\mathrm{S_1}}{\mathrm{S}} \quad \ldots\ldots\ldots\ldots\ldots\ldots\ldots (3.17)$$

Power Factor = Displacement Power Factor * Distortion Power Factor

where $\frac{P}{S_1}$ is Displacement Power Factor, $\frac{S_1}{S}$ is Distortion Power Factor and

S_1 is a fundamental apparent power and S is apparent power

$$\text{Power Factor} = \frac{\mathrm{P}}{\mathrm{S_1}} * \frac{1}{\left(\sqrt{1+\mathrm{THD_I^2}}\right)\left(\sqrt{1+\mathrm{THD_V^2}}\right)} \quad \ldots\ldots\ldots\ldots\ldots\ldots\ldots (3.18)$$

where THD_I is current total harmonic distortion and

THD_V is voltage total harmonic distortion

Thus, Displacement Power Factor = $\frac{P}{S_1}$

Distortion Power Factor = $\frac{1}{\left(\sqrt{1+THD_I^2}\right)\left(\sqrt{1+THD_V^2}\right)}$

The power factor correction is achieved by the harmonic power compensation of hybrid series active power filter expressed by applying Kirchhoff’s voltage at PCC.

$$V_{AF,AC} - Z_F * I_F - V_{PCC} = 0 \quad (3.19)$$

$$I_F = \frac{V_{AF,AC} - V_{PCC}}{Z_F} \quad (3.20)$$

$$Z_F = X_R = X_C + X_L \quad (3.21)$$

where V_{PCC} is the source voltage at the point of common coupling PCC

$V_{AF,AC}$ is the ac output voltage of harmonic source inverter

X_R is the resultant reactance of the passive filter

X_C is the capacitance of capacitor (C) in the filter

X_L is the inductance of inductor (L) in the filter

$$D = \frac{(V_{AF,AC} - V_{PCC})^2}{X_R} \quad (3.22)$$

where D is harmonic power corresponding to the selected compensation currents

Tuning frequency for harmonic filter

$$X_C = h^2 * X_L = h^2 * (X_R - X_C) = \frac{h^2 * X_R}{h^2 + 1} \quad (3.23)$$

$$C = \frac{1}{2\pi * f * X_C} \text{ and } L = \frac{X_C}{2\pi * f * h^2} \quad (3.24)$$

From Table 2.14 and Table 2.15, the maximum load conditions for the 11^{th} and 13^{th} current harmonic and harmonic or distortion power are considered. The values of 11^{th} & 13^{th} orders are determined and given in Table 3.4.

Table 3.4: Calculated values of 11^{th} & 13^{th} harmonic currents and powers

System parameters	Six traction motors
11^{th} Current Harmonic (A) = I_{11}	257.79
13^{th} Current Harmonic (A) = I_{13}	233.74
(11^{th} +13^{th}) Current Harmonic (A) = I_{11+13}	347.98
11^{th} Harmonic Power (kVA) = D_{11}	36.88
13^{th} Harmonic Power (kVA) = D_{13}	33.65
(11^{th} +13^{th}) Harmonic Power (kVA) = D_{11+13}	70.53
Vrms Phase-Phase at PCC (V) = V_{PCC}	569.84

The hybrid active power filter can inject compensation harmonic power to the network at PCC only when $V_{AF,AC} > V_{PCC}$.

$$D_{11+13} = \sqrt{3} * (V_{AF,AC} - V_{PCC}) * I_{11+13} \quad \text{(3.25)}$$

$$V_{AF,AC} = V_{PCC} + \frac{D_{11+13}}{\sqrt{3}\, I_{11+13}} = 569.84 + \frac{23.51*1000}{347.98\sqrt{3}} = 569.84 + 39.00 = 608.84V$$

For tuning the frequency of filters, the capacitor and inductor values are calculated.

a. Tuning 11th order single tuned passive filter

$$D_{11} = X_{R,11} * I_{11}^2 \Rightarrow X_{R,11} = \frac{D_{11}}{I_{11}^2} = \frac{12.29*1000}{257.79*257.79} = 0.185\Omega$$

$$X_{C,h} = \frac{h^2 * X_{R,h}}{h^2+1} \Rightarrow X_{C,11} = \frac{11^2 * X_{R,11}}{11^2+1} = \frac{121*0.185}{122} = 0.1835\Omega$$

$$C_{11} = \frac{1}{2\pi * f * X_{C,11}} = \frac{1}{2\pi*50*0.1835} = 17.347mF$$

$$L_{11} = \frac{X_{C,11}}{2\pi * f * h^2} = \frac{0.1835}{2\pi*50*11*11} = 4.827\mu H$$

b. Tuning 13th order single tuned passive filter

$$D_{13} = X_{R,13} * I_{13}^2 \Rightarrow X_{R,13} = \frac{D_{13}}{I_{13}^2} = \frac{11.22*1000}{233.74*233.74} = 0.2054\Omega$$

$$X_{C,13} = \frac{13^2 * X_{R,13}}{13^2+1} = \frac{13*13*0.2054}{170} = 0.2042\Omega$$

$$C_{13} = \frac{1}{2\pi * f * X_{C,13}} = \frac{1}{2\pi*50*0.2042} = 15.588mF$$

$$L_{13} = \frac{X_{C,13}}{2\pi * f * 13^2} = \frac{0.2054}{2\pi*50*13*13} = 3.869\mu H$$

3.4 Combined traction network model

MATLAB/Simulink traction model without hybrid active power is done in section 3.2. Hybrid active power filter design is also done in section 3.3. In this section, the combined traction network with hybrid active power filter is presented. For the effective operation of combined traction network system requirement are also included.

3.4.1 Traction network model with hybrid active power filter

The combined traction network with hybrid active power filter is shown below in Figure 3.14.

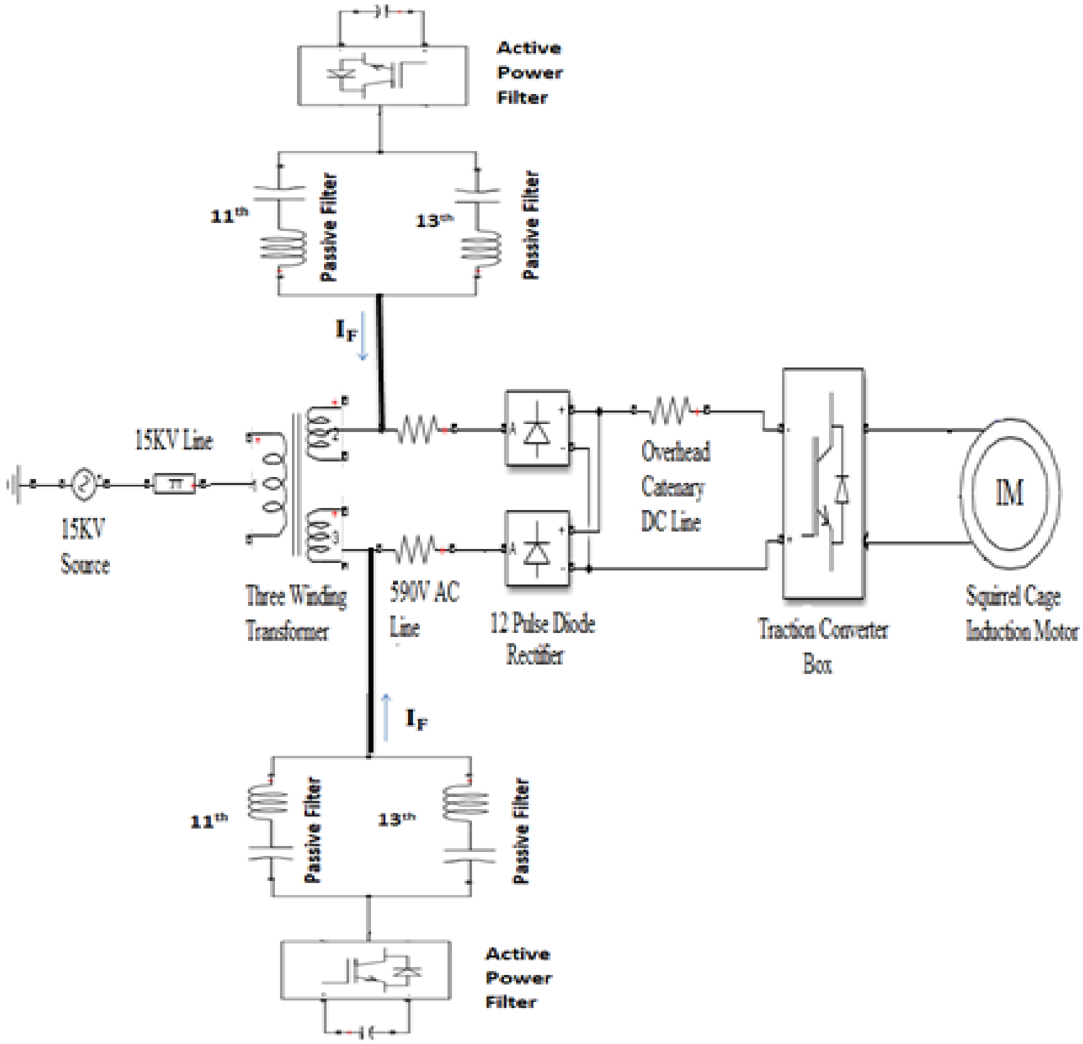

Figure 3.14: Single phase line diagram representation of railway traction network with hybrid active power filter

Three phase circuit diagram of single railway traction network with hybrid active power filter is given below in Figure 3.15.

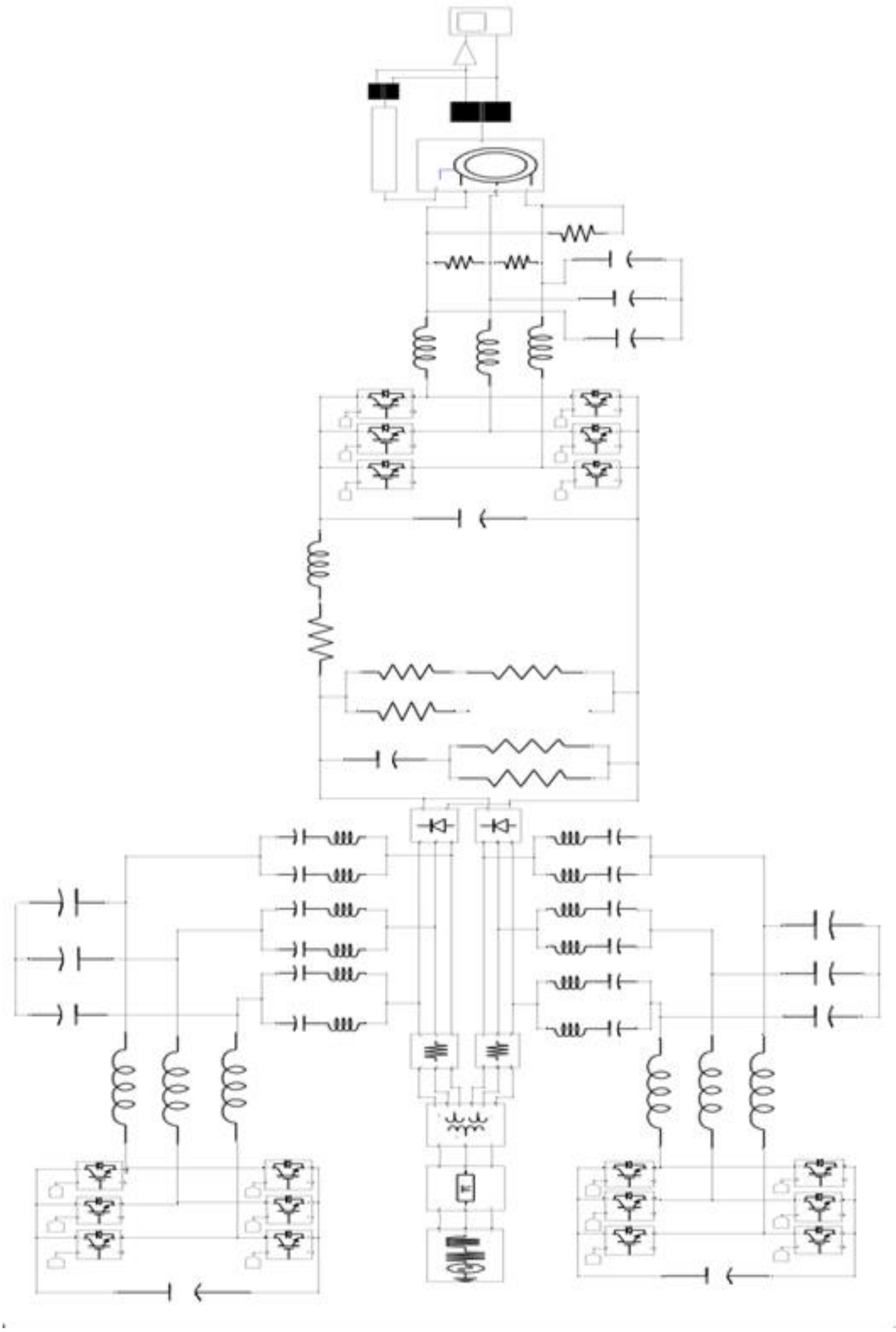

Figure 3.15: Three phase circuit diagram representation of single railway traction network with hybrid active power filter

3.4.2 The instantaneous P-Q theory in three phase three wire systems

The instantaneous p-q theory is implemented to generate the compensation current. It is the communication link between the traction network and the hybrid active power filter.

The traction substation system under the study is a three phase three wire system with instantaneous phase voltages V_a, V_b and V_c and instantaneous line currents i_a, i_b and i_c. Since zero sequence power in three phase three wire system is always zero, thus, zero sequence components of reactive and active power will not be included in the power mathematical equations [20].

The instantaneous active and reactive power p-q theory is based on a set of instantaneous values of active and reactive powers defined in the time domain. This theory is very efficient and flexible in designing controllers for power conditioners based on power electronics devices [18]. The p-q theory consists of an algebraic transformation (Clarke transformation) of three phase voltages and currents in the a-b-c coordinates. From this coordinates two orthogonal rotating vectors α and β are generated in the α-β-0 coordinates. These rotating vectors enable the calculation of the p-q instantaneous power components with simper mathematical steps. The p-q theory compensates the harmonic currents, corrects the power factor, and compensates dynamically and instantaneously [23]. The p-q theory is also balances the values of the currents supplied by the source to the load. The procedure for compensator current calculation is illustrated below in Figure 3.16.

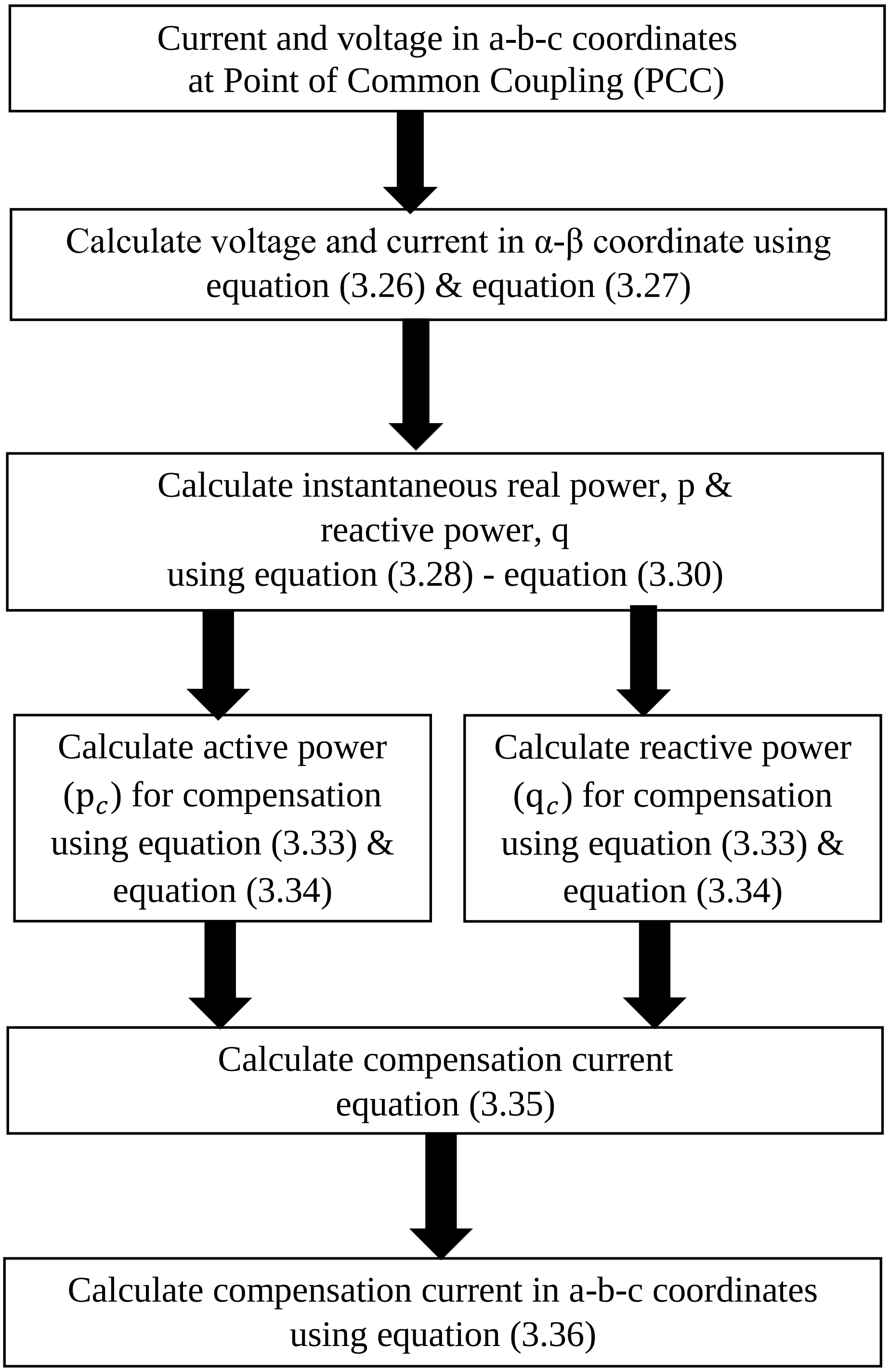

Figure 3.16: Procedure for compensator current calculation

The relation of the transformation between each component of three phase power system and orthogonal coordinates are expressed in α-β shown by the following equations in terms of voltage and current as shown in equation (3.26).

$$\begin{bmatrix} V_\alpha \\ V_\beta \end{bmatrix} = \sqrt{\frac{2}{3}} \begin{bmatrix} 1 & -\frac{1}{2} & -\frac{1}{2} \\ 0 & \frac{\sqrt{3}}{2} & -\frac{\sqrt{3}}{2} \end{bmatrix} \begin{bmatrix} V_a \\ V_b \\ V_c \end{bmatrix} \quad (3.26)$$

The three phase coordinates a-b-c is mutually orthogonal. As a result, the conventional power for three phase circuits can be derived by using the above equations. The instantaneous active power of the three phase circuit, p, can be calculated as shown in equation (3.27).

$$\begin{bmatrix} i_\alpha \\ i_\beta \end{bmatrix} = \sqrt{\frac{2}{3}} \begin{bmatrix} 1 & -\frac{1}{2} & -\frac{1}{2} \\ 0 & \frac{\sqrt{3}}{2} & -\frac{\sqrt{3}}{2} \end{bmatrix} \begin{bmatrix} i_a \\ i_b \\ i_c \end{bmatrix} \quad (3.27)$$

And the instantaneous real and reactive power can be defined as follows.

$$p = V_\alpha * i_\alpha + V_\beta * i_\beta \quad (3.28)$$

$$q = V_\alpha * i_\beta - V_\beta * i_\alpha \quad (3.29)$$

From these equations, the instantaneous power can be rewritten as

$$\begin{bmatrix} p \\ q \end{bmatrix} = \begin{bmatrix} V_\alpha & V_\beta \\ -V_\beta & V_\alpha \end{bmatrix} \begin{bmatrix} i_\alpha \\ i_\beta \end{bmatrix} \quad (3.30)$$

The α-β currents will be set as functions of voltages, real and imaginary powers p and q to explain the physical meaning of the powers defined in the p-q theory.

$$\begin{bmatrix} i_\alpha \\ i_\beta \end{bmatrix} = \begin{bmatrix} V_\alpha & V_\beta \\ -V_\beta & V_\alpha \end{bmatrix}^{-1} \begin{bmatrix} P \\ q \end{bmatrix} \quad (3.31)$$

Simplified form of equation (3.31) is given below,

$$\begin{bmatrix} i_\alpha \\ i_\beta \end{bmatrix} = \frac{1}{V_\alpha{}^2 + V_\beta{}^2} \begin{bmatrix} V_\alpha & -V_\beta \\ V_\beta & V_\alpha \end{bmatrix} \begin{bmatrix} p \\ q \end{bmatrix} \quad (3.32)$$

As stated above, the traction system is a three phase system without neutral wire and the zero sequence power is zero. Therefore, the compensator has to select the following powers as a reference to follow the control strategy.

Instantaneous active power supplied by the compensator:

$$p_c = - p \quad (3.33)$$

Instantaneous reactive power supplied by the compensator:

$$q_c = - q \quad (3.34)$$

3.4.3 Compensator reference current calculation

The compensator reference currents in α-β domain can be calculated as:

$$\begin{bmatrix} i^*_{ca} \\ i^*_{c\beta} \end{bmatrix} = \frac{1}{V_\alpha^2 + V_\beta^2} \begin{bmatrix} V_\alpha & -V_\beta \\ V_\beta & V_\alpha \end{bmatrix} \begin{bmatrix} p_c \\ q_c \end{bmatrix} \quad (3.35)$$

The compensator reference currents are transformed from α-β domain to a-b-c coordinates as following.

$$\begin{bmatrix} i^*_{ca} \\ i^*_{cb} \\ i^*_{cc} \end{bmatrix} = \sqrt{\frac{2}{3}} \begin{bmatrix} 1 & 0 \\ -\frac{1}{2} & \frac{\sqrt{3}}{2} \\ -\frac{1}{2} & -\frac{\sqrt{3}}{2} \end{bmatrix} \begin{bmatrix} i^*_{ca} \\ i^*_{c\beta} \end{bmatrix} \quad (3.36)$$

where i^*_{ca} , i^*_{cb} and i^*_{cc} denotes compensator current for phase A, B and C respectively

The reference current in equation (3.36) is compared with the current measurement of hybrid active power filter and then fed into three phase hysteresis controller to generate signaling pulses as following.

$$\begin{bmatrix} i_{a\,ref} \\ i_{b\,ref} \\ i_{c\,ref} \end{bmatrix} = \begin{bmatrix} i^*_{ca} \\ i^*_{cb} \\ i^*_{cc} \end{bmatrix} - \begin{bmatrix} i_{a,F} \\ i_{b,F} \\ i_{c,F} \end{bmatrix} \quad (3.37)$$

where $i_{a\,ref}$, $i_{b\,ref}$ and $i_{c\,ref}$ denote reference currents for phase A, B and C respectively. And where $i_{a,F}$, $i_{b,F}$ and $i_{c,F}$ denote HAPF current for phase A, B and C respectively.

3.4.4 Hysteresis current controller

The hysteresis band current control for hybrid active power filter is used to generate the switching patterns of the inverter. Hysteresis current control method is proven to be the best among other current control methods, because of its quick current controllability, easy implementation, unconditioned stability and fast control [18].

The actual compensation current is subtracted from its estimated reference current. The measured inverter phase currents ($i_{a,F}$, $i_{b,F}$, $i_{c,F}$) are compared, one by one, to the reference currents (i^*_{ca}, i^*_{cb}, i^*_{cc}). The resulting error is sent through a hysteresis controller to determine the appropriate switching pulses. The switching pulses are generated when actual compensation current reference crosses the upper and lower tolerance bands. If the actual compensation current reference is within a tolerance band then no switching pulses are generated. The controlled compensation current is injected such that the HAPF supply current follows the reference current.

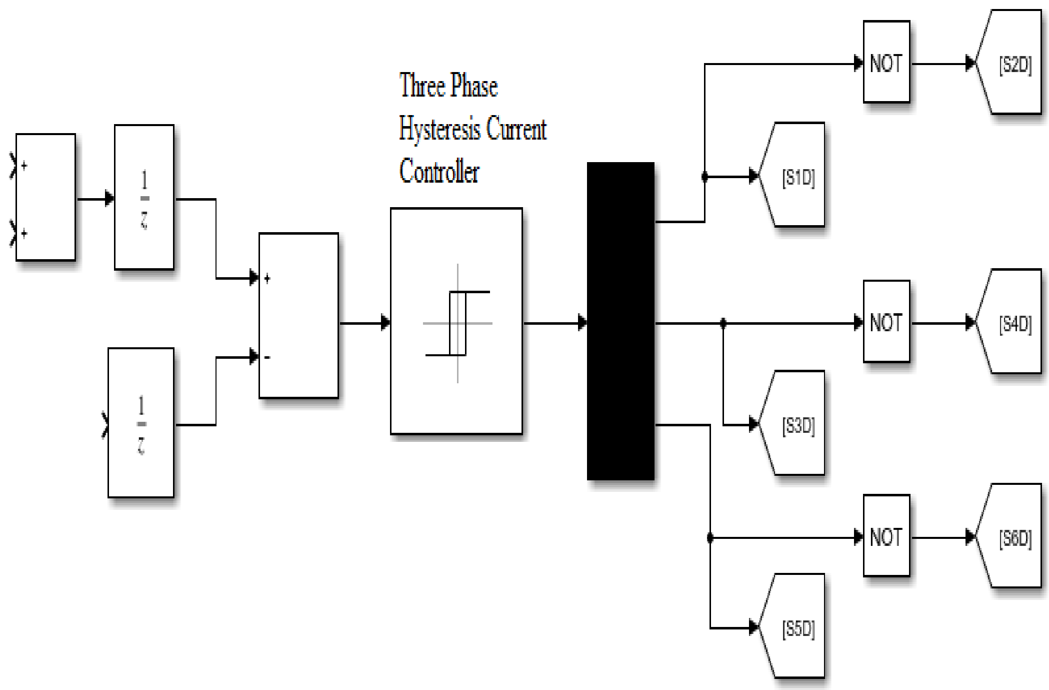

Figure 3.17: MATLAB/Simulink model representation of hysteresis current controller

The hysteresis current controller decides the switching patterns of the devices in the active power filter [24]. The switching logic is formulated as following.

If i_{ca} < (i_{ca}^* - hysteresis band tolerance) upper switch (S1D) is OFF and lower switch (S2D) is ON.

If i_{ca} > (i_{ca}^* - hysteresis band tolerance) upper switch (S1D) is ON and lower switch (S2D) is OFF.

If i_{cb} < (i_{cb}^* - hysteresis band tolerance) upper switch (S3D) is OFF and lower switch (S4D) is ON.

If i_{cb} > (i_{cb}^* - hysteresis band tolerance) upper switch (S3D) is ON and lower switch (S4D) is OFF.

If i_{cc} < (i_{cc}^* - hysteresis band tolerance) upper switch (S5D) is OFF and lower switch (S6D) is ON.

If i_{cc} > (i_{cc}^* - hysteresis band tolerance) upper switch (S5D) is ON and lower switch (S6D) is OFF.

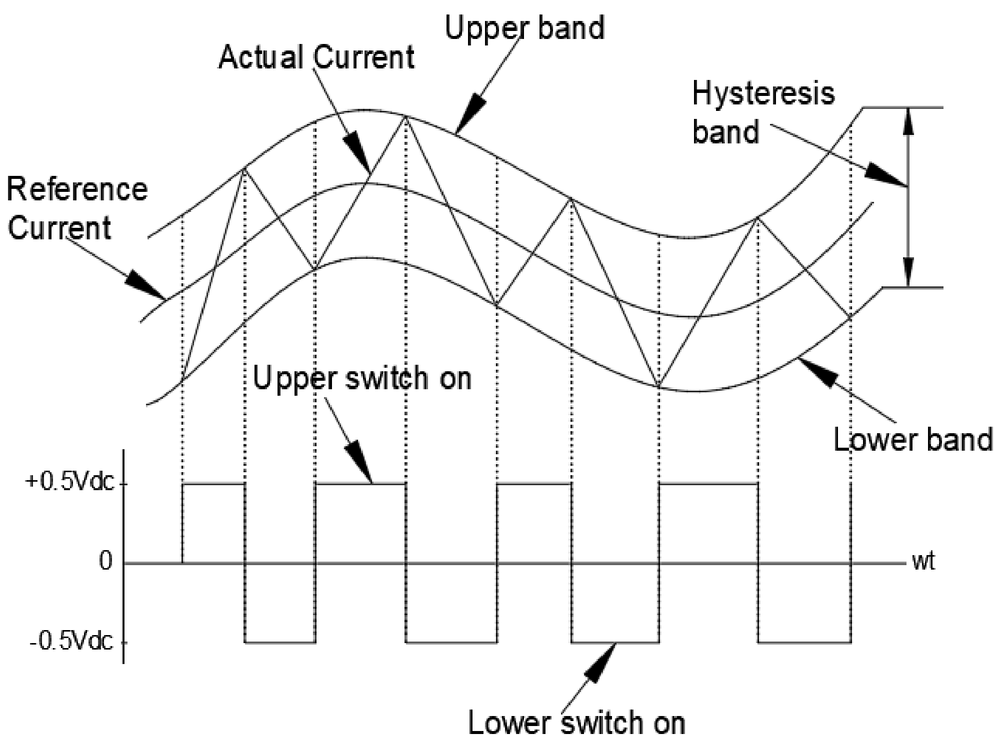

Figure 3.18: Switching signal pattern of hysteresis current controller

3.4.5 Gating signal generation method

In active power filter applications, the inverter delivers a current which compensates for harmonics and distortions absorbed by the load. The technique which is mostly used for the generation of gating pulses is pulsed width modulation and Hysteresis Current control (HCC) [24]. The generated switching signals are fed to VSI with a dc link capacitor across it. Based on these switching signals the inverter generates compensating current in phase opposition to the line current.

Output voltage of the inverter can be modified or controlled by controlling or modifying switching current, or in case of power switches, by controlling or modifying gate current. The compensating current is injected back into the power line at the PCC and thus suppressing the current harmonics present in the line.

Mathematical equations from equation (3.26) up to equation (3.37) for reference current calculation and gating signal generation are modeled using the MATLAB /Simulink as given in Figure 3.19.

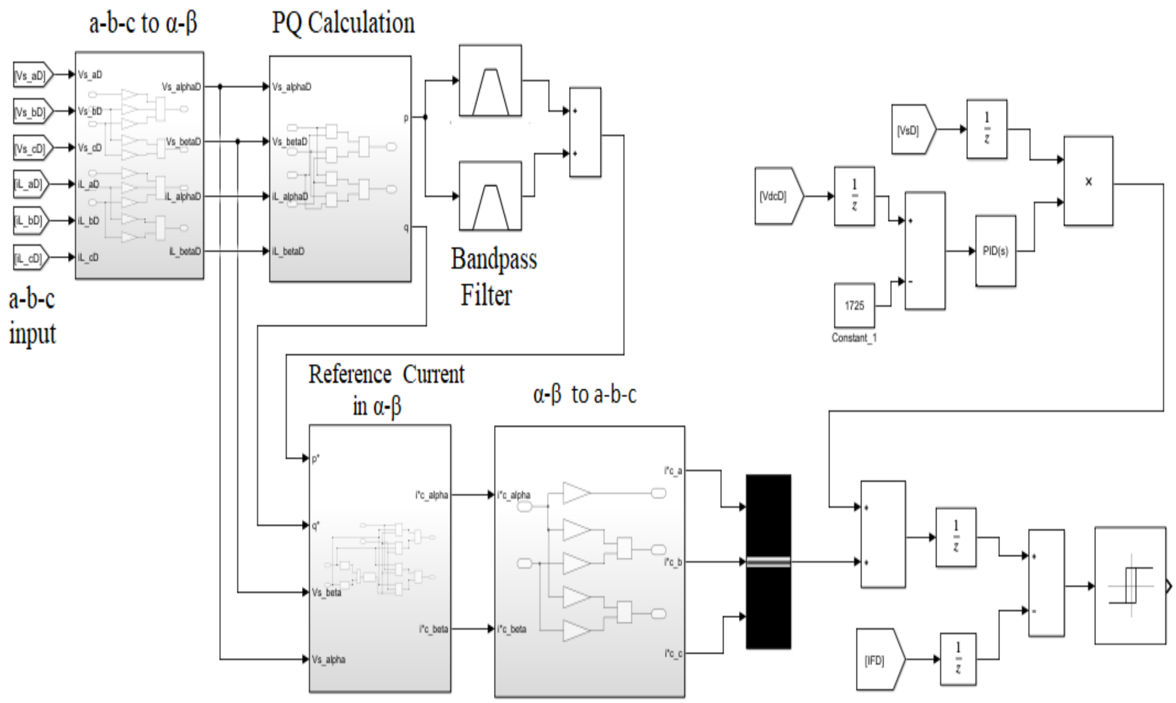

Figure 3.19: MATLAB/Simulink model representation of switching signal generation

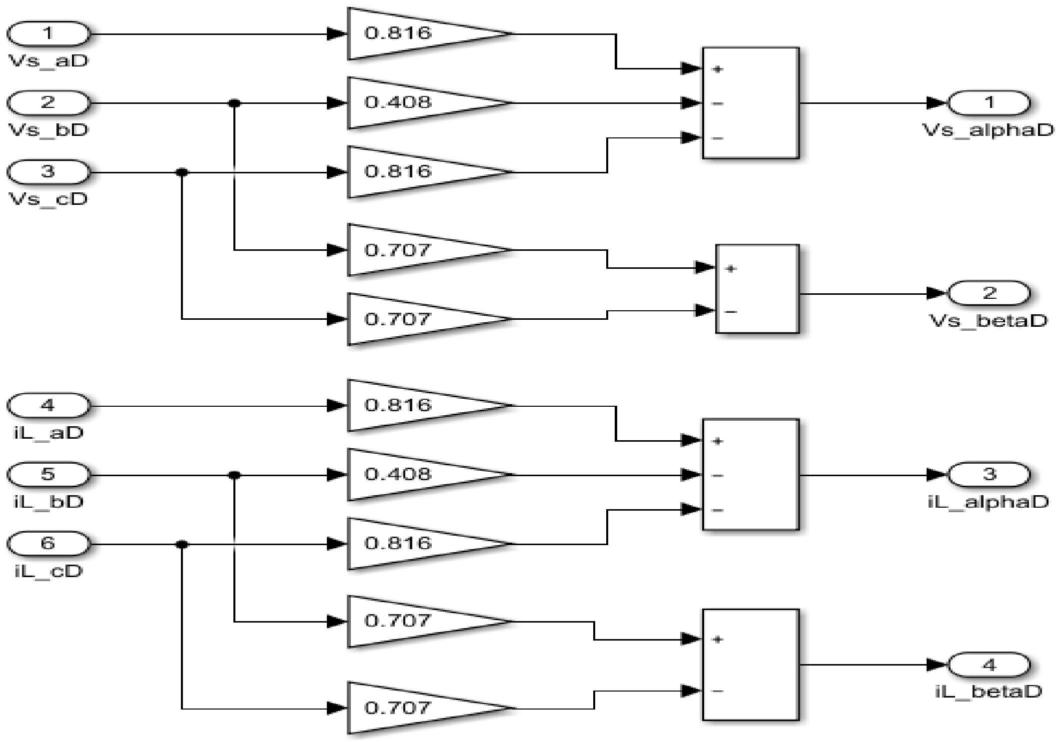

Figure 3.20: MATLAB/Simulink model representation of converting a-b-c axis to α-β axis

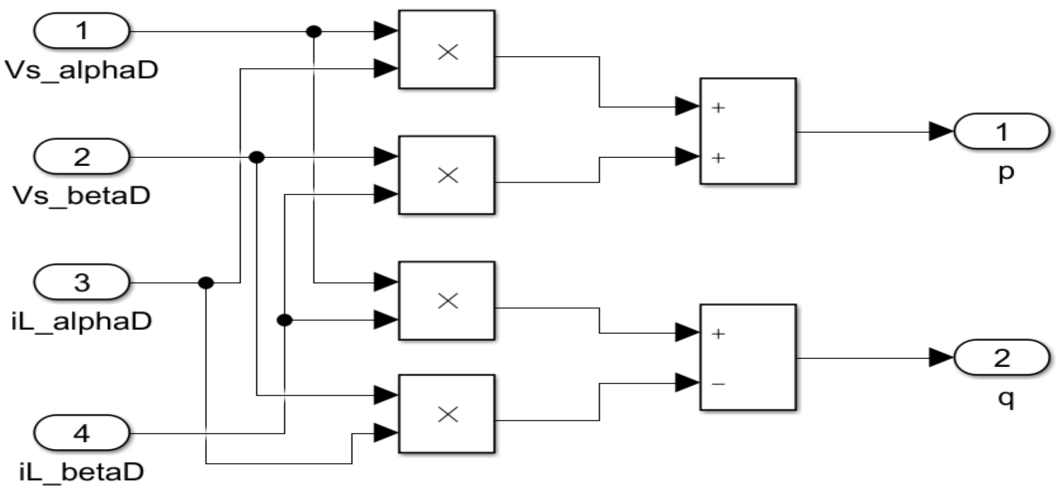

Figure 3.21: MATLAB/Simulink model representation of PQ calculation using α-β axis

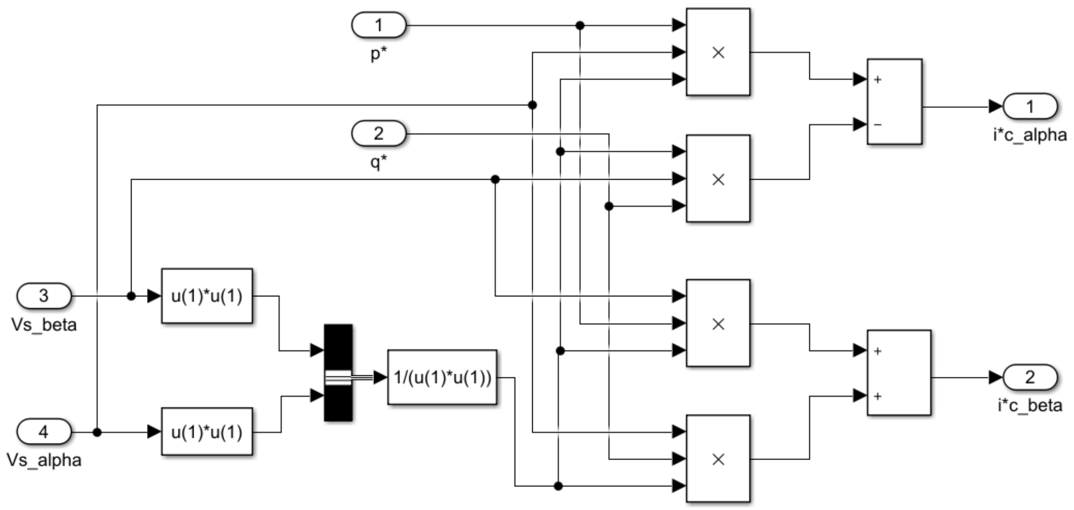

Figure 3.22: MATLAB/Simulink model representation of reference current calculation

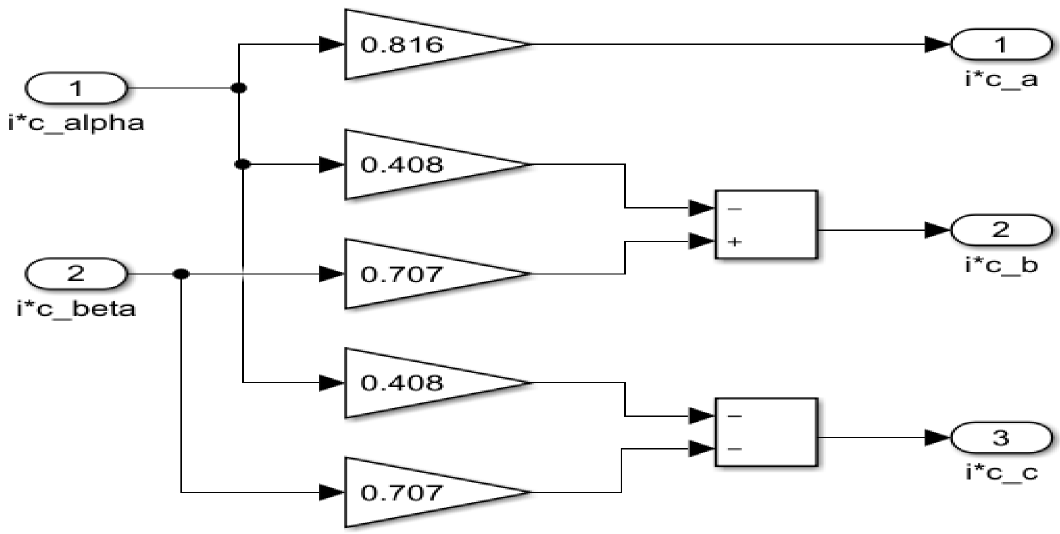

Figure 3.23: MATLAB/Simulink model representation of converting α-β reference current to a-b-c

3.4.6 Second order band pass filter

Band pass filter is one of the components of control circuit which is used to filter the harmonic power for the selected band of harmonic power orders. The band pass filter is designed for filtering 11th and 13th harmonic power based on their frequency spectrums.

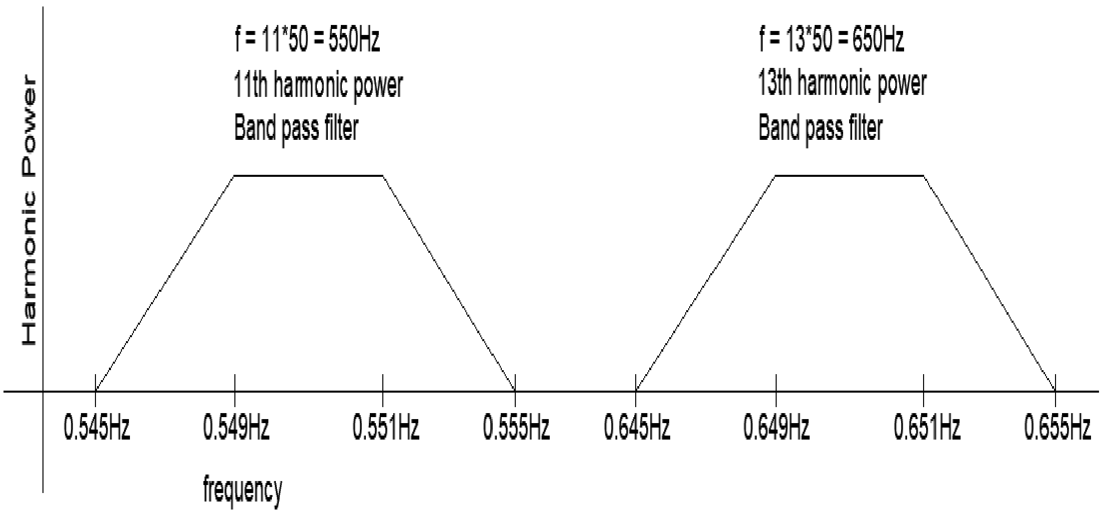

Figure 3.24: Band pass filter

3.4.7 DC bus voltage controller

It is one of the control circuit schemes of HAPF [25]. The main function of the DC bus voltage controller is to control power supply to the insulated gate bipolar transistor converter. This is done to avoid external power supply to the DC link capacitor. Thus, the charging and discharging phenomenon of capacitor is controlled by the DC bus voltage controller for maintaining the DC voltage level at constant and the transient response reached the stability.

Voltage controller of DC bus regulates the voltage of the capacitor on DC side of the converter and compensates losses of the inverter. The voltage of the capacitor is measured and then it is compared to constant value. The resultant difference is the fed into the PI controller. The proportional integral controller is used to develop the switching losses of the active power inverter through its proportional constant ($K_p = 1$) that determines the dynamic response of the DC link voltage by minimizing the instantaneous error and through its integration constant ($K_I = 2.5$) that determines the settling time by minimizing the steady state error. In this way, hybrid active power filter regulates and builds up the DC voltage of capacitor without using any external source.

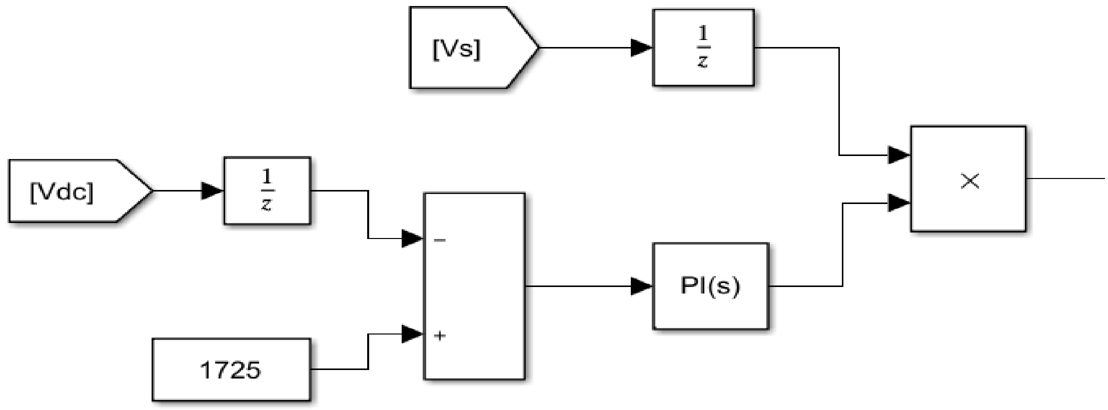

Figure 3.25: MATLAB/Simulink model representation of dc bus voltage controller

3.4.8 DC bus capacitor

The DC side capacitor serves to maintain a DC voltage with a less ripple in steady state and it serves as an energy storage element to supply the power difference between load and source during the transient period. In steady state, the power supplied by the source is equal to the required load power demand. In case, any change in load conditions, the power demand in load side changes. The difference in power between the source and the load is regulated by using DC capacitor. If DC capacitor voltage is attained the reference voltage, the power supplied by the source is equal to the load demand. The DC capacitor selection is based on the principle of instantaneous power flow on dc and ac side of PWM inverter.

The selection of C_{dc} can be governed by reducing the voltage ripple. As per the specification of peak to peak voltage ripple V_{P-P} (max) and rated filter current I_{RFC} , rated the DC side capacitor C_{dc} can be found from:

$$C_{dc} = \frac{I_{RFC}}{2\sqrt{3} * f * V_{P-P}(max)} \quad \text{...............................} (3.38)$$

V_{P-P} (max) = (608.84) – (- 608.84) =1217.68V

V_{P-P} (max) = 1218V

$$C_{dc} = \frac{347.98}{2\sqrt{3} * 50 * 1218)} = 1.65\text{mF}$$

3.4.9 Reference capacitor voltage $V_{dc,Ref}$

The hybrid active power filter can inject compensation harmonic power to the network at PCC only when $V_{AF} > V_{PCC}$. The PWM-VSI is assumed to operate in the linear modulation mode ($0 \leq m_a \leq 1$).

$$m_a = \frac{V_m}{V_{dc}/2} \qquad (3.39)$$

where $V_m = \sqrt{2} * V_{AF}$

For $m_a = 1$, $V_{dc} = 2\sqrt{2} * V_{AF} = 2\sqrt{2} * 608.84 = 1722.06V$

Therefore, V_{dc} = 1722.06V = 1722V

3.4.10 Interfacing inductor

The compensation current waveform generated by the active power filter is obtained by controlling the switching of the IGBTs in the voltage source inverter. The switching ripple of the compensation current is determined by the size of interfacing inductor, the driving voltage across the interface inductor, and switching frequency. In the HAPF case the driving voltage is DC bus voltage (V_{dc}). The IGBT DC bus voltage across the interfacing inductor determines the peak to peak switching ripple current (ΔI_{P-P}). The minimum interfacing inductor (L_{min}) is obtained from the following formula.

$$L_{min} = \frac{V_{dc}}{2(\Delta I_{P-P}) * f_{sw,max}} \qquad (3.40)$$

where $f_{sw,max}$ is the maximum frequency of switching ripple and ΔI_{P-P} is the peak to peak switching ripple of compensation current.

For V_{dc} = 1725V, $\Delta I_{P-P} = \sqrt{2}$ [347.98 - (-347.98)] = 984.24A, $f_{sw,max}$ = 4kHz

$$L_{min} = \frac{1725}{2 * 984.24 * 4000} = 219.08\mu H$$

Chapter Four

Simulation studies and analysis of result

4.1 Introduction

Simulation results of the traction network without HAPF and with HAPF are provided in numerical values and waveforms for six traction motors in the traction substation. Individual current harmonic distortion and total harmonic distortions are obtained from MATLAB/Simulink Fast Fourier Transform (FFT) analysis with harmonic spectrums representation and numerical lists. The numerical values for voltage and current are obtained from MATLAB/Simulink model voltmeters and ammeters. The current and voltage waveforms are also obtained from MATLAB/Simulink model oscilloscope (scope).

The simulation of MATLAB/Simulink model for traction network is carried in a discrete mode simulation type, variable step size solver type with ode45 (Dormand-Prince) solver which are selected in the parameter configuration panel.

The simulation results are carried out at three points of the traction substation network, namely at motor terminal, at PCC and at primary side of the transformer.

4.2 MATLAB/Simulink model simulation result without hybrid active power filter

Simulation results of the traction network without HAPF for voltage, current and total harmonic distortion at motor terminal, at PCC and at primary side of the transformer are given in Table 4.1 for comparison purpose.

Table 4.1: Comparison between measured values and simulation results

Description	Six traction motors (Design Rating/measured)	Six traction motors (Simulink model)
Voltage at motor terminal (V_{LL}) Vrms	500 – 510	502.30
Current at motor terminal (I_P) Arms	210	167.60
Voltage at PCC (V_{LL}) Vrms	590/569.84	590.60
Fundamental Voltage at PCC (V_1) Vrms	330.87	579.60
Current at PCC (I_P) Arms	640.83	643.70
Fundamental Current at PCC (I_1) Arms	422.53	400.50
Voltage THD at PCC (%)	27.60	28.52
Current THD at PCC (%)	153.03	88.19
Voltage at 15kV side (V_{LL}) Vrms	15,000	15,040

The traction network measured values and simulation results for individual current harmonics is given in Table 4.2. In this table, traction network modeling error determined using the measured values and simulation results is also presented.

Table 4.2: Traction network modeling error at PCC

PCC H_n	Measured Current Harmonics (%)	Simulink Current Harmonic (%)	Error (%)	H_n	Measured Current Harmonic (%)	Simulink Current Harmonic (%)	Error (%)
2	26.98	10.87	59.71	27	11.12	2.74	75.36
3	32.96	3.05	90.75	28	5.72	2.19	61.71
4	12.16	4.65	61.76	29	25.72	0.62	97.59
5	81.49	65.55	19.56	30	7.21	2.56	64.49
6	16.94	14.45	14.70	31	25.37	0.96	96.22
7	75.65	34.87	53.91	32	5.41	2.78	48.61
8	0	13.88		33	9.37	2.15	77.05
9	17.12	10.27	40.01	34	4.63	2.15	53.56
10	10.12	10.32	-1.98	35	20.21	2.09	89.66
11	61.01	26.99	55.76	36	5.77	1.92	66.72
12	14.45	6.53	54.81	37	19.21	1.88	90.21
13	55.32	11.05	80.03	38	4.1	2.04	50.24
14	9.91	7.17	27.65	39	7.99	1.71	78.60
15	15.32	6.84	55.35	40	4.05	1.89	53.33
16	8.09	9.59	-18.54	41	15.07	1.88	87.52
17	43	9.29	78.40	42	4.35	1.85	57.47
18	11.56	7.05	39.01	43	14.12	2.00	85.84
19	40.2	5.20	87.06	44	3.35	1.50	55.22
20	8.47	6.04	28.69	45	6.5	1.65	74.62
21	13.19	3.45	73.84	46	3.45	1.60	53.62
22	6.89	3.94	42.82	47	10.81	1.45	86.59
23	33.14	3.91	88.20	48	3.36	1.40	58.33
24	8.62	2.77	67.87	49	10.08	1.39	86.21
25	31.97	3.17	90.08	50	2.91	1.33	54.30
26	6.98	2.46	64.76	THD	153.03	88.19	42.37

4.2.1 Current waveforms without hybrid active power filter

The current waveforms from simulation results at motor terminals, at PCC and at primary side of transformer without hybrid active power filter is shown below in Figure 4.1, Figure 4.2 and Figure 4.3 respectively.

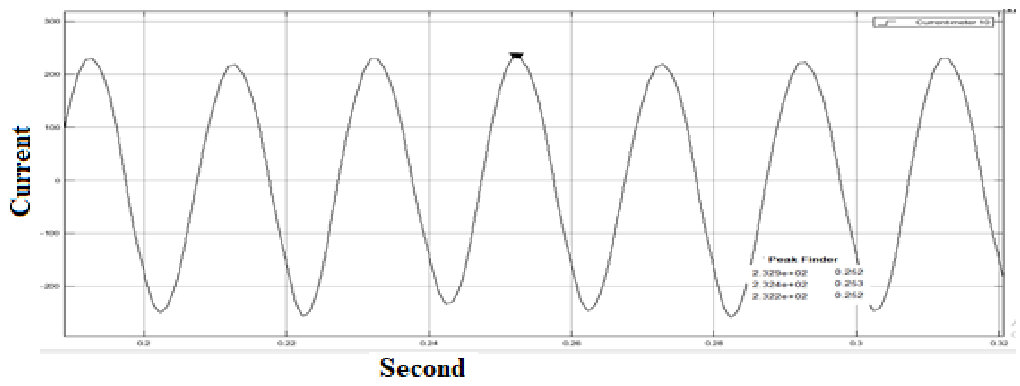

Figure 4.1: Current waveform at motor terminal without harmonic active power filter

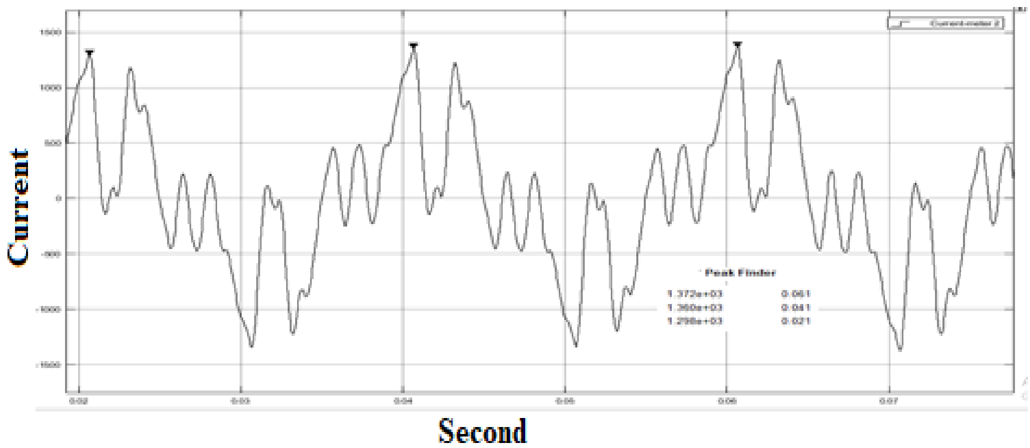

Figure 4.2: Current waveform at PCC without harmonic active power filter

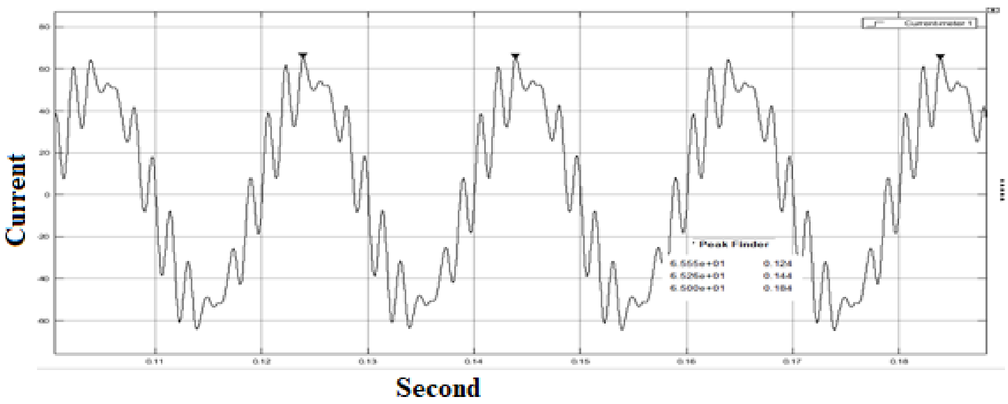

Figure 4.3: Current waveform at primary side of transformer without harmonic active power filter

4.2.2 Voltage waveforms without hybrid active power filter

The voltage waveforms from simulation results at motor terminals, at PCC and at primary side of transformer without hybrid active power filter is shown below in Figure 4.4, Figure 4.5 and Figure 4.5 respectively.

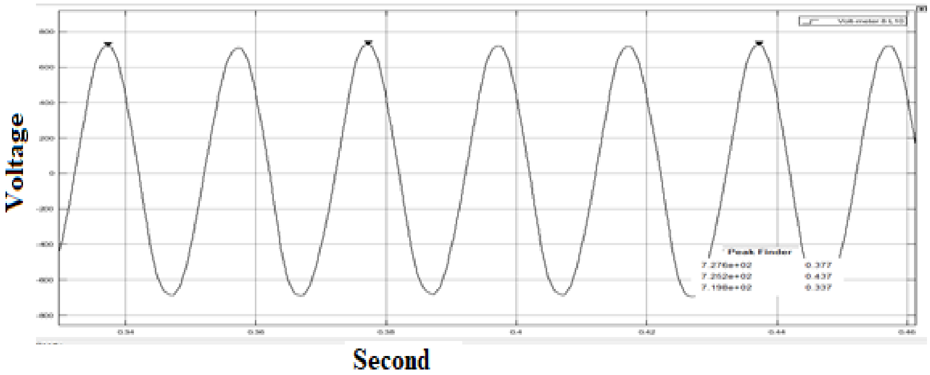

Figure 4.4: Voltage waveform at each motor terminal without harmonic active power filter

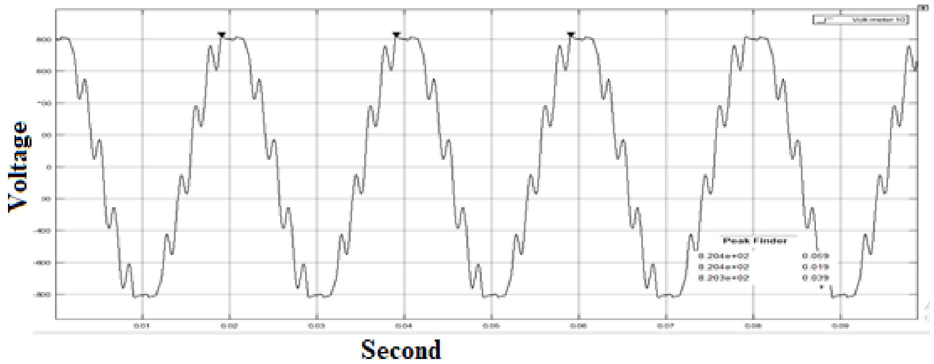

Figure 4.5: Voltage waveform at PCC without harmonic active power filter

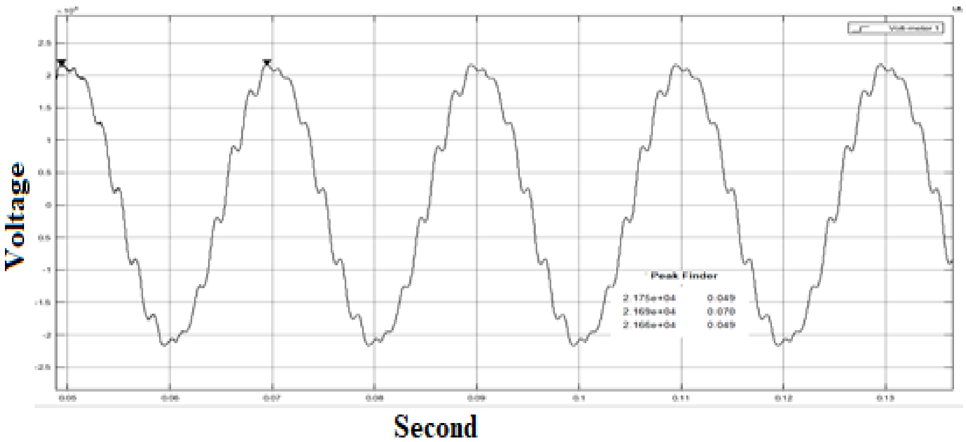

Figure 4.6: Voltage waveform at primary side of transformer without harmonic active power filter

4.2.3 Current harmonic spectrum without hybrid active power filter

The simulation results of individual current harmonic spectrums from Simulink FFT analysis at motor terminals, at PCC and at primary side of transformer without hybrid active power filter is shown below in Figure 4.7, Figure 4.8 and Figure 4.9 respectively.

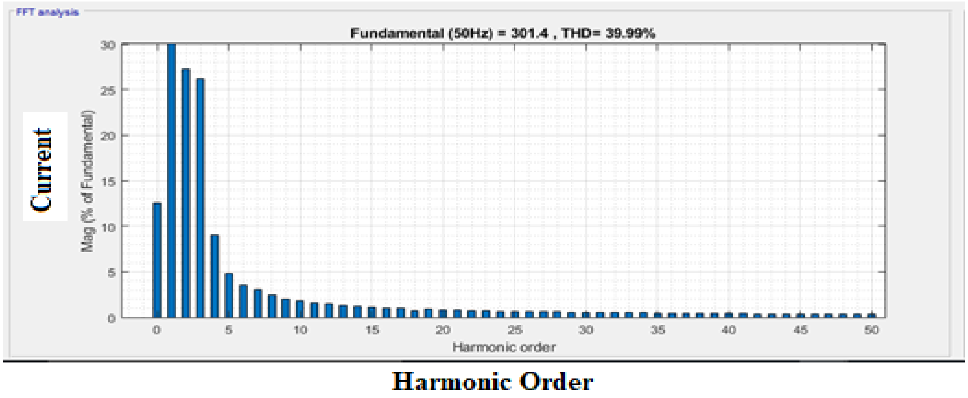

Figure 4.7: Individual current harmonic spectrums at motor terminal without harmonic active power filter

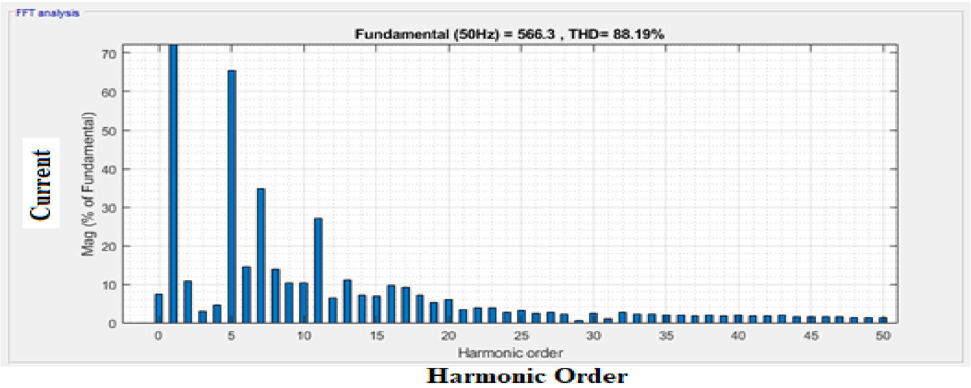

Figure 4.8: Individual current harmonic spectrums at PCC without hybrid active power filter

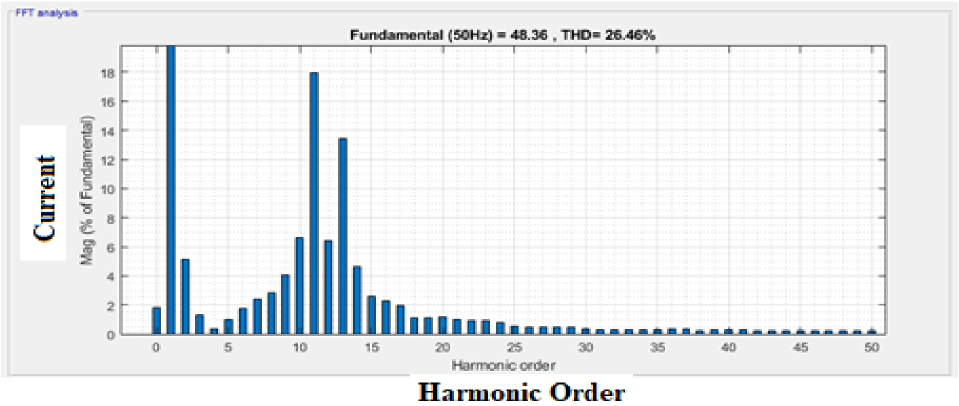

Figure 4.9: Individual current harmonic spectrums at primary side of transformer without harmonic active power filter

4.3 MATLAB/Simulink model simulation of six traction motors with hybrid active power filter

The result of simulation with hybrid active power filter for voltage, current and total harmonic distortion at motor terminal, at PCC and at primary side of transformer are given in Table 4.3.

Table 4.3: Simulation results without and with hybrid active power filter

System parameters values from Simulink output	Six traction motors (Without HAPF)	Six traction motors (With HAPF)
Voltage at motor terminal (V_{LL}) Vrms	502.30	503.90
Current at motor terminal (I_P) Arms	167.60	168.20
Current at PCC (I_P) Arms	643.70	785.40
Fundamental Current at PCC (I_1) Arms	400.50	549.50
Voltage at PCC (V_{LL}) Vrms	590.60	597.50
Fundamental Voltage at PCC (V_1) Arms	579.60	593.10
Voltage THD at PCC (%)	28.52	18.69
Current THD at PCC (%)	88.19	80.55
11^{th} harmonic Current at PCC (%)	26.99	3.75
13^{th} harmonic Current at PCC (%)	11.05	4.38
Voltage at 15kV side (V_{LL}) Vrms	15,040	15,200
Current at 15kV side (I_P) Arms	40.01	48.21
Fundamental Current at 15kV (I_1) Arms	34.20	49.27
11^{th} harmonic Current at 15kV (%)	17.99	1.55
13^{th} harmonic Current at 15kV (%)	13.43	0.89
Voltage THD at 15kV (%)	11.99	6.83
Current THD at 15kV (%)	26.46	6.88

The result of simulation for individual current harmonics at PCC with and without hybrid active power filter is given in Table 4.4

Table 4.4: Values of individual current harmonics at PCC

PCC H_n	Simulink Current Harmonic (Without HAPF) (%)	Simulink Current Harmonic (With HAPF) (%)		H_n	Simulink Current Harmonic (Without HAPF) (%)	Simulink Current Harmonic (With HAPF) (%)	
2	10.87	14.02		27	2.74	1.37	
3	3.05	10.97		28	2.19	1.23	
4	4.65	13.56		29	0.62	1.31	
5	65.55	57.75		30	2.56	1.16	
6	14.45	12.69		31	0.96	0.98	
7	34.87	47.70		32	2.78	0.98	
8	13.88	7.64		33	2.15	0.95	
9	10.27	3.24		34	2.15	0.91	
10	10.32	0.84		35	2.09	0.88	
11	26.99	3.75		36	1.92	0.85	
12	6.53	3.70		37	1.88	0.82	
13	11.05	4.38		38	2.04	0.77	
14	7.17	2.86		39	1.71	0.75	
15	6.84	3.41		40	1.89	0.75	
16	9.59	3.31		41	1.88	0.56	
17	9.29	2.51		42	1.85	0.65	
18	7.05	2.37		43	2.00	0.59	
19	5.20	2.25		44	1.50	0.55	
20	6.04	1.10		45	1.65	0.57	
21	3.45	1.67		46	1.60	0.54	
22	3.94	1.56		47	1.45	0.54	
23	3.91	1.52		48	1.40	0.55	
24	2.77	1.51		49	1.39	0.50	
25	3.17	1.46		50	1.33	0.45	
26	2.46	1.45		THD	88.19	80.55	

Similarly, the result of simulation for individual current harmonics at primary side of the transformer with and without hybrid active power filter is given in Table 4.5.

Table 4.5: Values of individual current harmonics at primary side of transformer

15KV	Simulink Current Harmonics (Without HAPF)	Simulink Current Harmonics (With HAPF)			Simulink Current Harmonics (Without HAPF)	Simulink Current Harmonics (With HAPF)	
H_n	(%)	(%)		H_n	(%)	(%)	
2	5.14	2.23		27	0.49	0.26	
3	1.31	0.99		28	0.46	0.24	
4	0.34	2.49		29	0.46	0.24	
5	0.99	2.29		30	0.38	0.23	
6	1.75	2.81		31	0.31	0.22	
7	2.42	3.25		32	0.32	0.21	
8	2.85	1.30		33	0.31	0.21	
9	4.06	1.05		34	0.31	0.20	
10	6.59	1.06		35	0.32	0.20	
11	17.99	1.55		36	0.38	0.19	
12	6.43	0.83		37	0.35	0.18	
13	13.43	0.89		38	0.26	0.18	
14	4.60	0.46		39	0.28	0.17	
15	2.62	0.47		40	0.28	0.17	
16	2.24	0.49		41	0.26	0.17	
17	1.92	0.36		42	0.25	0.16	
18	1.14	0.41		43	0.26	0.16	
19	1.15	0.41		44	0.25	0.15	
20	1.17	0.33		45	0.25	0.15	
21	0.97	0.33		46	0.25	0.14	
22	0.93	0.32		47	0.25	0.16	
23	0.92	0.32		48	0.22	0.15	
24	0.81	0.29		49	0.22	0.15	
25	0.56	0.28		50	0.22	0.14	
26	0.50	0.28		THD	26.46	6.88	

4.3.1 Current waveforms with hybrid active power filter

The current waveforms from simulation results at motor terminals, at PCC and at primary side of transformer with hybrid active power filter is shown below in Figure 4.10, Figure 4.11 and Figure 4.12 respectively.

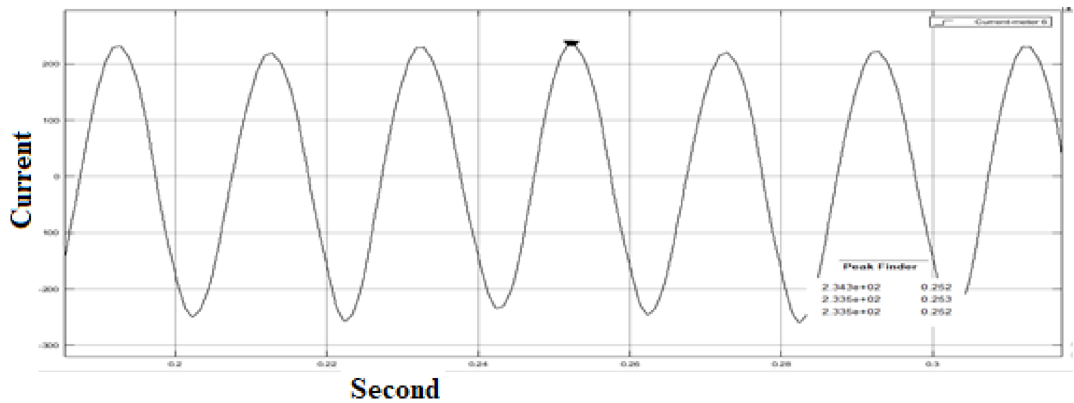

Figure 4.10: Current waveform at motor terminal with hybrid active power filter

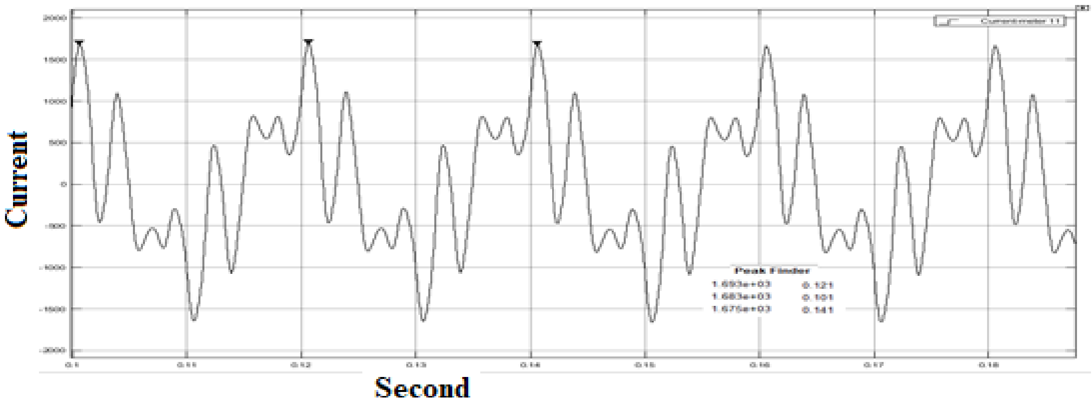

Figure 4.11: Current waveform at PCC with hybrid active power filter

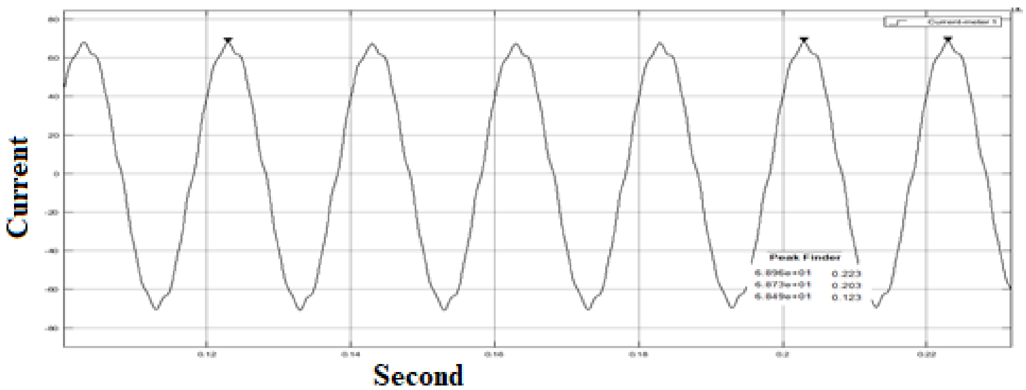

Figure 4.12: Current waveform at primary side of transformer with hybrid active power filter

4.3.2 Voltage waveforms with hybrid active power filter

The voltage waveforms from simulation results at motor terminals, at PCC and at primary side of transformer with hybrid active power filter is shown below in Figure 4.13, Figure 4.14 and Figure 4.15 respectively.

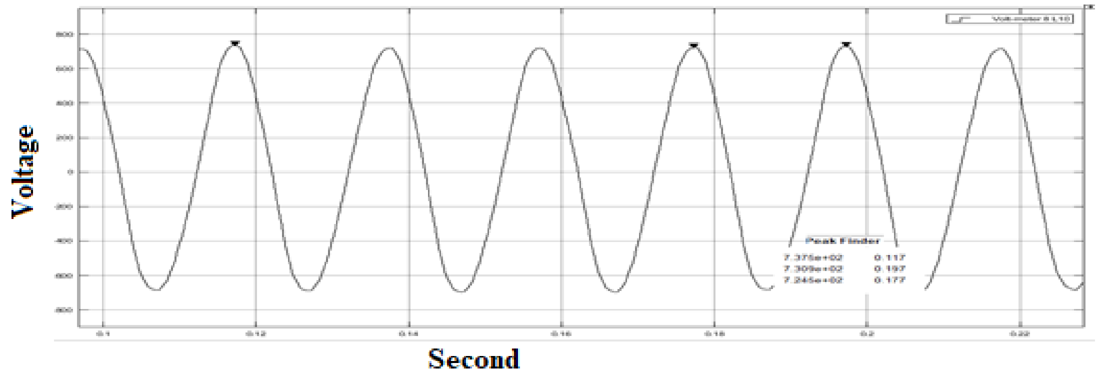

Figure 4.13: Voltage waveform at motor terminal with hybrid active power filter

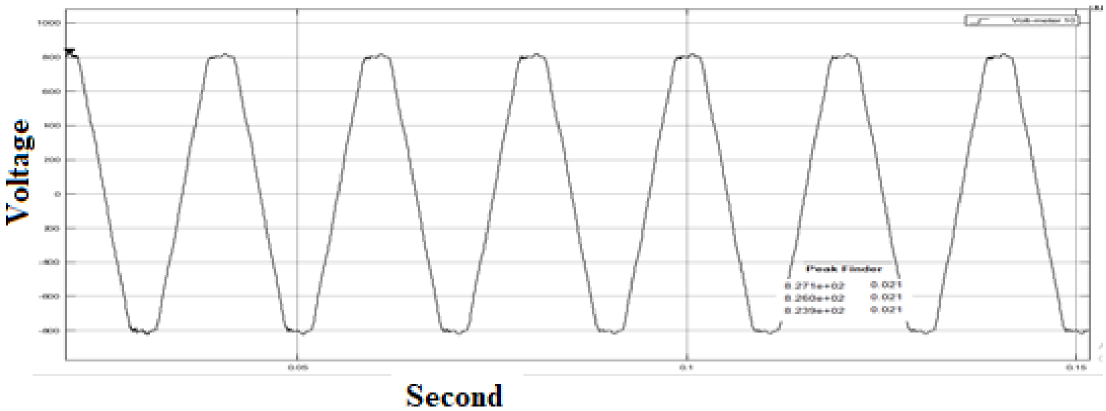

Figure 4.14: Voltage waveform at PCC with hybrid active power filter

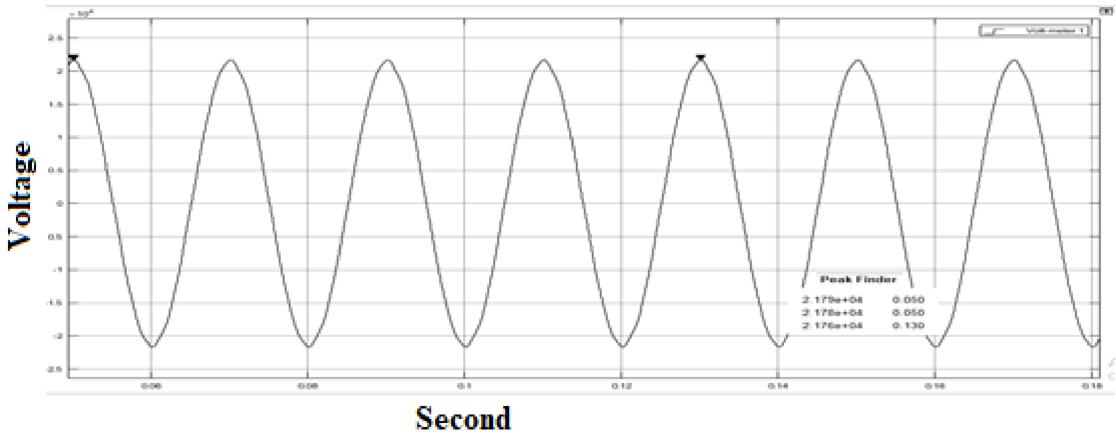

Figure 4.15: Voltage waveform at primary side of transformer with hybrid active power filter

4.3.3 Individual current harmonic spectrum with hybrid active power filter

The simulation results of individual current harmonic spectrums from Simulink FFT analysis at motor terminals, at PCC and at primary side of transformer with hybrid active power filter is shown below in Figure 4.16, Figure 4.17 and Figure 4.18 respectively.

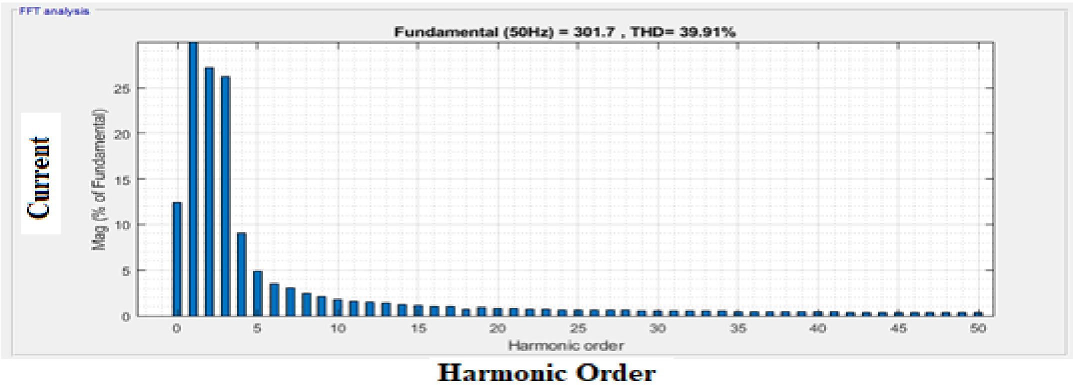

Figure 4.16: Individual current harmonic spectrums at motor terminal with harmonic active power filter

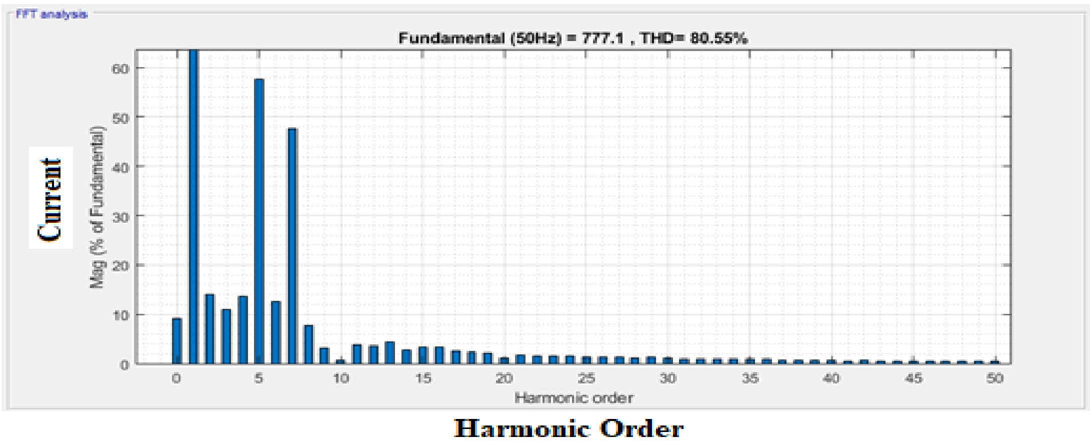

Figure 4.17: Individual current harmonic spectrums at PCC with harmonic active power filter

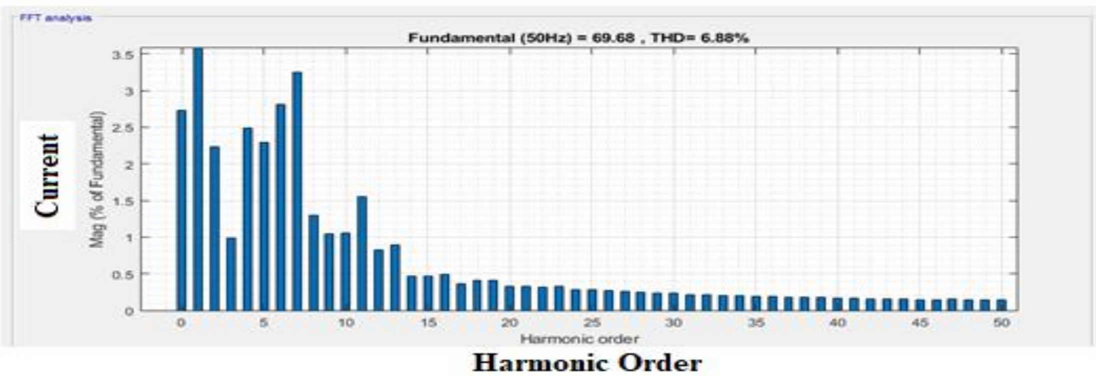

Figure 4.18: Individual current harmonic spectrums at primary side of transformer with harmonic active power filter

4.4 Compensator current waveform at PCC for six traction systems

Compensator current waveform generated by hybrid active power filter for six traction motors is given below in Figure 4.19.

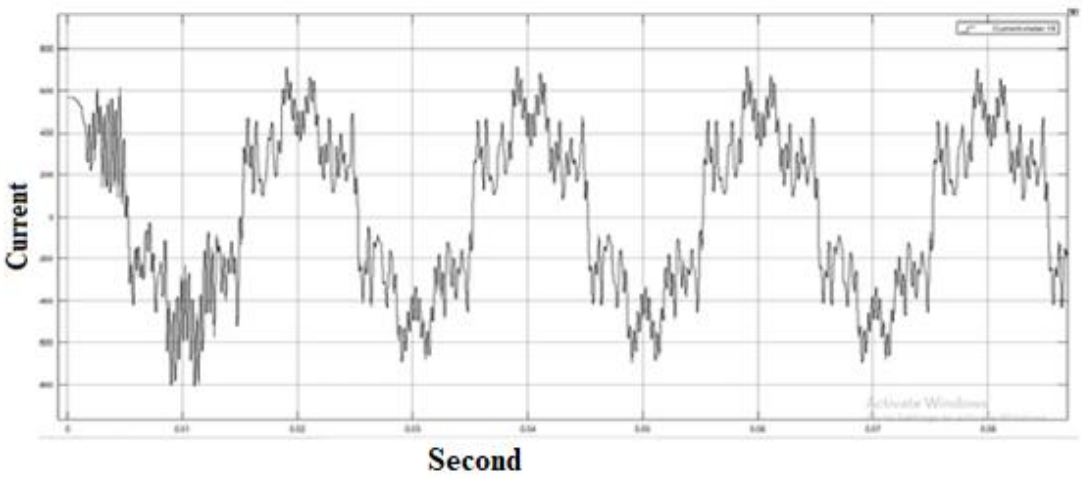

Figure 4.19: Compensator current waveform at PCC for six traction motors

4.5 MATLAB/Simulink results for one traction motor and three traction motors

The same HAPF design and model for six traction motors system is evaluated for one traction motor and three traction motors systems. The Simulink results of individual current harmonic values for 11^{th} and 13^{th} harmonic order at PCC and primary side of transformer are given in Table 4.6 for three traction motors and one traction motor inside the traction substation.

Table 4.6: Values of harmonics at PCC and primary side of transformer side

System parameters values from Simulink	One traction motor with HAPF	Three traction motors with HAPF
Voltage THD at PCC (%)	5.47	11.71
Current THD at PCC (%)	30.51	33.77
11^{th} harmonic Current at PCC (%)	1.27	1.56
13^{th} harmonic Current at PCC (%)	0.67	0.76
Voltage THD at 15kV (%)	1.55	2.66
Current THD at 15kV (%)	5.77	4.55
11^{th} harmonic Current at 15kV (%)	0.77	0.49
13^{th} harmonic Current at 15kV (%)	0.45	0.73

4.6 Distortion power factor comparison for six traction motors

The distortion power factor for six traction motors is determined by the current and voltage harmonic distortion results taken from Table 4.3. Distortion power factor is calculated by using the formula given below.

$$\text{Distortion Power Factor} = \frac{1}{\left(\sqrt{1+\mathrm{THD}_I^2}\right)\left(\sqrt{1+\mathrm{THD}_V^2}\right)}$$

Recalling Table 4.3, for current and voltage harmonic distortion results, the distortion power factor is calculated at PCC and 15kV side.

4.6.1 Distortion power factor without HAPF at PCC

THD_I = 88.19% = 0.8819 THD_V = 28.52% = 0.2852

Distortion Power Factor = 0.72

4.6.2 Distortion power factor with HAPF at PCC

THD_I = 80.55% = 0.8055 THD_V = 18.69% = 0.1869

Distortion Power Factor = 0.77

4.6.3 Distortion power factor without HAPF at 15kV side

THD_I = 26.46% = 0.2646 THD_V = 11.99% = 0.1199

Distortion Power Factor = 0.955

4.6.4 Distortion power factor for the traction network with HAPF at 15kV side

THD_I = 6.88% = 0.0688 THD_V = 6.83% = 0.0683

Distortion Power Factor = 0.995

Chapter Five

Conclusions, recommendations and suggestions of future work

5.1 Introduction

Conclusions are drawn based on measured values and improved values obtained from simulation results at PCC and at primary side of transformer.

Recommendations have been provided for Addis Ababa Light Rail Transit to include hybrid active power filter into the existing traction network for improved and safe operation of the network.

Suggestions have been included to improve traction network model for further study and investigation of the performance of the hybrid active power filter.

5.2 Conclusions

Hybrid active power filter is designed to mitigate 11^{th} and 13^{th} current harmonic orders. The simulation results of this filter indicates that the amount of 11^{th} and 13^{th} current harmonics is reduced and as result the distortion power factor is also improved. Thus, the total harmonic distortion of current is improved.

The simulation result shows that, 11^{th} current harmonic order at PCC is reduced from 26.99% to 3.75% and 13^{th} current harmonic order at PCC is reduced from 11.05% to 4.38%. The reduction of 11^{th} and 13^{th} current harmonic orders results the overall total harmonic distortion of current harmonic at PCC to reduce from 88.19% to 80.55%.

Correspondingly, 11^{th} current harmonic order at the primary side transformer is reduced from 17.99% to 1.55% and 13^{th} current harmonic order at the primary side transformer side is reduced from 13.43% to 0.89%. The reduction of 11^{th} and 13^{th} current harmonic orders results the overall total harmonic distortion of current harmonic at the primary side transformer side to reduce from 26.46% to 6.88%. The distortion power factor is also improved from 0.955 to 0.995. The effective values of fundamental current and voltage is also improved. The active power in the system is also improved with the reduced harmonic power due to the reduction of 11^{th} and 13^{th} harmonic currents. Hybrid active power filter technique is a selective harmonic mitigation method which is technically efficient to implement for selective harmonic current reduction.

5.3 Recommendations

By considering the current harmonic orders up to 50th order, the total number of current harmonic orders that exist in ideal six pulse rectifier is sixteen. But, for the practical six pulse rectifier which is made in this case study, it consists of forty nine current harmonics. Also, the value of individual current harmonics is exceeding the standard requirements of individual harmonic distortion which make the overall current harmonic distortion beyond the standard limit.

Therefore, Addis Ababa Light Railway Transit should install hybrid active power filter for the traction network to function effectively with improved power quality for safe and reliable operation of the network.

5.4 Suggestions for future work

All data presented in this thesis are measured at the site or taken from the manufacturer technical documents which could enable others to make further study and detail analysis.

In this thesis, the effect of 11th and 13th current harmonics have been investigated and analyzed. The effect of other current harmonics may be investigated and analyzed with respect to cost of implementation.

The analysis is done for six traction motors in the traction network. For the same hybrid active power filter considered in this thesis, further analysis of 11th and 13th current harmonics for additional traction motors in the traction network may be studied.

In future, attempt should be made to remove the deficiency in modeling and to improve the traction network model. Thus, the performance of hybrid active power filter may be carried out by using improved traction network model.

.

References

[1] "Technical Specification of Vehicles", China Railway Group Limited July 2013. (This document and others related design documents are found from Ethiopian Railway Corporation documentation store)

[2] Darwin Rivas, Luis Moran, Juan W. Dixon, and José R. Espinoza, "Improving Passive Filter Compensation Performance with Active Techniques," IEEE TRANSACTIONS ON INDUSTRIAL ELECTRONICS, VOL. 50, NO. 1, pp.161-164, FEBRUARY 2003.

[3] S. Suresh, Dr. N. Devarajan, V. Rajasekaran, "Modeling and Analysis of Shunt Hybrid Filter to Enhance Power Quality for Mitigation of Load Current Harmonics," Advances in Natural and Applied Sciences, pp. 1276-1282, 6(8): 2012 ISSN 1995 – 0772.

[4] B.Venkata Ramana, S.Dayasagar Chowdary, G.Venkata Ratnam, "Analysis of Active and Passive Power Filters for Power Quality Improvement under Different Load Conditions," International Journal of Advanced Research in Electrical, Electronics and Instrumentation Engineering (IJIRCCE) (An ISO 3297: 2007 Certified Organization) Vol. 3, Issue 8, pp.11104-11107, August 2014.

[5] Sahana C B, **"**Study on Mitigation of Harmonics by Using Passive Filter and Active Filter," International Journal of Innovative Research in Computer and Communication Engineering (IJIRCCE) an ISO 3297: 2007 Certified Organization Vol.3, Special Issue 5, pp.254-272, May 2015.

[6] Anumeha Kumari, Er. Roshan Nayak and Er. Anupam Masih, "Designing and Harmonic Analysis of Shunt Hybrid Filter with 24 Pulse Converter," IJISET – International Journal of Innovative Science, Engineering & Technology, Vol. 4 Issue 6, pp.2348 – 7968, June 2017 ISSN (Online), | Impact Factor (2016) – 5.264.

[7] Laxmi Devi Sahu, Satya Prakash Dubey, "ANN based Hybrid Active Power Filter for Harmonics Elimination with Distorted Mains," International Journal of Power Electronics and Drive System (IJPEDS) Vol. 2, No. 3, pp.241~248, September 2012.

[8] Jyotsana Kaiwart, Uma P. Bala Raju, "Harmonic Mitigation Techniques: A Review," International Journal of Advanced Research in Electrical, Electronics and Instrumentation Engineering (An ISO 3297: 2007 Certified Organization) Vol. 5, Issue 11, pp.8348-8350, November 2016.

[9] MEERA S NAIR, DEEPA SANKAR, “A Review of Hybrid filter topologies for power quality compensation’’, International Research Journal of Engineering and Technology (IRJET), Volume: 02 Issue: 04, pp.613-618, July-2015.

[10] Prashanta Kumar Das; Associate Professor, B. Srikanth; Research Student, “Modeling, Analysis and Simulation of Three Phase Hybrid Power Filter for Power Quality Improvement”, International Journal of Engineering Research and Applications (IJERA)ISSN: 2248-9622 www.ijera.com Vol. 2, Issue 3, pp.011-017 May-Jun 2012.

[11] Victor Fabián Corasaniti, Maria Beatriz Barbieri, Patricia Liliana Arnera and María Inés Valla, “Hybrid Active Filter for Reactive and Harmonics Compensation in a Distribution Network”, IEEE TRANSACTIONS ON INDUSTRIAL ELECTRONICS, VOL. 56, NO. 3, pp.671-673, MARCH 2009.

[12] P. Sathvik, A. Srinivasa Reddy, B. Sambasiva Rao, “Simulation of Shunt Active Power Filter with Pi and Fuzzy Logic Controller”, International Journal of Engineering and Advanced Technology (IJEAT) ISSN: 2249 – 8958, Volume-7 Issue-2, pp.89-91, December 2017.

[13] B. Shruti and, Dr. D. Bala Gangi Reddy, “Sliding Mode Control Based Hybrid Active Filter with Variable Conductance for Harmonic Resonance Suppression in Industrial Power Systems”, International Journal of Engineering Science and Computing (IJESC) Volume 6 Issue No.8, pp.2845-2849, August 2016.

[14] Swapnil S. Managule, Sanjay Dabhole, Sanjeev Gupta, “The Shunt Active Power Filter to Compensate Reactive Power and Harmonics with Optimized PI controller in a three Phase 3 Wire Distribution Network”, International Journal of Innovative Technology and Exploring Engineering (IJITEE) ISSN: 2278-3075, Volume-7 Issue-4, p.3, January 2018.

[15] P. Kishore Kumar, M.Sharanya, “Design of Hybrid Series Active Filters for Harmonic Reduction in Single Phase Systems”, International Journal of Modern Engineering Research (IJMER) www.ijmer.com, Vol. 3, Issue. 5, pp-3170-3176, Sep - Oct. 2013, ISSN: 2249-6645

[16] CH. RAVIKIRAN, G.INDIRA KISHORE, TLSV .AYYA RAO, and M. RAMBABU, “Effective Elimination of Harmonics By Means Of A Hybrid Series Active Filter (HSAF)”, International Journal of Engineering Research and Applications (IJERA) ISSN: 2248-9622 www.ijera.com Vol. 2, Issue 5, pp.096-101, September - October 2012.

[17] Tugce Demirdelen, R. Ilker Kayaalp and Mehmet Tumay, "Modeling and Analysis of a Multilevel Parallel Hybrid Active Power Filter", Engineering, Technology & Applied Science Research Vol. 6, No. 3, pp. 976-981, 2016.

[18] IRFAN ALI, VIRENDRA SHARMA, PRADEEP CHHAWCHHARIA, "CONTROL TECHNIQUES FOR ACTIVE POWER FILTER FOR HARMONIC ELIMINATION & POWER QUALITY IMPROVEMENT", International Journal of Electrical, Electronics And Data Communication, ISSN: 2320-2084 Volume-4, Issue-10, pp.25-28, Oct.-2016.

[19] Swati Pal, Pallavi Singh Bondriya, Yogesh Pahariya, "MATLAB-Simulink Model Based Shunt Active Power Filter Using Fuzzy Logic Controller to Minimize the Harmonics", International Journal of Scientific and Research Publications, Volume 3, Issue 12, pp.2-4, December 2013 1 ISSN 2250-3153.

[20] Almas Shintemirov, Astana, Kazakhstan, "Reference Signals Generation for Active Power Filter Compensation Using Mathematical Morphology", 4th International Conference on Power Engineering, Energy and Electrical Drives, Istanbul, Turkey, pp.1525-1527, 13-17 May 2013.

[21] H. R. Imani Jajarmi, A. Mohamed, H. Shareef, Subiyanto, "A New Method for Calculating the Reference Current of Shunt Active Power Filters Based on Recursive Discrete Fourier Transform", Article in International Review on Modelling and Simulations, pp.1-9, August 2012.

[22] M. Jawad Ghorbani, H. Mokhtari, "Impact of Harmonics on Power Quality and Losses in Power Distribution Systems", International Journal of Electrical and Computer Engineering (IJECE) Vol. 5, No. 1, pp. 166~174, February 2015, ISSN: 2088-8708.

[23] Arun Shankar V.K.a, Senthil Kumar N.b, "Implementation of Shunt Active Filter for Harmonic Compensation in a 3 Phase 3 Wire Distribution Network", 1st International Conference on Power Engineering, Computing and CONtrol, PECCON-2017, pp.173-175, 2- 4 March 2017, VIT University, Chennai Campus.

[24] Bhargav R. Gamit, Sanjay R. Vyas, "HARMONIC ELIMINATION IN THREE PHASE SYSTEM BY MEANS OF HYBRID ACTIVE FILTER", International Research Journal of Engineering and Technology (IRJET) e-ISSN: 2395-0056 Volume: 05 Issue: 04, pp.314-321, Apr-2018 www.irjet.net p-ISSN: 2395-0072.

[25] ZUBAIR AHMED MEMON, MOHAMMAD ASLAM UQAILI, AND MUKHTIAR AHMED UNAR, "Design of Three Phase Hybrid Active Power Filter for Compensating the Harmonic Currents of Three Phase System", Mehran University Research Journal of Engineering & Technology, Volume 31, No. 2, pp.347-350, April, 2012 [ISSN 0254-7821].

[26] ZUBAIR AHMED MEMON, MOHAMMAD ASLAM UQAILI, AND MUKHTIAR AHMED UNAR, "Estimation of Compensation Current Reference using Fuzzy Logic Controller for Three-Phase Hybrid Active Power Filter", Mehran University Engineering & Technology, International Journal of Computer Applications (0975 – 8887) Volume 43– No.11, pp.16-18, April 2012.

[27] M.Sahithullah, and Dr.A.Senthil Kumar, "Harmonic Reduction of Hybrid Active Power Filter Using Hysteresis Controller in Power System", 3rd International Conference on Latest Computational Technologies (ICLCT'2014) March 19-20, p.6, 2014 Abu Dhabi (UAE).

[28] C.S. Lam, M.C. Wong, and Y.D. Han, "Hysteresis current control of hybrid active power filters", Published in IET Power Electronics Received on 1st August 2011, pp.1175–1187, Revised on 28th December 2011 doi: 10.1049/iet-pel.2011.0300.

[29] Ch.V.Pujitha and A.Sambasiva Rao, "Mitigation of Harmonics Using Active Power Filters Based on Hysteresis Current Control", International Journal of Advanced Research in Electrical, Electronics and Instrumentation Engineering, (An ISO 3297: 2007 Certified Organization), (An ISO 3297: 2007 Certified Organization), Vol.4, Issue 4, pp.2667-2669, April 2015.

[30] B. NAYAK, B. MISRA and A. MOHAPATRA, "A PROPOSED REFERENCE CURRENT SIGNAL GENERATION TECHNIQUE FOR SHUNT ACTIVE POWER FILTER", Journal of Engineering Science and Technology Vol. 13, No. 6, pp.1837-1843, 2018, 1834 - 1849 © School of Engineering, Taylor's University.

[31] Prof. P. Parthasaradhy, Dr.Dola Gobinda Padhan and Chinmaya K A "Regulation of the DC Bus Voltage of a Three Phase Active Power Filter by PI and Fuzzy Logic Controller", The International Journal Of Engineering and Science (IJES) ISSN (e): 2319 – 1813 ISSN (p): 2319 – 1805, pp.78-80, 2014.

[32] Govindaraj.V, and Priya. M, "REVIEW OF HYBRID ACTIVE POWER FILTER TOPOLOGIES AND CONTROLLERS FOR ENHANCEMENT OF POWER QUALITY", International Journal of Pure and Applied Mathematics Volume 118, No. 11, pp. 29-35, 2018.

[33] Kavita Dewangan, Prof. Pawan C. Tapre, "Harmonic Reduction by Using Shunt Hybrid Power Filter", ISSN (e): 2250 – 3005 || Vol, 04 || Issue, 5, pp.41-46, May – 2014, International Journal of Computational Engineering Research (IJCER).

[34] M.Ghosh, C. Koley and N. K. Roy, "Improved Instantaneous PQ Theory based Reference Current Generation Algorithm for Shunt Active Power Filters", International Journal of Engineering Research in Electrical and Electronic Engineering (IJEREEE) Vol 3, Issue 12, pp.35-37, December 2017.

Appendix A: Case study location

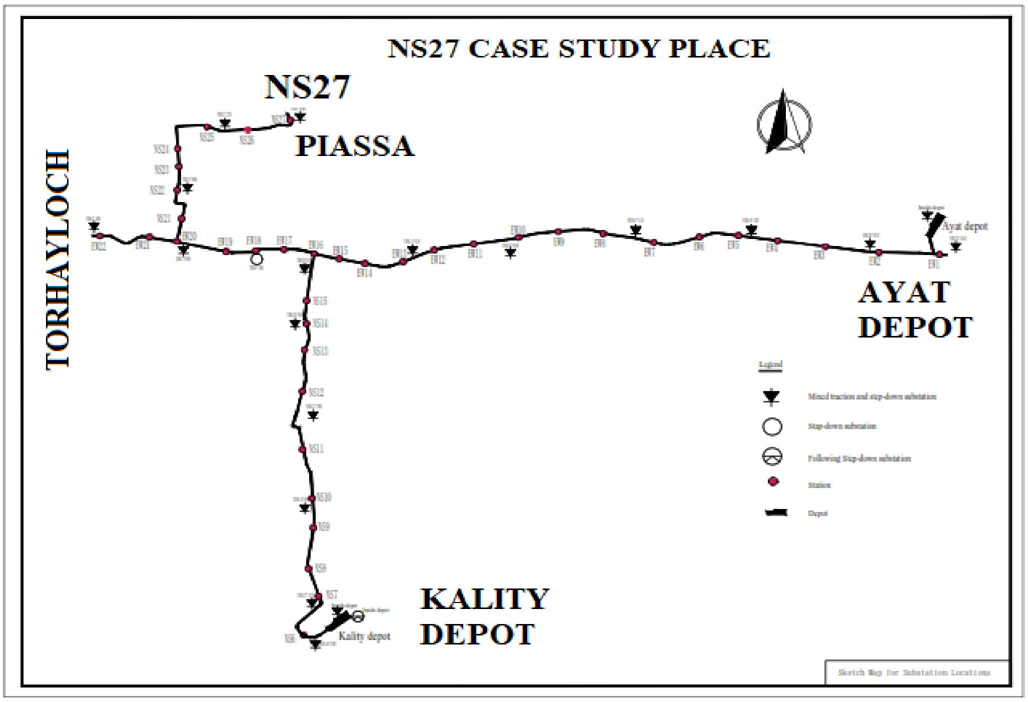

Appendix B: Manufacturer rectifier circuit

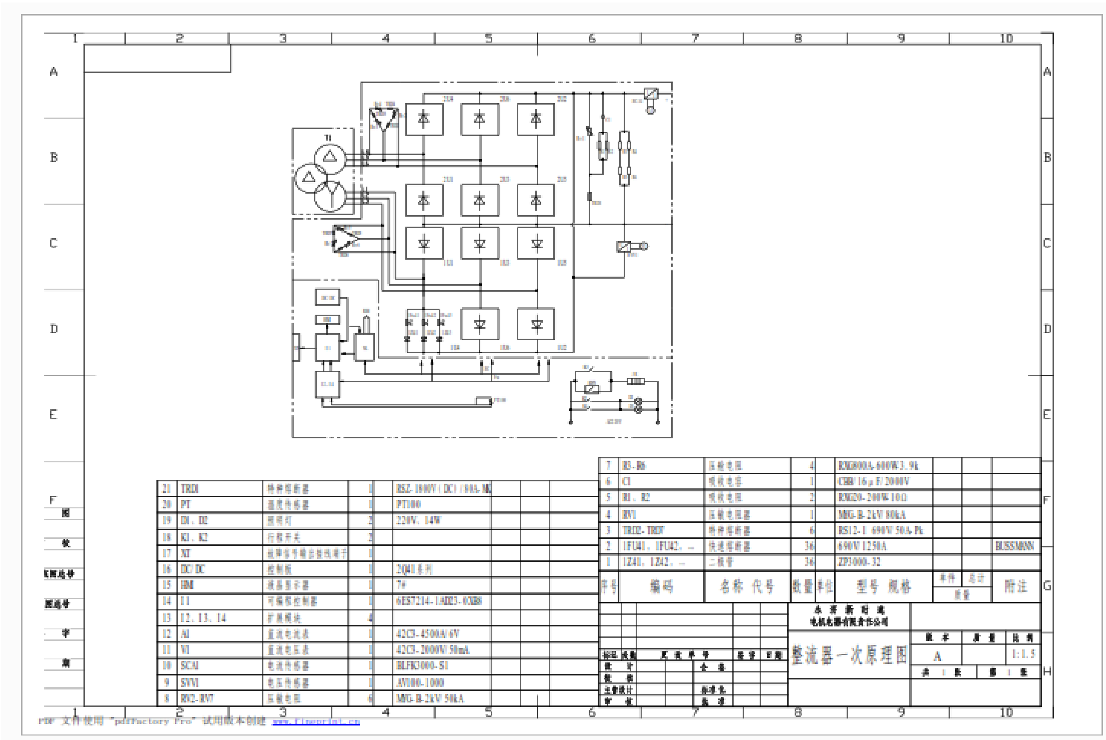

Appendix C: Short circuit current calculation

The short circuit current can be calculated from reactance percentage values of transformer and full load current of the system.

Percentage reactance is defined as:

$$\%X = \frac{I*X}{V} * 100\%$$

where I = transformer full load current,

V = transformer phase voltage,

X = transformer reactance in ohms per phase

Short circuit current I_{sc} in a circuit can be expressed as:

$$I_{sc} = \frac{V}{X} = \frac{V*I}{V.(\%X)} *100$$

$$I_{sc} = \frac{V}{X} = \frac{I}{\%X} *100$$